REPORT NO.
UC SESM 73-11

STRUCTURES AND MATERIALS RESEARCH
DEPARTMENT OF CIVIL ENGINEERING

NONLINEAR STATIC AND DYNAMIC ANALYSIS OF SHELLS OF REVOLUTION UNDER AXISYMMETRIC LOADING

by

S. NAGARAJAN

Report to
Picatinny Arsenal, Dover, New Jersey
Contract No. DAAA 21-72-C-0727

SEPTEMBER 1973

STRUCTURAL ENGINEERING LABORATORY
UNIVERSITY OF CALIFORNIA
BERKELEY CALIFORNIA

STRUCTURES AND MATERIALS RESEARCH

DEPARTMENT OF CIVIL ENGINEERING

Report No. UC-SESM 73-11

NONLINEAR STATIC AND DYNAMIC ANALYSIS OF SHELLS OF REVOLUTION UNDER AXISYMMETRIC LOADING

by

S. NAGARAJAN

Faculty Investigator: E. P. Popov

Report to

Picatinny Arsenal, Dover, New Jersey

Contract No. DAAA 21-72-C-0727

STRUCTURAL ENGINEERING LABORATORY

UNIVERSITY OF CALIFORNIA

BERKELEY, CALIFORNIA

September 1973

ABSTRACT

A method of analyzing nonlinear static and dynamic responses of deformable solids has been developed based on an incremental variational formulation using the Lagrangian mode of description. The material nonlinearity due to plasticity or viscoplasticity as well as the geometric nonlinearity due to large displacements are considered. The equations of motion are obtained in a linearized incremental form using the principle of virtual work and solved using step-by-step numerical integration procedures. Equilibrium check is made at the end of each step and the residual forces are added to the next increment for improved accuracy over the pure incremental method.

For elastic-plastic solutions the flow theory of plasticity is used along with the von Mises yield condition for isotropically hardening materials. The viscoplastic constitutive theory is also in the form of an associated flow law and capable of considering strain rate sensitive behavior. The viscoplastic strains are taken into account using an initial strain formulation.

The discretization of the structure is achieved by the use of degenerate isoparametric finite elements and the computer

codes that have been developed are capable of analyzing large axisymmetric deformations of shells of revolution. Inclusion of shear deformations in the elements permits both thin and moderately thick shells to be analyzed. Several numerical examples are presented to illustrate the capabilities of the programs for both static and dynamic analyses. The viscoplastic formulation is also shown to be capable of solving plasticity problems when the time parameter is used simply as an artifice.

ACKNOWLEDGEMENTS

I wish to express my deep gratitude and sincere appreciation to my research advisor, Professor E. P. Popov, for his continued encouragement and guidance during the course of this research. I am also grateful to Professors J. M. Kelly and R. S. Lehman for their perusal of the manuscript. My special thanks go to Dr. P. K. Larsen, a former graduate student and colleague in the department, for the many valuable discussions in the initial stages of this work. I am especially indebted to my wife Nadia for her patience, good cheer and moral support.

This work was partially supported by Contracts DAAA 21-72-C-0727 and -0729. The computer time and facilities were provided by the University of California, Berkeley.

TABLE OF CONTENTS

NOMENCLATURE

A list of important symbols is compiled in this section for convenience of reference. All symbols are defined in the text when they appear first. Symbols which have more than one meaning are clearly defined when used so as to avoid any confusion. All indices range from 1 to 3, unless specified to be otherwise.

A_{IJKL}	Strain transformation matrix, Eq. (3.25).
dA, da, $d\bar{a}$	Infinitesimal areas in B_0, B_1 and B_2, respectively.
B_0, B_1, B_2	Initial configuration, configuration 1 and configuration 2, respectively.
∂B_0, ∂B_1, ∂B_2	Surface areas of B_0, B_1, B_2 with prescribed tractions, respectively.
C^{IJKL}, C_{IJKL}	Stress-strain transformation tensor.
E, E_t	Young's modulus and tangent modulus.
E_{IJKL}	Stress-strain transformation tensor for generalized Hooke's law.
${}^1E_{IJ}$, ${}^2E_{IJ}$	Lagrangian strain in B_1 and B_2.
E_{IJ}	Increment of Lagrangian strain between B_1 and B_2.
${}^1\dot{E}_{IJ}$, ${}^2\dot{E}_{IJ}$	Lagrangian strain rates in B_1 and B_2.
${}^1\dot{E}^I_{IJ}$	Instantaneous Lagrangian strain rate in B_1.
${}^1\dot{E}^E_{IJ}$ ${}^1\dot{E}^P_{IJ}$ ${}^1\dot{E}^{VP}_{IJ}$	Elastic, plastic and viscoplastic strain rates in B_1, respectively.

F	Scalar yield function in viscoplasticity, Eq. (3.36).
${}^{1}F^{i}_{\cdot I}$	Deformation gradient in B_1 relative to B_0.
${}^{2}F^{\alpha}_{\cdot I}$, $F^{\alpha}_{\cdot i}$	Deformation gradients in B_2, relative to B_0 and B_1, respectively.
$\underset{\sim}{G}_I$, $\underset{\sim}{g}_i$, $\bar{\underset{\sim}{g}}_\alpha$	Base vectors in B_0, B_1 and B_2, respectively.
${}^{0}\underset{\sim}{G}_I$, ${}^{1}\underset{\sim}{G}_I$ ${}^{2}\underset{\sim}{G}_I$	Convected base vectors in B_0, B_1 and B_2, respectively.
G_{IJ}, g_{ij}, $\bar{g}_{\alpha\beta}$	Metric tensors associated with B_0, B_1 and B_2, respectively, in terms of base vectors $\underset{\sim}{G}_I$, $\underset{\sim}{g}_i$ and $\bar{\underset{\sim}{g}}_\alpha$.
${}^{0}G_{IJ}$, ${}^{1}G_{IJ}$, ${}^{2}G_{IJ}$	Metric tensors associated with B_0, B_1 and B_2, respectively, in terms of base vectors ${}^{0}\underset{\sim}{G}_I$, ${}^{1}\underset{\sim}{G}_I$ and ${}^{2}\underset{\sim}{G}_I$.
$G^{i}_{\ I}$, $G^{\alpha}_{\ I}$, $g^{\alpha}_{\ i}$	Shifters required to relate components of a vector in different coordinate systems, Eq. (2.5).
H'	Hardening parameter in plasticity, Eq. (3.9).
H	Slope of the uniaxial $\bar{\sigma}$ - $\bar{\varepsilon}^{P}$ curve.
I_2	Second invariant of viscoplastic strain rate tensor.
J_1, J_2, J_3	Invariants of deviatoric stress tensor.
$\underset{\sim}{N}$, $\underset{\sim}{n}$, $\bar{\underset{\sim}{n}}$	Normal vectors in B_0, $B_1$and B_2, respectively.

$\overset{2}{\underset{\sim}{R}}$	Generalized loads in B_2.
$\hat{\underset{\sim}{R}}$	Generalized incremental loads including out-of-balance forces, Eq. (4.8).
${}^1S^{IJ}$, ${}^2S^{IJ}$	2nd Piola-Kirchhoff stress in B_1 and B_2.
S^{IJ}	Increment of 2nd P-K stress between B_1 and B_2.
${}^1\dot{S}^{IJ}$, ${}^2\dot{S}^{IJ}$	Rates of 2nd P-K stress in B_1 and B_2.
$\bar{S}^{IJ}$	Deviatoric component of S^{IJ}.
S^I_{IJ}, S^{VP}_{IJ}	Instantaneous and "viscoplastic" increments of the P-K stress between B_1 and B_2, Eq. (2.92).
T_i	Period of vibration of mode i.
${}^1T^{ij}$, ${}^2T^{\alpha\beta}$	Cauchy stresses in B_1 and B_2.
${}^1\dot{T}^{ij}$, ${}^2\dot{T}^{\alpha\beta}$	Rates of the Cauchy stresses in B_1 and B_2.
dV, dv, $d\bar{v}$	Infinitesimal volumes in B_0, B_1 and B_2, respectively.
W_p	Plastic work.
${}^1W$, ${}^2W$	Strain energy functions in B_1 and B_2, section 2.5.
δW_1, δW_2	Virtual work in B_1 and B_2.
$\delta\tilde{W}_1$, $\delta\tilde{W}_2$	Defined in section 2.4.
X^I, x^i, $\bar{x}^\alpha$	Coordinates of material point in B_0, B_1 and B_2, respectively.
$\partial_{\underset{\sim}{x}}\cdot$, $\cdot\partial_{\underset{\sim}{x}}$	Right and left divergence operators.
c	Parameter for translation of yield surface in kinematic hardening, Eq. (3.7).

e_{IJ}	Linear part of E_{IJ}.
$\hat{e}_{IJ}$, $\hat{\hat{e}}_{IJ}$	Components of e_{IJ}, Eq. (2.19).
f	Yield surface.
${}^1\underset{\sim}{f}$, ${}^2\underset{\sim}{f}$	Body force vectors in B_1 and B_2.
g	Plastic potential.
h	Defined in section 3.1.
h_i	Shell thickness at node i.
k	Initial yield stress in pure shear.
${}^1p$, ${}^2p$, p	Normal pressure in B_1, B_2, and incremental pressure between B_1 and B_2, respectively.
r_i	Global coordinate of node i.
r	Radius.
${}^0ds$, ${}^1ds$, ${}^2ds$	Infinitesimal lengths in B_0, B_1, B_2.
s, t	Local orthogonal curvilinear coordinates, Fig. 5.2.
t	Time.
Δt	Time interval; time step for direct integration of equations of motion.
${}^0\underset{\sim}{t}$, ${}^1\underset{\sim}{t}$, ${}^2\underset{\sim}{t}$	Traction vectors in B_0, B_1, B_2.
${}^1\underset{\sim}{u}$, ${}^2\underset{\sim}{u}$, $\underset{\sim}{u}$	Displacement vector to B_1 and B_2 from B_0, and from B_1 to B_2, Fig. 2.1.
${}^1\dot{\underset{\sim}{u}}$, ${}^2\dot{\underset{\sim}{u}}$ $\dot{\underset{\sim}{u}}$	Velocity vectors.
${}^1\ddot{\underset{\sim}{u}}$, ${}^2\ddot{\underset{\sim}{u}}$, $\ddot{\underset{\sim}{u}}$	Acceleration vectors.
u_1, u_2	Local displacements relative to (s, t) coordinate system, Fig. 5.2.

u_i, w_i	Horizontal and vertical displacements at node i.
z_i	Global coordinate of node i.
α_i	Rotation of normal at node i.
α_{IJ}	Components of the tensor describing the incremental translation of the origin of yield surface.
α, β	Mass and stiffness proportional damping factors.
β	Defined in section 5.7.3.
β	Free parameter in Newmark family of integration methods.
γ	Free parameter in Newmark integration.
γ, $\bar{\gamma}$	Material viscosity coefficients, section 3.2.2.
δ	Virtual variation.
δ	Control parameter for introducing artificial damping in Newmark integration.
$\delta^I{}_J$, $\delta^i{}_j$	Kronecker delta.
ε_{ij}	Eulerian strain in B_1.
$\bar{\varepsilon}^P$, $\bar{\varepsilon}^{VP}$	Equivalent plastic and viscoplastic strains.
ζ	Defined in section 3.1.
η	Local coordinate, Fig. 5.2
η_{IJ}	Nonlinear part of E_{IJ}.
Θ	Parameter in the Wilson-Farhoomand integration method.

θ	Circumferential coordinate for shell.
θ_i	Normal angle at node i, see Fig. 5.2.
κ_p	Plastic hardening parameter.
λ	Lamé constant.
$\dot{\lambda}$, $d\lambda$	Proportionality factors in plasticity, Chapter 3.
μ	Lamé constant.
ν	Poisson's ratio.
ξ	Local coordinate, Fig. 5.2.
ρ_0, ρ, $\bar{\rho}$	Mass density in B_0, B_1, B_2.
ρ	Load proportionality factor.
$\bar{\sigma}$	Equivalent stress.
σ_y	Initial yield stress in simple tension.
τ	Pseudo-time step, defined in section 4.4.2.
Φ	Scalar function in viscoplasticity, Eq. (3.37).
$\phi_i(\xi, \eta)$	Interpolation polynomials, Chapter 5.
$\underset{\sim}{\chi}$	Mapping function from B_0
Ψ_i	Meridoinal angle at node i, Fig. 5.2.
[ ]	Matrix.
{ }	Column vector.
< >	Row vector.
< >	Singularity function defined in section 3.2.2.
[B]	Transformation matrix between displacement gradients and displacements, Eqs. (5.17, 18).

$[C]$	Damping matrix.
$[D]$	Transformed stress-strain matrix, Eq. (5.25).
$[D_1],[D_2],[D_3]$	Integrated forms of [D], Eq. (5.28).
$\{{}^1F^R\}$	Internal resisting forces.
$[H_{11}],[H_{22}],[H_{13}]$	Defined in section 5.3.
$[J]$	Jacobian matrix.
$[K_0]$	Incremental stiffness matrix.
$[K_1]$, $[K_2]$	Nonlinear stiffness matrices.
$[K_3]$	Stiffness matrix due to nonconservative loading.
$[K_G]$	Geometric stiffness matrix.
$[M]$	Mass matrix.
$<M_0>$, $<M_1>$, $<M_2>$	Defined in section 5.4.2.
$\{N_0\}$, $\{N_1\}$	Defined in section 5.7.1.
$\{Q_0\}$, $\{Q_1\}$	Defined in section 5.7.2.
$\{{}^2R\}$	Consistent nodal forces due to externally applied loading in B_2.
$\{R^{VP}\}$	Incremental viscoplastic pseudo-loading.
$\{r\}$	Vector of nodal point global coordinates.
$\{u\}$	Vector of radial displacements.
$\{Q\}$	Vector of nodal point displacements and rotations.
$\{u_\partial\}$	Vector of displacement gradients.
$\{w\}$	Vector of vertical displacements.
$\{z\}$	Vector of nodal point global coordinates.

$[\Gamma]_i$	Defined in section 5.3.
$[\Lambda]$	Defined in section 5.3
$[\Omega]_i$	Defined in section 5.3.
$[\pi]_i$	Defined in section 5.3.
$[\phi]$, $[\phi_u]$, $[\bar{\phi}_u]$	Matrices of interpolation polynomials, Chapter 5.

1. INTRODUCTION

The development of efficient and accurate techniques for static and dynamic analysis of deformable bodies is of considerable importance in various engineering fields. The study of shells of revolution is of particular significance because of the diverse fields in which structural components of this type are found - rocket casings, submarine hulls, fluid containers, nuclear reactors, pressure vessels, piping systems, etc. The ability to predict the response of such structures to blast pressure or impact loading is very essential from a design viewpoint. The objective of arriving at the most economical and optimum design requires that the analysis procedures take into consideration both physical and geometrical nonlinearities.

There are many practical problems involving rate dependent deformations that are of technical and industrial significance. Such examples may be found in explosive or impact forming of metal parts, impulsive loading of bars, plates, cylinders and spheres, etc. Both inertia and viscous type forces may become very important and the classical inviscid plasticity theory is inadequate for dealing with such problems and recourse must be made to constitutive theories which reflect strain rate sensitivity.

The application of well known linear theories to problems in solid mechanics remained the primary area of research activity until the onset of the age of high speed digital computers. Even in this area of linear analysis, exact closed form solutions to the governing differential equations of shells of revolution were possible only for the simplest of cases [1,2] and approximate methods had to

be devised to treat most practical problems. The classical field theories for nonlinear problems were formulated by Green et al. [3,4] and Truesdell et al. [5,6] but these theories are so complex that exact solutions may be found only for very few specific problems involving bodies with the most simple geometric shapes and boundary conditions. Even the classical approximate methods like asymptotic expansion and weighted residual methods could be applied only to relatively simple cases [7,8,9]. The advent of high speed digital computers with large capacity storage, along with the development of new numerical methods, made it possible to consider a much wider class of problems, and a considerable research effort has been under way over the last two decades in the area of nonlinear analysis.

The finite difference method [10] has been used for numerical solution of shell problems by Budiansky and Radkowski [11], Sepetoski et al. [12], and Bushnell and Almroth [13]. But this method is restricted to simple, regular geometries where the boundary conditions are not complex and the material properties can be expressed analytically. These difficulties can be overcome by the finite element method [14-17] which is an extension of the classical Ritz method for the solution of variational problems. This method is ideally suited for the analysis of complex structures since it can account for arbitrary geometries, boundary conditions, loadings and material property variations. Extensive references to recent research efforts may be found in several books and survey papers [18-22] and no attempt is made in the following to present a complete literature survey.

Most of the early work with the finite element method was focused on static analysis of linear systems but the use of incremental and/or iterative techniques have extended its applicability to nonlinear as well as dynamic problems. Turner et al. [23] presented the first attempt at solving nonlinear problems using the finite element method and a number of other investigators have studied the nonlinear behavior of various structural members [24-32]. Notable contributions were made by Marcal [33], Oden [34], Felippa [35], and a rigorous treatment of incremental equilibrium equations was given by Yaghmai [36]. Application of the finite element method to inelastic problems was studied by Argyris [24], Popov et al. [37], Khojasteh-Bakht [38], Marcal [39] and Zienkiewicz [40]. The combined effect of material and geometric nonlinearities was considered by Marcal [33], Yaghmai [36], Armen et al. [41], Hofmeister et al. [42] and Larsen [43]. Larsen also studied the large displacement behavior of shells of revolution for creep and viscoelastic problems. The extension of finite element methods for the solution of dynamic response analysis is rather straightforward. The mode superposition technique may be used for linear systems and various step-by-step algorithms may be applied for the solution of both linear and nonlinear systems [44-49]. However, use of the finite element methods for nonlinear dynamic analysis and their application to practical problems are still in the early stages of development.

There are many problems for which strain rate effects can be important and constitutive laws for rate sensitive materials have been proposed by several authors. These have been summarized and discussed by Perzyna [50], Lindholm [51], and Cristescu [52].

Although many experimental studies have been reported [53-57], application of finite element methods to this class of viscoplastic problems is lagging far behind and literature in this field is almost nonexistent, except for the work of Zienkiewicz and Cormeau [58] which studies some simple problems.

The objective of this investigation was the development of a method for the static and dynamic response analysis of shells of revolution subjected to axisymmetric loading, including the effect of both material and geometric nonlinearities. Lagrangian formulation is used in this study and the incremental equations of motion are derived using the principle of virtual work. The classical inviscid theory of plasticity using von Mises yield criterion as well as the viscoplasticity laws taking into account strain rate dependent deformations are both considered. The finite element idealization is based on the degenerate isoparametric elements and the solution is achieved by means of step-by-step numerical integration schemes along with equilibrium correction at each step. The numerical examples presented illustrate the effectiveness of the developed programs for a number of static and dynamic analysis problems and also demonstrate the use of the viscoplasticity formulation as an artifice for obtaining plasticity solutions.

2. THEORETICAL FORMULATION FOR LARGE DEFORMATIONS

2.1 Introduction

The most comprehensive accounts of the foundations of the field theories of continuum mechanics were presented by Truesdale and Toupin [5], and Truesdell and Noll [6]. Since then several texts have been have been published and the works of Truesdale [59], Eringen [60,6]], Jaunzemis [62], Leigh [63] and Malvern [64] may be cited for their unified presentation of fundamental principles and for extensive bibliographical references. However, these theories are so complex that numerical methods have to be resorted to in most practical problems. Many investigators have invoked variational principles and derived incremental equations for nonlinear problems. In particular, Yaghmai [36] and Larsen [43] have given detailed and rigorous treatments and the presentation here follows basically that of Larsen.

2.2 Kinematics

The mode of description of the motion of a continuum depends on the choice of the Euclidean space to be used as the reference configuration. The material particles of the body are used as primitive quantities in the material description of motion while the material coordinates in a reference configuration are used in the referential description. These are both commonly referred to as the Lagrangian description of motion and no distinction is drawn between the two in most practical applications. The spatial description or Eulerian description fixes attention on a given point in space and time instead of a particle of matter and observes

the motion of particles through this point. The relative description involves the use of a moving reference configuration wherein the configuration at time t is taken as the reference configuration. Finally, the convected description is involved when fixed coordinates are assigned to material points and motion is described in terms of deformation of the "body space".

The recomputation of several element matrices involving derivatives and the update of nodal point coordinates as the geometry changes are eliminated when the Lagrangian description is used. Although the constitutive equations for plasticity, viscoplasticity, creep, etc., may need transformation to this description, the Lagrangian mode of description of motion leads to a very efficient formulation and solution of the nonlinear equilibrium equations and is used throughout this study.

Consider three configurations in the path of deformation of a three-dimensional body, as shown in Fig. 2.1. The initial configuration is denoted by B_0, the current configuration by B_1, and a neighbouring configuration to B_1 is indicated by B_2. A fixed, orthogonal curvilinear coordinate system with coordinates X^I and base vectors $\underset{\sim}{G}_I$ is associated with configuration B_0 while configuration B_1 is described by the coordinates x^i and base vectors $\underset{\sim}{g}_i$, and B_2 by $\bar{x}^\alpha$ and $\bar{\underset{\sim}{g}}_\alpha$, all the indices having the range 1 to 3. The coordinate system X^I will be assumed to be a global system in which the motion is described. An auxiliary convected or intrinsic coordinate system is shown in Fig. 2.2 and can be obtained from the foregoing by selecting x^i and $\bar{x}^\alpha$ in such a way that the numerical value of these coordinates

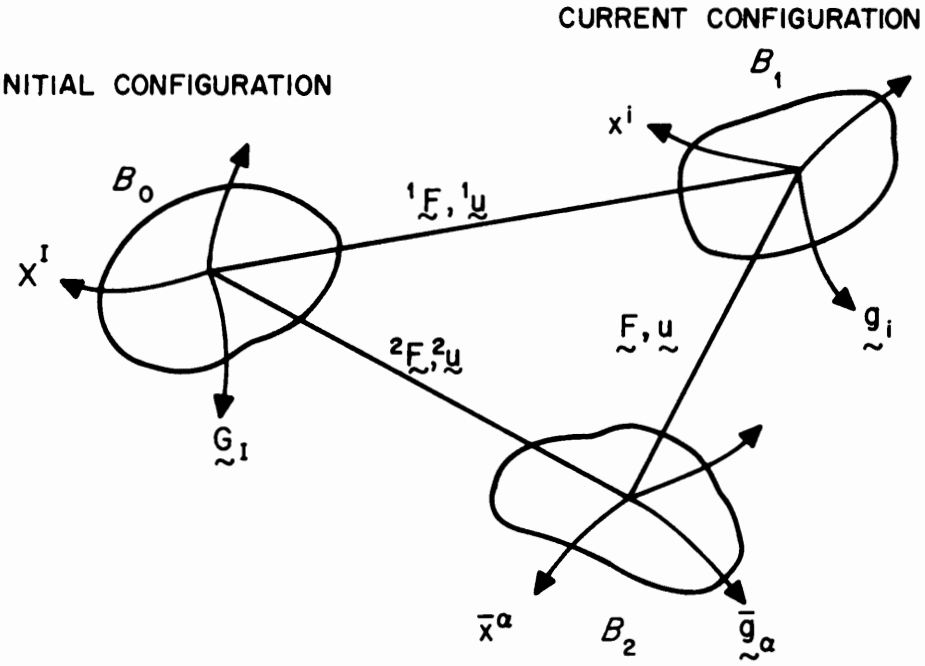

FIG. 2.1 DESCRIPTION OF MOTION

CONFIGURATIONS OF A BODY IN ITS PATH OF DEFORMATION

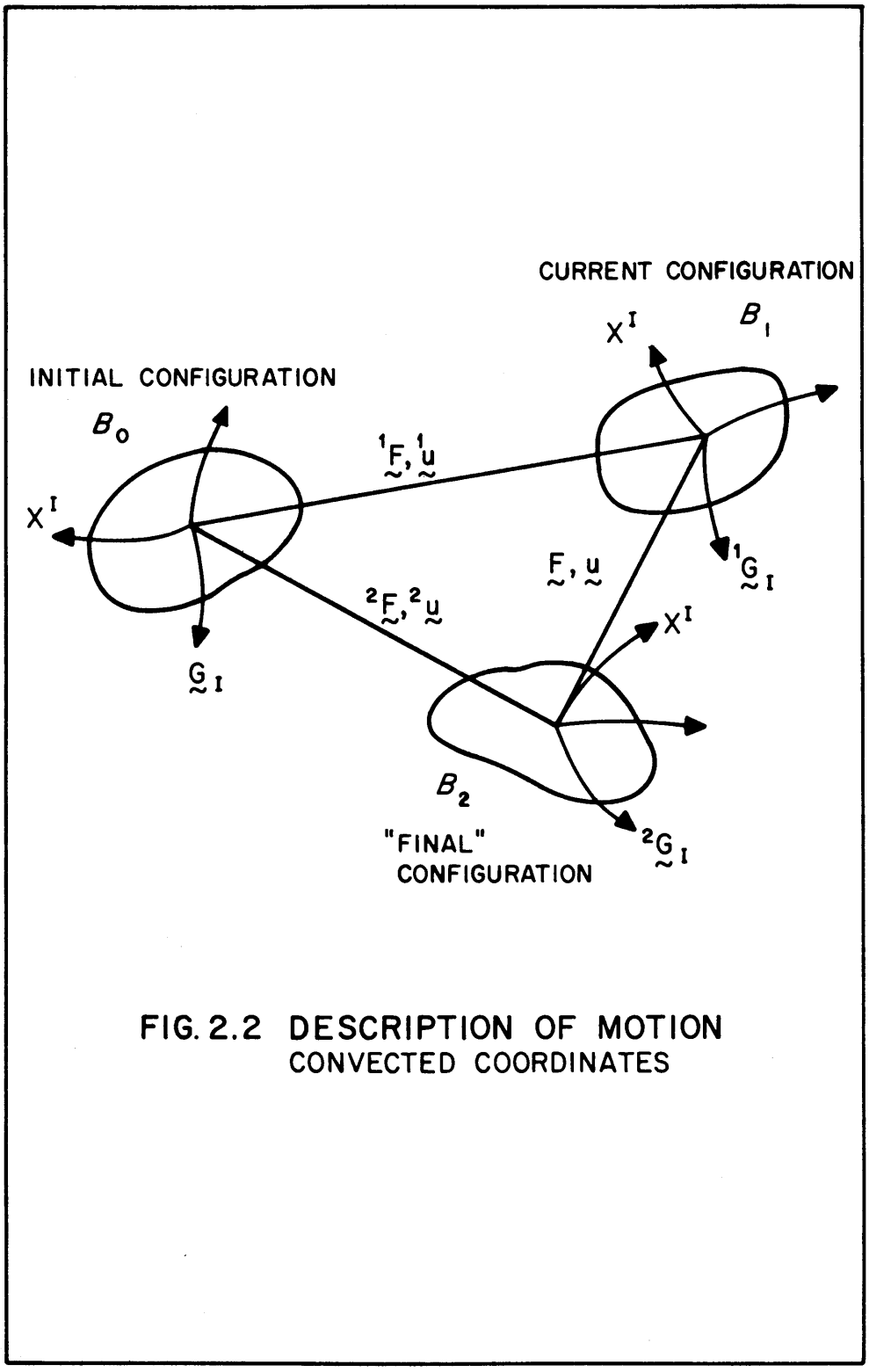

FIG. 2.2 DESCRIPTION OF MOTION
CONVECTED COORDINATES

of a given point remain the same as those of X^I. The base vectors in the initial configuration remain $\underset{\sim}{G}_I$; however, each deformed configuration requires a second set of base vectors. Thus, the coordinates remain X^I for all configurations while $\underset{\sim}{G}_I$, $^1\underset{\sim}{G}_I$ and $^2\underset{\sim}{G}_I$ are the base vectors associated with B_0, B_1 and B_2, respectively, in the convected system. This auxiliary system is useful in some coordinate transformations but will not be used in the description of motion as rate expressions become complicated in it.

The motion of the body causes any given material particle with material coordinates X^I to occupy a new spatial position with coordinates x^i. This is expressed by

$$x^i = x^i (X^I, t) \tag{2.1}$$

where $\underset{\sim}{\chi}$ is a mapping function from B_0 and the parameter t is time. This mapping function will take the value x^i in B_1 and $\bar{x}^\alpha$ in B_2, with reference to the base vectors in the respective spaces. These mappings are assumed to be single-valued and possess continuous partial derivatives. In order for a unique inverse mapping to exist, the jacobian J is not identically zero, i.e.

$$J \equiv \left| \frac{\partial x^i}{\partial X^I} \right| \neq 0 \tag{2.2}$$

This assumption is known as the axiom of continuity and expresses the concepts of indestructibility and impenetrability of matter.

Metric tensors and shifters

The inner product of the base vectors associated with each space defines the corresponding metric tensors, e.g.

$$G_{IJ} = \underset{\sim}{G}_I \cdot \underset{\sim}{G}_J$$

$$g_{ij} = \underset{\sim}{g}_i \cdot \underset{\sim}{g}_j$$

$$\bar{g}_{\alpha\beta} = \bar{\underset{\sim}{g}}_{\alpha} \cdot \bar{\underset{\sim}{g}}_{\beta}$$
$$^{1}G_{IJ} = {}^{1}\underset{\sim}{G}_{I} \cdot {}^{1}\underset{\sim}{G}_{J} \qquad (2.3)$$
$$^{2}G_{IJ} = {}^{2}\underset{\sim}{G}_{I} \cdot {}^{2}\underset{\sim}{G}_{J}$$

The reciprocal base vectors are defined by the orthonormality conditions,

$$\underset{\sim}{G}_{I} \cdot \underset{\sim}{G}^{J} = \delta_{I}^{\ J},$$
$$\underset{\sim}{g}_{i} \cdot \underset{\sim}{g}^{j} = \delta_{i}^{\ j}, \text{ etc.} \qquad (2.4)$$

In order to relate components of a vector in two coordinate systems, it is useful to define the following shifters:

$$G^{i}_{\ I} = \underset{\sim}{g}^{i} \cdot \underset{\sim}{G}_{I}$$
$$G^{\alpha}_{\ I} = \bar{\underset{\sim}{g}}^{\alpha} \cdot \underset{\sim}{G}_{I} \qquad (2.5)$$
$$g^{\alpha}_{\ i} = \bar{\underset{\sim}{g}}^{\alpha} \cdot \underset{\sim}{g}_{i}$$

The shifters are two-point tensor fields, i.e., they transform as tensors with respect to the transfromation of both coordinates, e.g. X^{I} and x^{i} in the case of the shifter $G^{i}_{\ I}$.

Deformation gradients

The deformation gradient tensors are defined as tensors which operate on infinitesimal material vectors in one space to associate them to infinitesimal material vectors in another space. ${}^{2}\underset{\sim}{F}$, ${}^{1}\underset{\sim}{F}$, and $\underset{\sim}{F}$ are the deformation gradient tensors between B_0 and B_2, B_0 and B_1, and B_1 and B_2, respectively. The operations are given by

$$d\bar{\underset{\sim}{x}} = {}^{2}\underset{\sim}{F} \cdot d\underset{\sim}{X}$$
$$d\underset{\sim}{x} = {}^{1}\underset{\sim}{F} \cdot d\underset{\sim}{X} \qquad (2.6)$$
$$d\bar{\underset{\sim}{x}} = \underset{\sim}{F} \cdot d\underset{\sim}{x}$$

and the components of these deformation gradient tensors are given by

$$
\begin{aligned}
{}^{2}F^{\alpha}_{\cdot I} &= \bar{x}^{\alpha}\,\big|_{I} = \bar{x}^{\alpha}\,\big|_{i}\; x^{i}\,\big|_{I} \\
{}^{1}F^{i}_{\cdot I} &= x^{i}\,\big|_{I} \\
F^{\alpha}_{\cdot i} &= \bar{x}^{\alpha}\,\big|_{i}
\end{aligned}
\tag{2.7}
$$

where the vertical bars indicate covariant differentiation.

Strain tensors

The expressions for the Green strain are derived by considering the difference of the squares of line elements in different configurations. Denoting these as $({}^{0}ds)^{2}$, $({}^{1}ds)^{2}$ and $({}^{2}ds)^{2}$ in B_0, B_1 and B_2, respectively,

$$
\begin{aligned}
({}^{0}ds)^{2} &= d\underset{\sim}{X} \cdot d\underset{\sim}{X} = G_{IJ}\, dX^{I}\, dX^{J} \\
({}^{1}ds)^{2} &= d\underset{\sim}{x} \cdot d\underset{\sim}{x} = g_{ij}\, dx^{i}\, dx^{j} = {}^{1}G_{IJ}\, dX^{I}\, dX^{J} \\
({}^{2}ds)^{2} &= d\underset{\sim}{\bar{x}} \cdot d\underset{\sim}{\bar{x}} = \bar{g}_{\alpha\beta}\, d\bar{x}^{\alpha}\, d\bar{x}^{\beta} = {}^{2}G_{IJ}\, dX^{I}\, dX^{J}
\end{aligned}
\tag{2.8}
$$

Using the relations given by Eqs. (2.6, 7), these can be rewritten as

$$
\begin{aligned}
({}^{0}ds)^{2} &= G_{IJ}\, dX^{I}\, dX^{J} \\
({}^{1}ds)^{2} &= g_{ij}\, {}^{1}F^{i}_{\cdot I}\, {}^{1}F^{j}_{\cdot J}\, dX^{I}\, dX^{J} = {}^{1}G_{IJ}\, dX^{I}\, dX^{J} \\
({}^{2}ds)^{2} &= \bar{g}_{\alpha\beta}\, F^{\alpha}_{\cdot i}\, F^{\beta}_{\cdot j}\, {}^{1}F^{i}_{\cdot I}\, {}^{1}F^{j}_{\cdot J}\, dX^{I}\, dX^{J} = {}^{2}G_{IJ}\, dX^{I}\, dX^{J}
\end{aligned}
\tag{2.9}
$$

The Green strain tensors are defined as

$$
\begin{aligned}
2\,{}^{2}E_{IJ} &= \bar{g}_{\alpha\beta}\, F^{\alpha}_{\cdot i}\, F^{\beta}_{\cdot j}\, {}^{1}F^{i}_{\cdot I}\, {}^{1}F^{j}_{\cdot J} - G_{IJ} = {}^{2}G_{IJ} - G_{IJ} \\
2\,{}^{1}E_{IJ} &= g_{ij}\, {}^{1}F^{i}_{\cdot I}\, {}^{1}F^{j}_{\cdot J} - G_{IJ} = {}^{1}G_{IJ} - G_{IJ} \\
2\,E_{IJ} &= 2({}^{2}E_{IJ} - {}^{1}E_{IJ}) = {}^{2}G_{IJ} - {}^{1}G_{IJ}
\end{aligned}
\tag{2.10}
$$

where ${}^2E_{IJ}$, ${}^1E_{IJ}$ and E_{IJ} are components of the Green strain between B_0 and B_2, B_0 and B_1, and B_1 and B_2, respectively, with all components referred to the base vectors in B_0. If the strain increment between B_1 and B_2 is required with reference to the space B_1, one can rewrite $({}^2ds)^2$ in terms of $d\underset{\sim}{x}$, i.e.

$({}^2ds)^2 = d\bar{\underset{\sim}{x}} \cdot d\bar{\underset{\sim}{x}} = \bar{g}_{\alpha\beta}\, d\bar{x}^\alpha\, d\bar{x}^\beta$ from Eq. (2.8) is transformed to

$$({}^2ds)^2 = \bar{g}_{\alpha\beta}\, F^\alpha_{\cdot i}\, F^\beta_{\cdot j}\, dx^i\, dx^j \tag{2.11}$$

which then yields

$$2\,\varepsilon_{ij} = \bar{g}_{\alpha\beta}\, F^\alpha_{\cdot i}\, F^\beta_{\cdot j} - g_{ij} \tag{2.12}$$

Using Eqs. (2.10), this can be related to E_{IJ} as

$$E_{IJ} = {}^1F^i_{\cdot I}\, {}^1F^j_{\cdot J}\, \varepsilon_{ij} \tag{2.13}$$

The components of Green strain are next expressed in terms of displacements by deriving expressions for the metric tensors ${}^1G_{IJ}$ and ${}^2G_{IJ}$ and substituting them in Eqs. (2.10).

The equation of motion from Eq. (2.1) can be written as $\underset{\sim}{x} = \underset{\sim}{X} + {}^1\underset{\sim}{u}$ when going from B_0 to B_1. The convected base vectors ${}^1\underset{\sim}{G}$ can be expressed as

$${}^1\underset{\sim}{G}_I = \frac{\partial \underset{\sim}{x}}{\partial X^I} = \frac{\partial \underset{\sim}{X}}{\partial X^I} + \frac{\partial\, {}^1\underset{\sim}{u}}{\partial X^I}$$

or,

$${}^1\underset{\sim}{G}_I = \underset{\sim}{G}_I + {}^1u_{K|I}\, \underset{\sim}{G}^K \tag{2.14}$$

The metric tensor ${}^1G_{IJ}$ can then be obtained as

$${}^1G_{IJ} = (\underset{\sim}{G}_I + {}^1u_{K|I}\, \underset{\sim}{G}^K) \cdot (\underset{\sim}{G}_J + {}^1u_{L|J}\, \underset{\sim}{G}^L)$$

$$= G_{IJ} + \delta^K_J\, {}^1u_{K|I} + \delta_I^L\, {}^1u_{L|J} + {}^1u_{K|I}\, {}^1u_{L|J}\, G^{KL}$$

$$\therefore\ {}^{1}G_{IJ} = G_{IJ} + {}^{1}u_{J|I} + {}^{1}u_{I|J} + {}^{1}u_{K|I}\, G^{KL}\, {}^{1}u_{L|J}$$

Using the property of metric tensors with regard to the lowering and raising of the indices of vectors, one gets

$$ {}^{1}G_{IJ} = G_{IJ} + {}^{1}u_{I|J} + {}^{1}u_{J|I} + {}^{1}u_{K|I}\, {}^{1}u^{K}{}_{|J} \tag{2.15}$$

Hence, the Green strain is given as

$$2\,{}^{1}E_{IJ} = {}^{1}G_{IJ} - G_{IJ} = {}^{1}u_{I|J} + {}^{1}u_{J|I} + {}^{1}u_{K|I}\, {}^{1}u^{K}{}_{|J} \tag{2.16}$$

A similar expression can be derived for ${}^{2}E_{IJ}$, viz.,

$$2\,{}^{2}E_{IJ} = {}^{2}G_{IJ} - G_{IJ} = {}^{2}u_{I|J} + {}^{2}u_{J|I} + {}^{2}u_{K|I}\, {}^{2}u^{K}{}_{|J} \tag{2.17}$$

Since $\overset{2}{\underset{\sim}{u}} = \overset{1}{\underset{\sim}{u}} + \underset{\sim}{u}$, the expression for E_{IJ} can be derived in terms of displacements $\overset{1}{\underset{\sim}{u}}$ in the current configuration B_1 and the displacement increments $\underset{\sim}{u}$.

$$\begin{aligned} 2\,E_{IJ} &= 2({}^{2}E_{IJ} - {}^{1}E_{IJ}) \\ &= {}^{2}u_{I|J} - {}^{1}u_{I|J} + {}^{2}u_{J|I} - {}^{1}u_{J|I} \\ &\quad + {}^{2}u_{K|I}\, {}^{2}u^{K}{}_{|J} - {}^{1}u_{K|I}\, {}^{1}u^{K}{}_{|J} \\ &= u_{I|J} + u_{J|I} + ({}^{1}u_{K|I} + u_{K|I})\,({}^{1}u^{K}{}_{|J} + u^{K}{}_{|J}) \\ &\quad - {}^{1}u_{K|I}\, {}^{1}u^{K}{}_{|J} \end{aligned}$$

$$\therefore\ 2\,E_{IJ} = u_{I|J} + u_{J|I} + {}^{1}u_{K|I}\, u^{K}{}_{|J} + u_{K|I}\, {}^{1}u^{K}{}_{|J} + u_{K|I}\, u^{K}{}_{|J} \tag{2.18}$$

Defining, $2\,\hat{e}_{IJ} = u_{I|J} + u_{J|I}$

$$2\,\hat{\hat{e}}_{IJ} = {}^{1}u_{K|I}\,u^{K}{}_{|J} + u_{K|I}\,{}^{1}u^{K}{}_{|J} \tag{2.19}$$

$$2\,\eta_{IJ} = u_{K|I}\,u^{K}{}_{|J}$$

the strain increment can be written as

$$E_{IJ} = \hat{e}_{IJ} + \hat{\hat{e}}_{IJ} + \eta_{IJ} = e_{IJ} + \eta_{IJ} \tag{2.20}$$

The linear part of the strain increment is represented by

$$e_{IJ} = \hat{e}_{IJ} + \hat{\hat{e}}_{IJ} \tag{2.21}$$

and the nonlinear part is given by η_{IJ}.

During each increment the strains can be updated using

$${}^{2}E_{IJ} = {}^{1}E_{IJ} + E_{IJ} \tag{2.22}$$

or

$${}^{2}E_{IJ} = {}^{1}E_{IJ} + {}^{1}F^{i}_{\cdot I}\,{}^{1}F^{j}_{\cdot J}\,\varepsilon_{ij} \tag{2.23}$$

Strain rate, velocity, acceleration

The expression for the rate of Green strain can be written as

$${}^{1}\dot{\underset{\sim}{E}} = \frac{d}{dt}\left({}^{1}E_{IJ}\,\underset{\sim}{G}^{I}\,\underset{\sim}{G}^{J}\right) = {}^{1}\dot{E}_{IJ}\,\underset{\sim}{G}^{I}\,\underset{\sim}{G}^{J}, \tag{2.24}$$

$\underset{\sim}{G}^{I}$ and $\underset{\sim}{G}^{J}$ being fixed base vectors in B_0 and

hence independent of time.

$$\text{Define} \quad {}^{1}\dot{E}_{IJ} = \lim_{\Delta t \to 0} \frac{{}^{2}E_{IJ} - {}^{1}E_{IJ}}{\Delta t} = \lim_{\Delta t \to 0} \frac{E_{IJ}}{\Delta t} \tag{2.25}$$

For sufficiently small time increments, the Green strain increments can be expressed as

$$E_{IJ} = {}^{1}\dot{E}_{IJ}\, dt \tag{2.26}$$

The expressions for velocity and acceleration will be needed in later development, and can be written in terms of displacements as shown below.

Velocity: $\underset{\sim}{v} = \frac{d}{dt} \underset{\sim}{x}^{i} (\underset{\sim}{X},t)|_{\underset{\sim}{X}} = \text{constant}$

$$= \frac{d}{dt} (\underset{\sim}{X} + {}^{1}\underset{\sim}{u})|_{\underset{\sim}{X}} = \text{constant}$$

$$\therefore \underset{\sim}{v} = \frac{d}{dt} ({}^{1}\underset{\sim}{u}) \tag{2.27}$$

Similarly,

Acceleration: $\underset{\sim}{a} = \frac{d^2}{dt^2} ({}^{1}\underset{\sim}{u})$ (2.28)

The same equations will be valid in configuration B_2 if ${}^{1}\underset{\sim}{u}$ is replaced by ${}^{2}\underset{\sim}{u}$.

2.3 Stress

The 2nd Piola-Kirchhoff stress tensor is used in this study as it is a stress measure which is conjugate to the Green strain tensor in an energy sense. This stress tensor, ${}^{1}\underset{\sim}{S}$, in configuration B_1 has components ${}^{1}S^{IJ}$ which

are defined as forces in B_1 per unit area in the reference configuration B_0, and referred to the base vectors $\underset{\sim}{G}_I$ in B_0. On the other hand, the Cauchy stress tensor, ${}^1\underset{\sim}{T}$, in configuration B_1, has components ${}^1T^{ij}$ which are defined as forces per unit area of the deformed configuration and referred to the orthogonal base vectors $\underset{\sim}{g}_i$ in B_1. The relationship between the Cauchy and the Piola-Kirchhoff stress tensors will be required in further development and can be obtained as shown below.

Consider the stress tractions ${}^0\underset{\sim}{t}$ and ${}^1\underset{\sim}{t}$, as shown in Fig. 2.3, acting over the areas dA and da in configuration B_0 and B_1, respectively.

Using Cauchy's theorem,

$$ {}^0\underset{\sim}{t} = {}^1\underset{\sim}{S} \cdot \underset{\sim}{N} \tag{2.29} $$

$$ {}^1\underset{\sim}{t} = {}^1\underset{\sim}{T} \cdot \underset{\sim}{n} \tag{2.30} $$

where

$$ \begin{aligned} {}^1\underset{\sim}{S} &= {}^1S^{IJ}\, \underset{\sim}{G}_I\, \underset{\sim}{G}_J, \qquad \underset{\sim}{N} = N_K\, \underset{\sim}{G}^K, \\ {}^1T &= {}^1T^{ij}\, \underset{\sim}{g}_i\, \underset{\sim}{g}_j, \qquad \underset{\sim}{n} = n_k\, \underset{\sim}{g}^k, \end{aligned} \tag{2.31} $$

$\underset{\sim}{N}$ and $\underset{\sim}{n}$ being unit normals to dA and da, respectively.

The pseudo force ${}^0\underset{\sim}{t}$ on dA is defined in such a way that it has the same relation to ${}^1\underset{\sim}{t}$ that a material vector $d\underset{\sim}{X}$ at $\underset{\sim}{X}$ has to the spatial vector $d\underset{\sim}{x}$ at $\underset{\sim}{x}$, i.e.

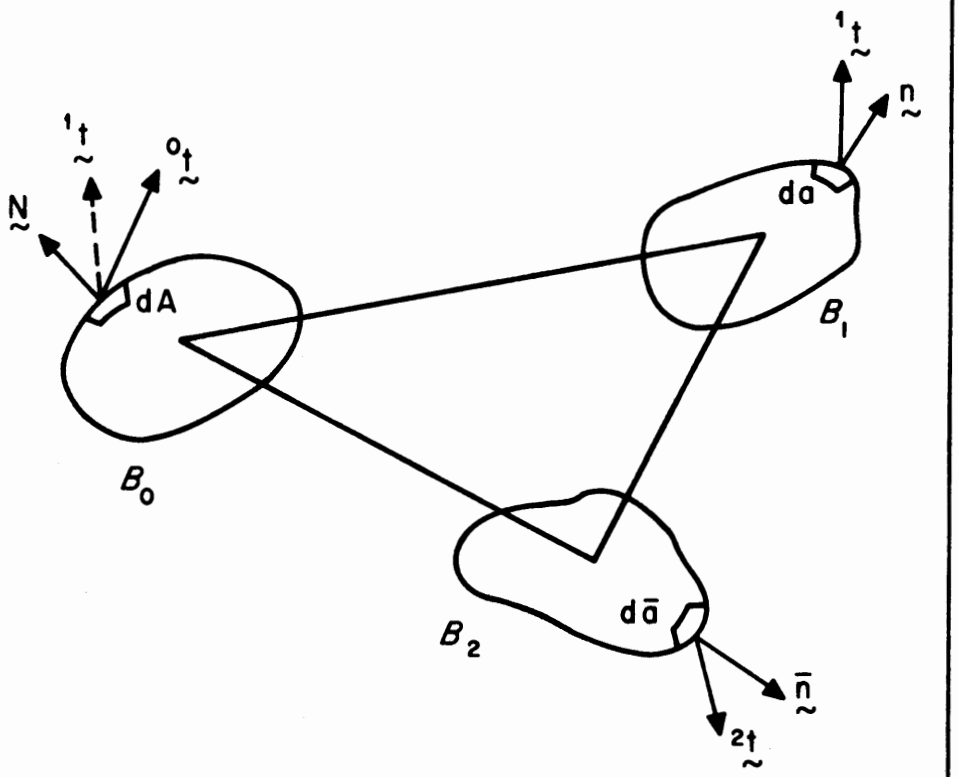

FIG. 2.3 TRACTION VECTORS AND NORMALS FOR PIOLA-KIRCHHOFF STRESS DEFINITION

$$ {}^{1}\underset{\sim}{t} = {}^{1}\underset{\sim}{F} \cdot {}^{0}\underset{\sim}{t} \tag{2.32} $$

Then,

$$ {}^{1}\underset{\sim}{t}\, da = {}^{1}\underset{\sim}{F} \cdot {}^{0}\underset{\sim}{t}\, dA \tag{2.33} $$

and, using Nanson's formula [64]

$$ \underset{\sim}{n}\, da = \frac{\rho_0}{\rho} \left({}^{1}\underset{\sim}{F}^{-1}\right)^{T} \cdot \underset{\sim}{N}\, da \tag{2.34} $$

one gets, for the left side of Eq. (2.33)

$$ {}^{1}\underset{\sim}{t}\, da = {}^{1}\underset{\sim}{T} \cdot \underset{\sim}{n}\, da = \underset{\sim}{T} \frac{\rho_0}{\rho} \left({}^{1}\underset{\sim}{F}^{-1}\right)^{T} \cdot \underset{\sim}{N}\, da \tag{2.35} $$

Substituting Eq. (2.29) into the right side of Eq. (2.33)

$$ {}^{1}\underset{\sim}{F} \cdot {}^{0}\underset{\sim}{t}\, dA = {}^{1}\underset{\sim}{F} \cdot {}^{1}\underset{\sim}{S} \cdot \underset{\sim}{N}\, dA \tag{2.36} $$

Equating Eqs. (2.35, 36), and comparing terms

$$ {}^{1}\underset{\sim}{T} \frac{\rho_0}{\rho} \left({}^{1}F^{-1}\right)^{T} = {}^{1}\underset{\sim}{F} \cdot {}^{1}\underset{\sim}{S} \tag{2.37} $$

or

$$ {}^{1}\underset{\sim}{T} = \frac{\rho}{\rho_0} {}^{1}\underset{\sim}{F} \cdot {}^{1}\underset{\sim}{S} \cdot {}^{1}\underset{\sim}{F}^{T} \tag{2.38} $$

In terms of components,

$$ {}^{1}T^{ij} = \frac{\rho}{\rho_0} {}^{1}F^{i}_{\cdot I}\, {}^{1}F^{j}_{\cdot J}\, {}^{1}S^{IJ} \tag{2.39} $$

which simplifies in Cartesian coordinates to

$$ {}^{1}T_{ij} = \frac{\rho}{\rho_0} \frac{\partial x_i}{\partial X_I} \frac{\partial x_j}{\partial X_J} {}^{1}S_{IJ} \tag{2.40} $$

The inverse relation gives Piola-Kirchhoff stresses in terms of Cauchy stresses, i.e.

$$ {}^{1}\underset{\sim}{S} = \frac{\rho_0}{\rho} \left({}^{1}\underset{\sim}{F}^{-1}\right) \cdot {}^{1}\underset{\sim}{T} \cdot \left({}^{1}\underset{\sim}{F}^{-1}\right)^{T} \tag{2.41} $$

The 2nd Piola-Kirchhoff stress tensor is symmetric whenever the Cauchy stress tensor is symmetric, i.e. ${}^{1}\underset{\sim}{S}^{IJ} = {}^{1}\underset{\sim}{S}^{JI}$, and hence preferred over the 1st Piola-Kirchhoff stress tensor (not discussed here) which is, in general, not symmetric.

Stress rates

The time rates of the Piola-Kirchhoff and Cauchy stress tensors are given by

$$ {}^{1}\dot{\underset{\sim}{S}} = \frac{d}{dt}\left({}^{1}S^{IJ}\ \underset{\sim}{G}_I\ \underset{\sim}{G}_J\right) = {}^{1}\dot{S}^{IJ}\ \underset{\sim}{G}_I\ \underset{\sim}{G}_J \tag{2.42} $$

$$ {}^{1}\dot{\underset{\sim}{T}} = \frac{d}{dt}\left({}^{1}T^{ij}\ \underset{\sim}{g}_i\ \underset{\sim}{g}_j\right) = {}^{1}\dot{T}^{ij}\ \underset{\sim}{g}_i\ \underset{\sim}{g}_j + {}^{1}T^{ij}\ \dot{\underset{\sim}{g}}_i\ \underset{\sim}{g}_j + {}^{1}T^{ij}\ \underset{\sim}{g}_i\ \dot{\underset{\sim}{g}}_j \tag{2.43} $$

The time derivative of base vectors $\underset{\sim}{g}_i$ do not vanish and remain in the rate expression for the Cauchy stress tensor.

Define $$ {}^{1}S^{IJ} = \lim_{\Delta t \to 0} \frac{{}^{2}S^{IJ} - {}^{1}S^{IJ}}{\Delta t} = \frac{S^{IJ}}{\Delta t} \tag{2.44} $$

and, for sufficiently small time increments, the increments can be expressed as

$$ S^{IJ} = {}^{1}\dot{S}^{IJ}\ dt \tag{2.45} $$

2.4 Principle of Virtual Work

An incremental variational expression will be derived to describe the motion of a body from its current configuration $\bar{B}_1$ to a neighbouring configuration B_2 in terms of the incremental state variables between B_1 and B_2, and the current states of stresses and deformations of the body in B_1. The virtual work expressions in B_1 and B_2 have to be written with respect to a common reference state. The choice of $\bar{B}_2$ as the reference state leads to an Eulerian description while the choice of B_1 leads to a relative description and that of B_0 to the Lagrangian description. Yaghmai [36] was the first to propose these approaches for large deformation analysis and adopted the relative description in his work while later Larsen [43] made use of the Lagrangian description. As stated earlier, the latter will be used in this study.

The virtual work of the external surface tractions and body forces in B_1 and B_2 during infinitesimal virtual displacements are given by

$$\delta W_2 = \int_{\partial B_2} \delta \underset{\sim}{u} \cdot {}^{2}\underset{\sim}{t}\, d\bar{a} + \int_{B_2} \bar{\rho}\, \delta \underset{\sim}{u} \cdot {}^{2}\underset{\sim}{f}\, d\bar{v} \tag{2.46}$$

$$\delta W_1 = \int_{\partial B_1} \delta \underset{\sim}{u} \cdot {}^{1}\underset{\sim}{t}\, da + \int_{B_1} \rho\, \delta \underset{\sim}{u} \cdot {}^{1}\underset{\sim}{f}\, dv \tag{2.47}$$

Using Cauchy's principle,

$${}^{2}\underset{\sim}{t} = {}^{2}\underset{\sim}{T} \cdot \bar{n}\,, \qquad {}^{1}\underset{\sim}{t} = {}^{1}\underset{\sim}{T} \cdot \underset{\sim}{n} \tag{2.48}$$

Eqs. (2.46, .47) can be written as

$$\delta W_2 = \int_{\partial B_2} \delta \underset{\sim}{u} \cdot {}^2\underset{\sim}{T} \cdot \bar{\underset{\sim}{n}}\, d\bar{a} + \int_{B_2} \bar{\rho}\, \delta \underset{\sim}{u} \cdot {}^2\underset{\sim}{f}\, d\bar{v} \qquad (2.49)$$

and

$$\delta W_1 = \int_{\partial B_1} \delta \underset{\sim}{u} \cdot {}^1\underset{\sim}{T} \cdot \underset{\sim}{n}\, da + \int_{B_1} \rho\, \delta \underset{\sim}{u} \cdot {}^1\underset{\sim}{f}\, dv \qquad (2.50)$$

Nanson's formula, Eq. (2.34), and the transformation law, Eq. (2.38), expressing Cauchy stress tensors in terms of the 2nd Piola-Kirchhoff stress tensors can now be used to obtain δW_2 and δW_1 in configuration B_0.

$$\delta W_2 = \int_{\partial B_0} \delta \underset{\sim}{u} \cdot \left(\frac{\bar{\rho}}{\rho_0}\, {}^2\underset{\sim}{F} \cdot {}^2\underset{\sim}{S} \cdot {}^2\underset{\sim}{F}^T\right) \cdot \frac{\rho_0}{\bar{\rho}} \left({}^2F^{-1}\right)^T \cdot \underset{\sim}{N}\, dA + \int_{B_0} \rho_0\, \delta \underset{\sim}{u} \cdot {}^2\underset{\sim}{f}\, dV$$

or

$$\delta W_2 = \int_{\partial B_0} \delta \underset{\sim}{u} \cdot \left({}^2\underset{\sim}{F} \cdot {}^2\underset{\sim}{S}\right) \cdot \underset{\sim}{N}\, dA + \int_{B_0} \rho_0\, \delta \underset{\sim}{u} \cdot {}^2\underset{\sim}{f}\, dV \qquad (2.51)$$

and,

$$\delta W_1 = \int_{\partial B_0} \delta \underset{\sim}{u} \cdot \left(\frac{\rho}{\rho_0}\, {}^1\underset{\sim}{F} \cdot {}^1\underset{\sim}{S} \cdot {}^1\underset{\sim}{F}^T\right) \cdot \frac{\rho_0}{\rho} \left({}^1F^{-1}\right)^T \cdot \underset{\sim}{N}\, dA + \int_{B_0} \rho_0\, \delta \underset{\sim}{u} \cdot {}^1\underset{\sim}{f}\, dV$$

or

$$\delta W_1 = \int_{\partial B_0} \delta \underset{\sim}{u} \cdot \left({}^1\underset{\sim}{F} \cdot {}^1\underset{\sim}{S}\right) \cdot \underset{\sim}{N}\, dA + \int_{B_0} \rho_0\, \delta \underset{\sim}{u} \cdot {}^1\underset{\sim}{f}\, dV \qquad (2.52)$$

The Green-Gauss theorem enabling transformation of

surface integrals to volume integrals is given as

$$\int_{\partial B_0} \underset{\sim}{b} \cdot \underset{\sim}{N}\, dA = \int_{B_0} \text{div. } \underset{\sim}{b}\, dV \tag{2.53}$$

for any vector field $\underset{\sim}{b}$. Using this theorem,

$$\delta W_2 = \int_{B_0} [(\partial_{\underset{\sim}{X}} \cdot \delta \underset{\sim}{u}) \cdot ({}^2\underset{\sim}{F} \cdot {}^2\underset{\sim}{S}) + \delta \underset{\sim}{u} \cdot \{({}^2\underset{\sim}{F} \cdot {}^2\underset{\sim}{S}) \cdot \partial_{\underset{\sim}{X}} + \rho_0\, {}^2\underset{\sim}{f}\}]\, dV \tag{2.54}$$

and,

$$\delta W_1 = \int_{B_0} [(\partial_{\underset{\sim}{X}} \cdot \delta \underset{\sim}{u}) \cdot ({}^1\underset{\sim}{F} \cdot {}^1\underset{\sim}{S}) + \delta \underset{\sim}{u} \cdot \{({}^1\underset{\sim}{F} \cdot {}^1\underset{\sim}{S}) \cdot \partial_{\underset{\sim}{X}} + \rho_0\, {}^1\underset{\sim}{f}\}]\, dV \tag{2.55}$$

The equations of motion in the reference state are given by [64]

$$\begin{aligned} ({}^2\underset{\sim}{F} \cdot {}^2\underset{\sim}{S}) \cdot \partial_{\underset{\sim}{X}} + \rho_0\, {}^2\underset{\sim}{f} &= \rho_0\, {}^2\ddot{\underset{\sim}{u}} \\ ({}^1\underset{\sim}{F} \cdot {}^1\underset{\sim}{S}) \cdot \partial_{\underset{\sim}{X}} + \rho_0\, {}^1\underset{\sim}{f} &= \rho_0\, {}^1\ddot{\underset{\sim}{u}} \end{aligned} \tag{2.56}$$

and the left sides of these equations are found in the virtual work expressions, Eqs. (2.54, 55). Replacing these by the corresponding right hand side terms from Eqs. (2.56),

$$\delta W_2 = \int_{B_0} [(\delta \underset{\sim}{u} \cdot \rho_0\, {}^2\ddot{\underset{\sim}{u}}) + (\partial_{\underset{\sim}{X}} \cdot \partial \underset{\sim}{u}) \cdot ({}^2\underset{\sim}{F} \cdot {}^2\underset{\sim}{S})]\, dV \tag{2.57}$$

$$\delta W_1 = \int_{B_0} [(\delta \underset{\sim}{u} \cdot \rho_0 \, {}^1\ddot{\underset{\sim}{u}}) + (\partial_{\underset{\sim}{X}} \cdot \partial \underset{\sim}{u}) \cdot ({}^1\underset{\sim}{F} \cdot {}^1\underset{\sim}{S})] \, dV \tag{2.58}$$

The vectors and tensors can now be replaced by their components and the expressions for δW_2 and δW_1 can be simplified.

$$\delta W_2 = \int_{B_0} [\rho_0 \, {}^2\ddot{u}_J \, \delta u_J + (\delta u_\alpha)|_K \, {}^2F^\alpha_{\cdot J} \, {}^2S^{JK}] \, dV \tag{2.59}$$

$$\delta W_1 = \int_{B_0} [\rho_0 \, {}^1\ddot{u}_J \, \delta u_J + (\delta u_i)|_K \, {}^1F^i_{\cdot J} \, {}^1S^{JK}] \, dV \tag{2.60}$$

The second terms of Eqs. (2.59, 60) need further simplification. Let $\delta\tilde{W}_2$ and $\delta\tilde{W}_1$ denote these terms, i.e.

$$\delta\tilde{W}_2 = \int_{B_0} (\delta u_\alpha)|_K \, {}^2F^\alpha_{\cdot J} \, {}^2S^{JK} \, dV \tag{2.61}$$

$$\delta\tilde{W}_1 = \int_{B_0} (\delta u_i)|_K \, {}^1F^i_{\cdot J} \, {}^1S^{JK} \, dV \tag{2.62}$$

$$\text{Now} \quad \delta(u_\alpha) = \delta\,(G_\alpha{}^M \, u_M) = G_\alpha{}^M \delta u_M, \qquad \text{and} \quad \delta(u_i) = \delta\,(G_i{}^N \, u_N) = G_i{}^M \, \delta u_N \tag{2.63}$$

as the shifters can be taken as constants during differentiation and variation. Further, since the motion is given by

$$\bar{\underset{\sim}{x}} = \underset{\sim}{x} + \underset{\sim}{u} = \underset{\sim}{X} + {}^1\underset{\sim}{u} + \underset{\sim}{u}, \text{ or } \bar{x}^\alpha = G^\alpha{}_I \, (X^I + {}^1u^I + u^I),$$

$$\text{and} \qquad \underset{\sim}{x} = \underset{\sim}{X} + {}^1\underset{\sim}{u}, \text{ or} \qquad x^i = G^i{}_I \, (X^I + {}^1u^I), \tag{2.64}$$

the deformation gradients can be expressed as

$$
\begin{aligned}
{}^{2}F^{\alpha}_{\cdot J} &= G^{\alpha}{}_{I}\ (\delta^{I}{}_{J} + {}^{1}u^{I}|_{J} + u^{I}|_{J}) \\
{}^{1}F^{i}_{\cdot J} &= G^{i}{}_{I}\ (\delta^{I}{}_{J} + {}^{1}u^{I}|_{J})
\end{aligned}
\tag{2.65}
$$

The expressions for $\delta\tilde{W}_2$ and $\delta\tilde{W}_1$ can now be rewritten, using Eqs. (2.63, 65), as

$$
\delta\tilde{W}_2 = \int_{B_0} (\delta u_M)|_K\ G_{\alpha}{}^{M}\ G^{\alpha}{}_{I}\ (\delta^{I}{}_{J} + {}^{1}u^{I}|_{J} + u^{I}|_{J})\ {}^{2}S^{JK}\ dV \tag{2.66}
$$

$$
\delta\tilde{W}_1 = \int_{B_0} (\delta u_N)|_K\ G_{i}{}^{N}\ G^{i}{}_{I}\ (\delta^{I}{}_{J} + {}^{1}u^{I}|_{J})\ {}^{1}S^{JK}\ dV \tag{2.67}
$$

But $\quad G_{\alpha}{}^{M}\ G^{\alpha}{}_{I} = \delta^{M}{}_{I}\ ; \qquad (\delta u_M)|_K\ \delta^{M}{}_{I} = (\delta u_I)|_K$

and $\quad G_{i}{}^{N}\ G^{i}{}_{I} = \delta^{N}{}_{I}\ ; \qquad (\delta u_N)|_K\ \delta^{N}{}_{I} = (\delta u_I)|_K$

Hence,
$$
\delta\tilde{W}_2 = \int_{B_0} (\delta u_I)|_K\ (\delta^{I}{}_{J} + {}^{1}u^{I}|_{J} + u^{I}|_{J})\ {}^{2}S^{JK}\ dV \tag{2.68}
$$

$$
\delta\tilde{W}_1 = \int_{B_0} (\delta u_I)|_K\ (\delta^{I}{}_{J} + {}^{1}u^{I}|_{J})\ {}^{1}S^{JK}\ dV \tag{2.69}
$$

Examining each term of Eqs. (2.68, 69), and using the symmetry property of the 2nd Piola-Kirchhoff stress tensors, one gets

$$
\begin{aligned}
(\delta u_I)|_K\ \delta^{I}{}_{J}\ {}^{2}S^{JK} &= (\delta u_J)|_K\ {}^{2}S^{JK} \\
&= \tfrac{1}{2}\ [\ (\delta u_J)_{|K}\ {}^{2}S^{JK} + (\delta u_K)|_J\ {}^{2}S^{KJ}]
\end{aligned}
$$

$$
\therefore\quad (\delta u_I)|_K\ \delta^{I}{}_{J}\ {}^{2}S^{JK} = \tfrac{1}{2}\ \delta\ (u_{J|K} + u_{K|J})\ {}^{2}S^{JK}
$$

$$
(\delta u_I)|_K\ {}^{1}u^{I}|_{J}\ {}^{2}S^{JK} = \tfrac{1}{2}\ [\ \delta u_{I|K}\ {}^{1}u^{I}|_{J} + \delta u_{I|J}\ {}^{1}u^{I}|_{K}]\ {}^{2}S^{JK}
$$

$$
\therefore\quad (\delta u_I)|_K\ {}^{1}u^{I}|_{J}\ {}^{2}S^{JK} = \tfrac{1}{2}\ \delta\ (u_{I|K}\ {}^{1}u^{I}{}_{J} + u_{I|J}\ {}^{1}u^{I}|_{K})\ {}^{2}S^{JK}
$$

$$(\delta u_I)|_K \, u^I|_J \, {}^2S^{JK} = \frac{1}{2} \left[\delta u_{I|K} \, u^I|_J + \delta u_{I|J} \, u^I|_K \right] {}^2S^{JK}$$

$$\therefore \quad (\delta u_I)|_K \, u^I|_J \, {}^2S^{JK} = \frac{1}{2} \, \delta \left(u_{I|K} \, u^I|_J \right) {}^2S^{JK}$$

Similarly,

$$(\delta u_I)|_K \, \delta^I_J \, {}^1S^{JK} = \frac{1}{2} \, \delta \left(u_{J|K} + u_{K|J} \right) {}^1S^{JK}$$

$$\text{and } (\delta u_I)|_K \, {}^1u^I|_J \, {}^1S^{JK} = \frac{1}{2} \, \delta \left(u_{I|K} \, {}^1u^I|_J + u_{I|J} \, {}^1u^I|_K \right) {}^1S^{JK}$$

Using the expressions for strain tensors shown in Eqs. (2.19), it can be seen that

$$\begin{aligned}
(\delta u_I)|_K \, \delta^I_J \, {}^2S^{JK} &= {}^2S^{JK} \, \delta \, \hat{e}_{JK} \\
(\delta u_I)|_K \, {}^1u^I|_J \, {}^2S^{JK} &= {}^2S^{JK} \, \delta \, \hat{\hat{e}}_{JK} \\
(\delta u_I)|_K \, u^I|_J \, {}^2S^{JK} &= {}^2S^{JK} \, \delta \, \eta_{IJ} \\
(\delta u_I)|_K \, \delta^I_J \, {}^1S^{JK} &= {}^1S^{JK} \, \delta \, \hat{e}_{JK} \\
(\delta u_I)|_K \, {}^1u^I|_J \, {}^1S^{JK} &= {}^1S^{IJ} \, \delta \, \hat{\hat{e}}_{JK}
\end{aligned} \tag{2.70}$$

Substituting these expressions into Eqs. (2.68, 69), taking the difference and noting that ${}^2S^{JK} = {}^1S^{JK} + S^{JK}$,

$$\delta\tilde{W}_2 - \delta\tilde{W}_1 = \int_{B_0} [S^{JK} \left(\delta\hat{e}_{JK} + \delta\hat{\hat{e}}_{JK} + \delta\eta_{JK} \right) + {}^1S^{JK} \, \delta\eta_{JK}] \, dV$$

or,

$$\delta\tilde{W}_2 - \delta\tilde{W}_1 = \int_{B_0} (S^{JK} \, \delta E_{JK} + {}^1S^{JK} \, \delta\eta_{JK}) \, dV \tag{2.71}$$

where

$$E_{JK} = \hat{e}_{JK} + \hat{\hat{e}}_{JK} + \eta_{JK} = e_{JK} + \eta_{JK} \tag{2.72}$$

Subtracting Eq. (2.60) from Eq. (2.59), the incremental virtual work expression is obtained as

$$\delta W_2 - \delta W_1 = \int_{B_0} \rho_0 \left({}^2\ddot{u}_I - {}^1\ddot{u}_I\right) \delta u_I \, dV + \delta\tilde{W}_2 - \delta\tilde{W}_1$$

or,

$$\delta W_2 - \delta W_1 = \int_{B_0} [\, \rho_0 \, \ddot{u}_I \, \delta u_I + (S^{IJ} \, \delta E_{IJ} + {}^1S^{IJ} \, \delta\eta_{IJ})] \, dV \quad (2.73)$$

In the displacement formulation of the finite element method, the first term gives rise to a consistent mass or lumped mass matrix depending on the approximation to be used, and the terms in the paranthesis give rise to the stiffness matrices.

Virtual work due to the applied loads

The incremental virtual work expression for the prescribed tractions and body forces may be obtained from Eqs. (2.46, 47) as

$$\delta W_2 - \delta W_1 = \int_{\partial B_2} \delta\underset{\sim}{u} \cdot {}^2\underset{\sim}{t} \, d\bar{a} + \int_{B_2} \bar{\rho} \, \delta\underset{\sim}{u} \cdot {}^2\underset{\sim}{f} \, d\bar{v} - \int_{\partial B_1} \delta\underset{\sim}{u} \cdot {}^1\underset{\sim}{t} \, da - \int_{B_1} \rho \, \delta\underset{\sim}{u} \cdot {}^1\underset{\sim}{f} \, dv \quad (2.74)$$

But the use of the finite element method, while ensuring global force equilibrium of the system, does not guarantee local stress equilibrium equations and gives an internal stress field that is not necessarily in equilibrium with the applied load at any instant. This lack of equilibrium can be accounted for in the load increment by using the expression for δW_1 in terms of the internal stress field instead of Eq. (2.47) in the computation of incremental work derived in Eq. (2.74).

Using the Eqs. (2.60, 69, 70 d, 70 e) it can be seen that

$$\delta W_1 = \int_{B_0} [\rho_0 \, {}^1\ddot{u}_I \, \delta u_I + {}^1S_{IJ} \, (\delta \hat{e}_{IJ} + \delta \hat{\hat{e}}_{IJ})] \, dV$$

or

$$\delta W_1 = \int_{B_0} (\rho_0 \, {}^1\ddot{u}_I \, \delta u_I + {}^1S_{IJ} \, \delta e_{IJ}) \, dV \tag{2.75}$$

Now, subtracting Eq. (2.75) from Eq. (2.46),

$$\delta W_2 - \delta W_1 = \int_{\partial B_2} \delta u_I \, {}^2t_I \, d\bar{a} + \int_{B_2} \bar{\rho} \, \delta u_I \, {}^2f_I \, d\bar{v}$$

$$- \int_{B_0} (\rho_0 \, {}^1\ddot{u}_I \, \delta u_I + {}^1S_{IJ} \, \delta e_{IJ}) \, dV \tag{2.76}$$

This general expression must now be specialized for conservative and nonconservative loading and the integrals transformed from B_2 to B_0. This problem has been discussed by Oden [18, 31] and Larsen [43], and Larsen and Popov [65, 66].

Conservative loading consists of forces which do not change direction during deformation and can be derived from a potential function. Nonconservative loads, on the other hand, do change direction such as in the case of a pressure type loading.

Nonconservative Loads

For a pressure type loading, the traction vector ${}^2\underset{\sim}{t}$ is given by

$${}^2\underset{\sim}{t} \, d\bar{a} = - \, {}^2p \, \underset{\sim}{\bar{n}} \, d\bar{a} \tag{2.77}$$

where ${}^2p$ is the pressure on the surface element $d\bar{a}$ whose outward normal is $\underset{\sim}{\bar{n}}$.

Using Nanson's formula Eq. (2.34) to transform $\bar{\underset{\sim}{n}}\, d\bar{a}$ in B_2 to $\underset{\sim}{N}\, dA$ in B_0,

$$ {}^2\underset{\sim}{t}\, d\bar{a} = - {}^2p\, \bar{\underset{\sim}{n}}\, d\bar{a} = - {}^2p\, \frac{\rho_0}{\bar{\rho}}\, ({}^2\underset{\sim}{F}^{-1})^T \cdot \underset{\sim}{N}\, dA \qquad (2.78) $$

Since ${}^2\underset{\sim}{F}^{-1}$ is defined in terms of gradients with respect to B_2 it cannot be determined directly and an approximate expression is obtained by imposing the restrictions that

i) the displacement increments $\underset{\sim}{u}$ between B_1 and B_2 are small compared to ${}^1\underset{\sim}{u}$, and

ii) the rotations associated with $\underset{\sim}{u}$ are small compared to unity.

Hence, one can assume

$$ \frac{\rho}{\bar{\rho}} \doteq 1 $$

$$ \frac{\partial}{\partial \bar{x}^J} \doteq \frac{\partial}{\partial x^J} \qquad (2.79) $$

and ${}^2\underset{\sim}{F}^{-1}$ can be written in rectangular Cartesian coordinates as

$$ {}^2F^{-1}_{IJ} = \frac{\partial X_I}{\partial \bar{x}_J} = \frac{\partial X_I}{\partial x_K} \frac{\partial x_K}{\partial \bar{x}_J} = \frac{\partial X_I}{\partial x_K} \frac{\partial}{\partial \bar{x}_J} (\bar{x}_K - u_K) $$

$$ \doteq \frac{\partial X_I}{\partial x_K} \delta_{JK} - \frac{\partial X_I}{\partial x_K} \frac{\partial X_M}{\partial x_J} \frac{\partial u_K}{\partial X_M} $$

or,

$$ {}^2F^{-1}_{IJ} \doteq \frac{\partial X_I}{\partial x_J} - \frac{\partial X_I}{\partial x_K} \frac{\partial X_M}{\partial x_J} \frac{\partial u_K}{\partial X_M} \qquad (2.80) $$

This leads to the approximate virtual work expression

$$ \delta W_2 - \delta W_1 \doteq - \int_{\partial B_0} {}^2p\, \frac{\rho_0}{\rho}\, \delta u_I \left(\frac{\partial X_J}{\partial x_I} - \frac{\partial X_J}{\partial x_K} \frac{\partial X_M}{\partial x_I} \frac{\partial u_K}{\partial X_M} \right) N_J\, dA $$

$$-\int_{B_0}(\rho_0\ {}^{1}\ddot{u}_I\ \delta u_I + {}^{1}S_{IJ}\ \delta e_{IJ})\ dV$$

$$+\int_{B_0}\rho_0\ {}^{2}f_I\ \delta u_I\ dV \qquad (2.81)$$

The second term in the paranthesis of the integrand in the surface integral is linear in the displacement increment $\underset{\sim}{u}$ and will give rise to an additional stiffness term. It should be noted that this term is nonsymmetric and usually neglected for most engineering applications because its effect on the total stiffness of the system is negligible and the additional computational effort needed to solve a set of equations with an unsymmetric coefficient matrix is significant. However, it is essential to include this term in cases where both the strains and rotations are large, as in the case of pneumatic structures.

Conservative Loads

In the case of conservative loading, the loads are usually given in terms of vectors with fixed directions in space. A difficulty arises in the transformation of these loads from B_2 to B_0 due to the lack of transformation rules for such vectors. This was overcome by Larsen [65, 66] who suggested that the load be redefined in terms of the convected base vectors in B_2, i.e. ${}^{2}\underset{\sim}{G}_I$, which are governed by known transformation rules, e.g.,

$${}^{2}\underset{\sim}{G}_I = ({}^{2}F^{-1})_{JI}\ {}^{0}\underset{\sim}{G}_J \qquad (2.82)$$

where ${}^{0}\underset{\sim}{G}_J \equiv \underset{\sim}{G}_J$ is the set of base vectors in B_0 as defined in section 2.2. For gravity load vector ${}^{2}\underset{\sim}{q}$, whose norm and direc-

tion are known, one then obtains

$$\bar{\rho}\ {}^{2}\underset{\sim}{f}\ d\bar{v} = \bar{\rho}\ {}^{2}q_I\ {}^{2}\underset{\sim}{G}_I\ d\bar{v} = \rho_0\ {}^{2}q_I\ ({}^{2}F^{-1})_{JI}\ {}^{0}\underset{\sim}{G}_J\ dV \qquad (2.83)$$

where the components ${}^{2}q_I$ of the gravity loads relative to the convected base vectors ${}^{2}\underset{\sim}{G}_I$ are deformation dependent and must be computed in B_2. For the surface traction vector ${}^{2}\underset{\sim}{t}$, the load intensities change according to the ratio $d\bar{a}/dA$. Thus, ${}^{2}\bar{\underset{\sim}{t}}\ dA = {}^{2}\underset{\sim}{t}\ d\bar{a}$ defines ${}^{2}\bar{\underset{\sim}{t}}$, the traction vector in B_2 measured per unit area in B_0. For most structures the distinction between ${}^{2}\underset{\sim}{t}$ and ${}^{2}\bar{\underset{\sim}{t}}$ is insignificant. Once again, the norm and direction of the vector ${}^{2}\bar{\underset{\sim}{t}}$ are known and its components ${}^{2}\bar{t}_I$ relative to ${}^{2}\underset{\sim}{G}_I$ must be computed. Then one obtains

$${}^{2}\bar{t}_I\ {}^{2}\underset{\sim}{G}_I\ dA = {}^{2}\bar{t}_I\ ({}^{2}F^{-1})_{JI}\ {}^{0}\underset{\sim}{G}_J\ dA$$

As in the case of nonconservative loading discussed earlier, the deformation gradient ${}^{2}\underset{\sim}{F}^{-1}$ cannot be obtained directly and approximations must be introduced. The final expression for the incremental virtual work in the case of conservative loading is obtained as

$$\begin{aligned}\delta W_2 - \delta W_1 = &\int_{\partial B_0} \delta u_I\ {}^{2}\bar{t}_J \left(\frac{\partial X_I}{\partial x_J} - \frac{\partial X_I}{\partial x_K}\frac{\partial X_M}{\partial x_J}\frac{\partial u_K}{\partial X_M}\right) dA \\ &+\int_{B_0} \delta u_I\ \rho_0\ {}^{2}q_J \left(\frac{\partial X_I}{\partial x_J} - \frac{\partial X_I}{\partial x_K}\frac{\partial X_M}{\partial x_J}\frac{\partial u_K}{\partial X_M}\right) dV \\ &-\int_{B_0} (\rho_0\ \ddot{u}_I\ \delta u_I + {}^{1}S_{IJ}\ \delta\ e_{IJ})\ dV \qquad (2.84)\end{aligned}$$

2.5 Incremental Constitutive Equations in Elasticity

The incremental virtual work expressions derived in the previous section are not restricted to any particular constitutive law of material behavior. For an elastic continuum, the constitutive laws assume rather simple forms and this section presents the incremental equations in terms of the Green strain tensor and the 2nd Piola-Kirchhoff stress tensor.

A strain energy function W, per unit mass in the undeformed configuration, exists for hyperelastic materials and is a function of the Green strain tensor. As a consequence of the law of conservation of energy, it can be shown that

$$ {}^{2}S^{IJ} = \rho_0 \frac{\partial\, {}^{2}W}{\partial\, {}^{2}E_{IJ}} \qquad (2.85) $$

and

$$ {}^{1}S^{IJ} = \rho_0 \frac{\partial\, {}^{1}W}{\partial\, {}^{1}E_{IJ}} $$

where ${}^{2}W$ and ${}^{1}W$ are the strain energies in configurations B_2 and B_1, respectively. Assuming that W may be expressed as a polynomial function of the strains,

$$ \rho_0\, {}^{i}W = C^{IJ}\, {}^{i}E_{IJ} + \tfrac{1}{2} C^{IJKL}\, {}^{i}E_{IJ}\, {}^{i}E_{KL} + \tfrac{1}{3} C^{IJKLMN}\, {}^{i}E_{IJ}\, {}^{i}E_{KL}\, {}^{i}E_{MN} + \cdots\cdots $$

Taking derivatives with respect to ${}^{i}E_{IJ}$, one gets

$$ {}^{i}S^{IJ} = C^{IJ} + C^{IJKL}\, {}^{i}E_{KL} + C^{IJKLMN}\, {}^{i}E_{KL}\, {}^{i}E_{MN} + \cdots\cdot $$

As a consequence of the material being assumed elastic, C^{IJ} must vanish and linear elastic behavior demands that C^{IJKLMN} and all higher order terms must be taken as zero. Hence, for linear elastic material,

$$\rho_0 \, {}^{i}W = \frac{1}{2} C^{IJKL} \, {}^{i}E_{IJ} \, {}^{i}E_{KL}$$
$$(2.86)$$
$${}^{i}S^{IJ} = C^{IJKL} \, {}^{i}E_{KL}$$

The incremental constitutive relationship then takes the form

$$({}^{2}S^{IJ} - {}^{1}S^{IJ}) = C^{IJKL} \, ({}^{2}E_{KL} - {}^{1}E_{KL}) \qquad (2.87)$$

or

$$S^{IJ} = C^{IJKL} \, E_{KL}$$

where

$$C^{IJKL} = \mu \, (\delta^{IK} \, \delta^{JL} + \delta^{IL} \, \delta^{JK}) + \lambda \, \delta^{IJ} \, \delta^{KL}$$

for an isotropic, linear elastic material. λ and μ are the Lamé constants,

$$\lambda = \frac{\nu E}{(1+\nu)(1-2\nu)} \qquad \mu = \frac{E}{2(1+\nu)}$$

where ν = Poisson's ratio.

2.6 Modification of the Virtual Work Expression for Viscoplasticity

The application of the virtual work expressions derived in section 2.4 for viscoplastic material behavior is straightforward and based on the following assumptions:

i) The additive decomposition law is valid for the Green

strain rate tensor, i.e.

$$\dot{E}_{IJ} = \dot{E}^{I}_{IJ} + \dot{E}^{VP}_{IJ} \tag{2.88}$$

where $\dot{E}^{I}_{IJ}$, the instantaneous strain rate, and $\dot{E}^{VP}_{IJ}$, the viscoplastic strain rate, are assumed to be defined by constitutive relations. For sufficiently small time steps, a similar equation is valid for the strain increments.

ii) There exists a linear relationship between the increment of P-K stress and the instantaneous strain increment, i.e.

$$S_{IJ} = C_{IJKL}\, E^{I}_{KL} \tag{2.89}$$

Although the additive decomposition of the strain rates is not the only method of decomposing kinematic variables, it is the most convenient form for use in Lagrangian description. While these component strain rates do not in general satisfy kinematics, they are obtained directly from constitutive equations formulated so as to satisfy the principles of thermodynamics, and given the same invariance properties as the total strain rate. A comparative discussion of the many different approaches adopted for the kinematic decomposion of finite inelastic deformations has been presented by Larsen [43].

In viscoplasticity, the instantaneous strain E^{I}_{IJ} equals the elastic strain E^{E}_{IJ}. In the case of problems involving classical inviscid plasticity, E^{VP}_{IJ} equals zero, and the instantaneous strain rate is decomposed into elastic and plastic strain rates, i.e.

$$\dot{E}_{IJ} = \dot{E}^{I}_{IJ} = \dot{E}^{E}_{IJ} + \dot{E}^{P}_{IJ} \tag{2.90}$$

The viscoplastic strain rate is assumed to be independent of the stress rate and is considered as an initial strain increment in the virtual work expressions. Combining Eqs. (2.88, 89) gives

$$S_{IJ} = C_{IJKL}\,(E_{KL} - E^{VP}_{KL}) = S^{I}_{IJ} - S^{VP}_{IJ} \tag{2.91}$$

where

$$S^{I}_{IJ} = C_{IJKL}\,E_{KL}$$

and (2.92)

$$S^{VP}_{IJ} = C_{IJKL}\,E^{VP}_{KL}$$

may be defined as the "instantaneous" and "viscoplastic" stress increments, respectively, possessing the same invariance properties as S_{IJ}. The virtual work expression, Eq. (2.73), can now be modified for viscoplasticity problems by the substitution into it of Eq. (2.91) for the stress increment S_{IJ}, which results in

$$\begin{aligned}\delta W_2 - \delta W_2 &= \int_{B_0}[\rho_0\,\ddot{u}_I\,\delta u_I + (S^{I}_{IJ} - S^{VP}_{IJ})\,\delta E_{IJ} + {}^{1}S_{IJ}\,\delta\eta_{IJ}]\,dV \\ &= \int_{B_0}(\rho_0\,\ddot{u}_I\,\delta u_I + S^{I}_{IJ}\,\delta E_{IJ} - S^{VP}_{IJ}\,\delta e_{IJ} - S^{VP}_{IJ}\,\delta\eta_{IJ} \\ &\qquad + {}^{1}S_{IJ}\,\delta\eta_{IJ})\,dV\end{aligned}$$

$$\therefore\quad \delta W_2 - \delta W_2 = \int_{B_0}[\rho_0\,\ddot{u}_I\,\delta u_I + S^{I}_{IJ}\,\delta E_{IJ} + ({}^{1}S_{IJ} - S^{VP}_{IJ})\,\delta\eta_{IJ} - S^{VP}_{IJ}\,\delta e_{IJ}]\,dV \tag{2.93}$$

Comparison of Eq. (2.93) with Eq. (2.73) reveals two changes arising from the consideration of the viscoplastic strain. The

last term in the integrand of Eq. (2.93) gives rise to a viscoplastic pseudo-loading term. Also, the initial stresses caused by the viscoplastic strains make a contribution to the geometric stiffness of the system.

3. INCREMENTAL CONSTITUTIVE RELATIONS FOR PLASTICITY AND VISCOPLASTICITY

3.1 Incremental Theory of Plasticity

The mathematical theory of plasticity is divided into two subclasses - one which treats the deformations in a material to be path-independent and relates the total plastic strain components to the current state of stress; the other which is an incremental theory and relates the increments of plastic strain to the increments of stress, the current state of stress and the accumulated plastic strains. The former, referred to as the deformation (or Hencky) theory, is similar to nonlinear elasticity except for the concept of elastic unloading in the plastic region, while the latter, referred to as the flow or incremental theory, is a path-dependent theory and necessitates integration along the loading path to determine the total strains. The two theories can be shown to be equivalent in the case of proportional or radial loading where ratios between the stress components remain unchanged during the deformation process. For nonradial loading, however, it has been established that the deformation theory is inadequate, especially during load reversals, and superior results are obtained through the use of the flow theory. Finally, although the deformation theory is the more tractable of the two from the analytical point of view, the flow theory can be employed without difficulty in the solution of problems using the incremental techniques of numerical analysis and is used in

this investigation.

In flow theory, the response of an elastic-plastic material is governed by three conditions [71]:

i) initial yield condition

ii) flow rule

iii) hardening rule

The initial yield condition specifies the state of stress for which plastic flow sets in, the flow rule relates the plastic strain increments to the stresses, stress increments and plastic strains, and the hardening rule governs the modification of the yield function during the deformation process.

Although many mathematical forms have been proposed for the yield condition, the most general representations express the initial yield function as a surface in the stress space, convex and containing the origin. The extension of the infinitesimal theory of plasticity to the special case of small strains, large rotations is based on the use of the 2nd Piola-Kirchhoff stress and the postulate that the physical components of the Cauchy stress tensor in surface coordinates of the deformed shell are approximately equal to the components of the P-K stress in the undeformed configuration [43]. It follows from this that the mathematical representation of the yield function is the same in both the Cauchy and P-K stress spaces.

Consider a deformable body, in its current configuration B_1 at time t, as it moves through the deformation space

from an initial configuration B_0 to a "final" configuration B_2 (see Fig. 2.1). The yield condition in this current configuration B_1 may be expressed as

$$f({}^1S_{IJ},\ {}^1E^P_{IJ},\ H) = 0 \tag{3.1}$$

where H is the hardening parameter depending on the entire history of motion of the body, and the plastic strain tensor ${}^1E^P_{IJ}$ is obtained through the use of constitutive relations and not from the kinematics of deformation.

The initial yield surface is only a function of the stress. In the case of initially isotropic materials it reduces to a function of invariants of the stress tensor. Further, since hydrostatic pressure of the order of the yield stress does not affect the yielding and plastic deformation of metals [67], the yield condition can be written as

$$F(J_2,\ J_3) = k \tag{3.2}$$

where k is a constant, and J_2 and J_3 are the second and third invariants of the deviatoric stress tensor ${}^1\bar{S}_{IJ}$ defined as

$${}^1\bar{S}_{IJ} = {}^1S_{IJ} - \frac{1}{3}\ {}^1S_{KK}\ \delta_{IJ} \tag{3.3}$$

and

$$J_1 = {}^1\bar{S}_{II} = 0$$

$$J_2 = \frac{1}{2} {}^1\bar{S}_{IJ} {}^1\bar{S}_{IJ} \tag{3.4}$$

$$J_3 = \frac{1}{3} {}^1\bar{S}_{IJ} {}^1\bar{S}_{JK} {}^1\bar{S}_{KI}$$

Experimental evidence indicates that the yield condition can be approximated by the von Mises yield criterion [68,69]

$$F({}^1S_{IJ}) = F(J_2) = J_2 = k^2 \tag{3.5}$$

where

k = initial yield stress in pure shear.

Using the isotropic hardening law, the subsequent yield surfaces, also referred to as the loading surfaces, can be written as

$$f = F({}^1S_{IJ}) - H({}^1E^P_{IJ}) = 0 \tag{3.6}$$

This hardening law implies that the shape of the yield surface remains unchanged but undergoes uniform expansion in stress space, Fig. 3.1(a). The Bauschinger effect is not accounted for by this law; in fact, it predicts a negative Bauschinger effect. To account for this, one may use the kinematic hardening rule suggested by Prager [70] or the modification of it proposed by Ziegler [71]. In the case of Prager's kinematic hardening rule, Fig. 3.1(b), the initial yield surface is translated in the direction of the increment of strain, i.e.,

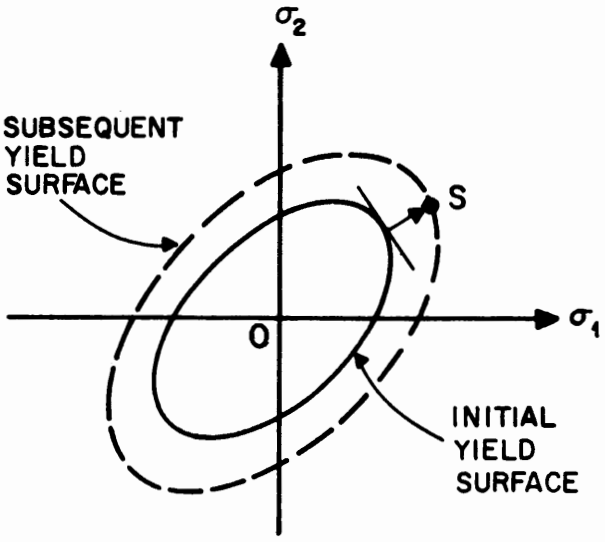

(a) ISOTROPIC HARDENING

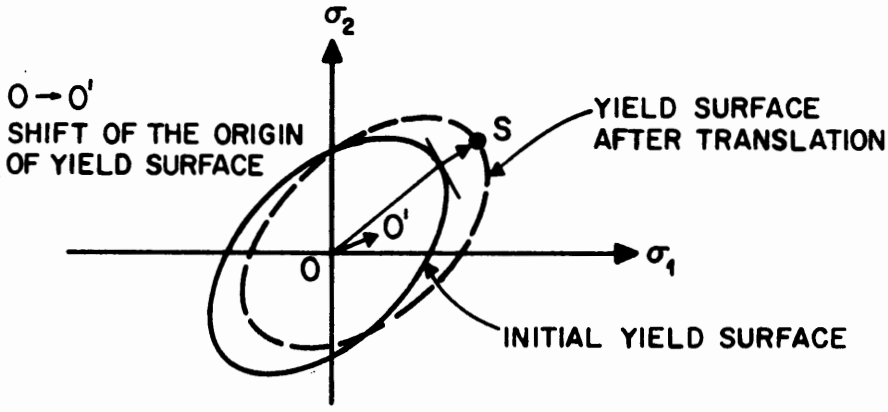

(b) KINEMATIC HARDENING

FIG.3.1 HARDENING LAWS IN PLASTICITY

$$\alpha_{IJ} = c\, E^{P}_{IJ}$$

and (3.7)

$$^{2}\alpha_{IJ} = {}^{1}\alpha_{IJ} + \alpha_{IJ}$$

where the parameter c is determined experimentally and α_{IJ} is a tensor representing the incremental translation of the yield surface. The loading surfaces can then be represented as

$$f = F(^{1}S_{IJ} - {}^{1}\alpha_{IJ}) = 0 \qquad (3.8)$$

It must be noted that the use of a constant parameter c, termed the hardening co-efficient, in Eq. (3.7), regardless of the state of stress, restricts the kinematic hardening law to linear hardening materials. Although some empirical methods have been proposed [72,73] for obtaining a variable hardening co-efficient for nonlinear hardening, there exists no theoretically established procedure for the evaluation of this parameter and further research must be directed toward this subject. This study makes use of the isotropic hardening law alone and the presentation that follows is based on this rule.

The hardening parameter H for isotropic hardening may also be written as

$$H(^{1}E^{P}_{IJ}) = H(\kappa_p) \qquad (3.9)$$

where two measures of hardening are possible for κ_p. The

work-hardening parameter is given by

$$\kappa_P = \kappa_P\left(\int_0^{{}^1E^P_{IJ}} dW_P\right) \tag{3.10}$$

where the increment of plastic work is given by

$$dW_P = {}^1S_{IJ}\ {}^1\dot{E}^P_{IJ}\ dt = {}^1S_{IJ}\ E^P_{IJ} \tag{3.11}$$

while the strain-hardening parameter is expressed as

$$\kappa_P = \kappa_P\left(\int_0^{{}^1E^P_{IJ}} d\bar{\varepsilon}^P\right) \tag{3.12}$$

where the equivalent plastic strain is defined as

$$d\bar{\varepsilon}^P = \left(\frac{2}{3} E^P_{IJ}\ E^P_{IJ}\right)^{\frac{1}{2}} \tag{3.13}$$

Both of these measures are identical for isotropic hardening [74]. The form of the function κ_P is determined from some experiment, e.g., a simple uniaxial tension test may be used.

Assuming the existence of a plastic potential g, the flow law is given as

$${}^1\dot{E}^P_{IJ} = \dot{\lambda}\ \frac{\partial g}{\partial\ {}^1S_{IJ}} \tag{3.14}$$

where $\dot{\lambda}$ is a non-negative scalar. As a result of Drucker's normality rule which asserts that the incremental plastic strain vector is normal to the yield surface, the plastic potential g is taken to be the same as the yield function f and Eq. (3.14)

becomes

$$ {}^{1}\dot{E}^{P}_{IJ} = \dot{\lambda} \frac{\partial f}{\partial {}^{1}S_{IJ}} \tag{3.15} $$

which is then referred to as the associated flow rule.

During loading from one plastic state to another, the consistency condition df = 0 is imposed on the yield function. Since f is a function of ${}^{1}S_{IJ}$ and ${}^{1}E^{P}_{IJ}$, from Eq. (3.6), this gives

$$ df = \frac{\partial f}{\partial {}^{1}S_{IJ}} S_{IJ} + \frac{\partial f}{\partial {}^{1}E^{P}_{IJ}} E^{P}_{IJ} = 0 \tag{3.16} $$

The plastic strain increment E^{P}_{IJ} can be determined from Eq. (3.15) if the proportionality factor $\dot{\lambda}$ can be determined,

$$ E^{P}_{IJ} = d({}^{1}E^{P}_{IJ}) = \dot{\lambda}\, dt \frac{\partial f}{\partial {}^{1}S_{IJ}} = d\lambda \frac{\partial f}{\partial {}^{1}S_{IJ}} \tag{3.17} $$

The generalized Hooke's law is given as

$$ S_{IJ} = E_{IJKL} (E_{KL} - E^{P}_{KL}) \tag{3.18} $$

where

$$ E_{IJKL} = \mu(\delta_{IK}\delta_{JL} + \delta_{IL}\delta_{JK}) + \lambda\delta_{IJ}\delta_{KL} \tag{3.19} $$

and μ, λ are the Lame constants defined in section 2.5. Substituting Eq. (3.18) into Eq. (3.16), one gets

$$ df = \frac{\partial f}{\partial {}^{1}S_{IJ}} E_{IJKL} (E_{KL} - E^{P}_{KL}) + \frac{\partial f}{\partial {}^{1}E^{P}_{IJ}} E^{P}_{IJ} = 0 \tag{3.20} $$

Now, using the flow rule, Eq. (3.17), for the plastic strain

increments in Eq. (3.20), one gets

$$\frac{\partial f}{\partial {}^{I}S_{IJ}} E_{IJKL} \left(E_{KL} - d\lambda \frac{\partial f}{\partial {}^{I}S_{KL}}\right) + d\lambda \frac{\partial f}{\partial {}^{I}E^{P}_{IJ}} \frac{\partial f}{\partial {}^{I}S_{IJ}} = 0 \quad (3.21)$$

which can then be solved for $d\lambda$,

$$d\lambda = h\, E_{IJKL} \frac{\partial f}{\partial {}^{I}S_{IJ}} E_{KL} \quad (3.22)$$

where

$$h^{-1} = \frac{\partial f}{\partial {}^{I}S_{IJ}} \frac{\partial f}{\partial {}^{I}S_{KL}} E_{IJKL} - \frac{\partial f}{\partial {}^{I}S_{IJ}} \frac{\partial f}{\partial {}^{I}E^{P}_{IJ}} \quad (3.23)$$

Substitution of Eq. (3.22) into Eq. (3.17) gives

$$E^{P}_{IJ} = A_{IJKL} E_{KL} \quad (3.24)$$

where

$$A_{IJKL} = h \frac{\partial f}{\partial {}^{I}S_{IJ}} \frac{\partial f}{\partial {}^{I}S_{MN}} E_{MNKL} \quad (3.25)$$

This gives an expression for the plastic strain increments in terms of the strain increments. Finally, substituting Eq. (3.24) into the generalized Hooke's law, Eq. (3.18), the incremental stress-strain law is obtained as

$$S_{IJ} = C_{IJKL} E_{KL} \quad (3.26)$$

where

$$C_{IJKL} = E_{IJKL} - E_{IJMN} A_{MNKL} \quad (3.27)$$

For von Mises yield criterion and isotropic hardening, the partial derivatives are given by [38]

$$\frac{\partial f}{\partial {}^1S_{IJ}} = \frac{3}{2\bar{\sigma}} {}^1\bar{S}_{IJ}$$

$$\frac{\partial f}{\partial {}^1E^P_{IJ}} = \frac{\partial f}{\partial \bar{\varepsilon}^P} \frac{\partial \bar{\varepsilon}^P}{\partial W_P} \frac{\partial W_P}{\partial {}^1E^P_{IJ}} = -\frac{1}{\bar{\sigma}} H' {}^1S_{IJ} \tag{3.28}$$

where

$$\bar{\sigma} = \text{equivalent stress} = \sqrt{3J_2} \tag{3.29}$$

and $H' = \dfrac{\partial f}{\partial \bar{\varepsilon}^P}$ can be determined from a uniaxial tension test, Fig. 3.2. It can be shown that

$$\frac{1}{H'} = \frac{1}{E_t} - \frac{1}{E} \tag{3.30}$$

Defining $\zeta = E_t/E$, one can get [38]

$$h = \frac{1}{3\mu+H'} = \frac{2(1+\nu)(1-\zeta)}{E[3-\zeta(1-2\nu)]} \tag{3.31}$$

Eq. (3.25, 27) can then be simplified to

$$A_{IJKL} = \frac{9\mu h}{2\bar{\sigma}^2} {}^1\bar{S}_{IJ} {}^1\bar{S}_{KL} \tag{3.32}$$

and

$$C_{IJKL} = \mu(\delta_{IK}\delta_{JL} + \delta_{IL}\delta_{JK}) + \lambda\delta_{IJ}\delta_{KL} - 9\mu^2 h {}^1\bar{S}_{IJ} {}^1\bar{S}_{KL} / \bar{\sigma}^2 \tag{3.33}$$

These equations will have to be modified for the generalized

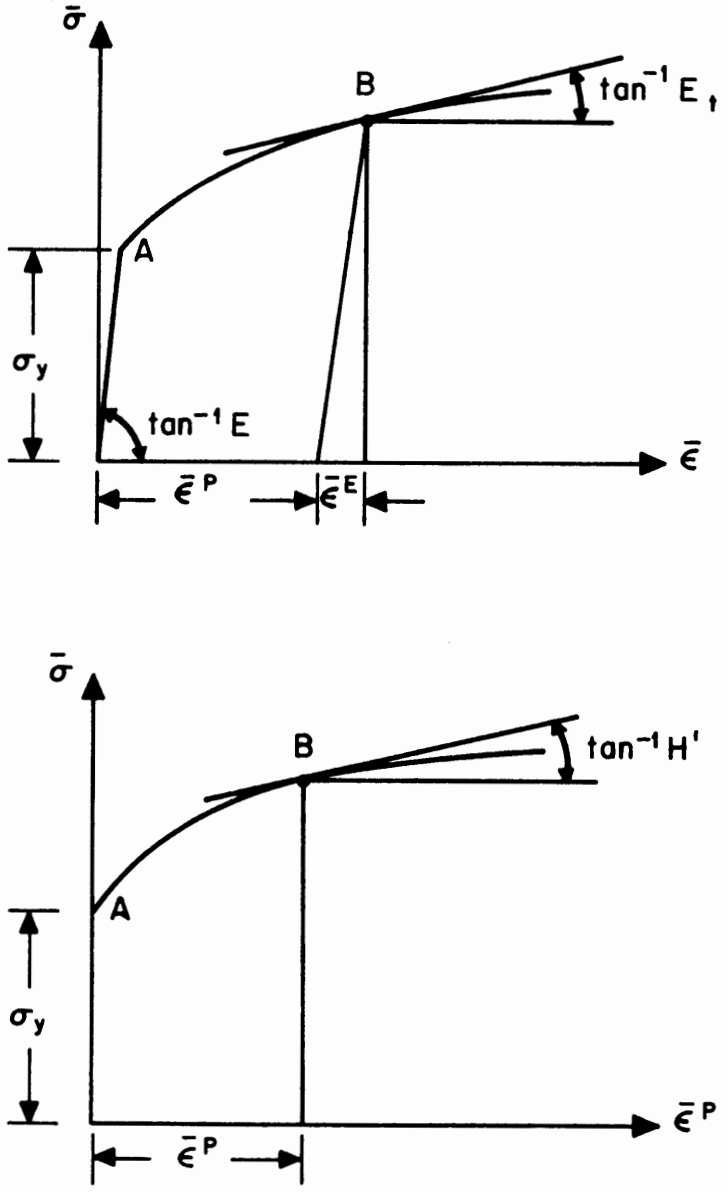

FIG.3.2 UNIAXIAL STRESS – STRAIN CURVES

plane stress state used in the analysis of shells.

In addition to the constitutive relations, it is also necessary to have criteria for loading and unloading in the incremental solution procedure. Three types of behavior are recognized and are termed

i) Loading,

ii) Neutral loading, and

iii) Unloading.

The state of stress is examined to see if $f < 0$ or $f = 0$, the former indicating an elastic state and the latter a plastic state; $f > 0$ constitutes an inadmissible state.

The three paths associated with the plastic state are characterized by

$$\dot{f} \gtrless 0$$

or (3.34)

$$\frac{\partial f}{\partial {}^{1}S_{IJ}} \, {}^{1}\dot{S}_{IJ} \gtrless 0$$

Loading is a change from one plastic state to another accompanied with strain hardening; $f = 0$, $\dot{f} > 0$.

Unloading is said to occur when the plastic strain rate reduces to zero (${}^{1}\dot{E}^{P}_{IJ} = 0$); $f = 0$, $\dot{f} < 0$.

Neutral loading is a change from one plastic state to another without any change in the plastic strain rate; $f = 0$, $\dot{f} = 0$.

3.2 Constitutive Theories for Viscoplasticity

3.2.1 General

The classical theories of plasticity are restricted to inviscid media so that time effects may be disregarded. As such, these theories are inadequate for dealing with the many practical problems involving highly strain rate sensitive material behavior. There have been numerous experimental investigations to study the behavior of materials under high rates of loading, providing useful information in the development of constituitve theories. Most metals exhibit some degree of rate sensitivity in their stress-strain relations depending on several factors like crystalline structure, magnitude of strain rate and temperature. In the case of metals with face centered cubic (FCC) structure as in Aluminum, there is no appreciable strain rate effect over a large strain rate region and temperature variation, but beyond about 10^{4} sec.$^{-1}$ pure Aluminum exhibits considerable increase in yield stress over the static value. But metals with body centered cubic (BCC) structure are fairly rate sensitive over a large range of strain rates. For example, steel has an athermal zone between 300 to 400° F. but shows considerable rate sensitivity at lower temperatures; the yield stress of mild steel increases by a factor of 2.5 over a range of 10^{-6} to 10^{2} sec.$^{-1}$ in strain rate [75].

Many attempts have been made to formulate constitutive laws for rate sensitive materials, motivated primarily by the need to study elastic-plastic wave propagation and permanent

deformation of structures subjected to blast or impact loadings, as for example in the explosive forming of metal parts, projectile impact on armor plates, etc. There is also a class of problems for which strain rate effects may be important although the inertia terms remain small.

3.2.2 Flow Theory for Viscoplasticity

The uniaxial behavior of viscoplastic materials was described by Malvern [76] in terms of reference, static stress-strain functions. The viscoplastic strain rate was considered to be proportional to the excess stress above this reference, the proprotionality factor being a function of the material viscosity. Lubliner [77] proposed a quasi-linear differential form of constitutive equation that contained as special cases the rate-dependent theories of Sokolovsky [78] and Malvern [76] as well as the rate-independent theories of von Karman [79], Rakhmatulin [80], and Taylor [81]. Also, Lubliner modified Malvern's theory by imposing a limiting maximum dynamic stress-strain curve. Perzyna [82] gave a multi-axial form of Malvern's law by the generalization of a more restricted viscoplastic law introduced by Hohenemeser and Prager [83]. Perzyna and Wojno [84] extended the multiaxial theory to finite strains. The basic assumption of all these theories is that viscoplastic deformations occur only when a certain threshold static yield surface is exceeded below which the response is purely elastic. Linearized versions of

of these viscoplastic laws have been used for the analytical solution of some simple cases [85,86] but more complex problems may be considered by the use of numerical techniques such as the finite element methods.

Following Perzyna, the viscoplastic strain rate is assumed to be given by

$$ {}^{1}\dot{E}_{IJ}^{VP} = \bar{\gamma} < \Phi\ (F) > \frac{\partial F}{\partial\ {}^{1}S_{IJ}} \tag{3.35} $$

where

$\bar{\gamma}$ is a material viscosity co-efficient and

F is a scalar yield function.

In terms of the static loading surface, Eq. (3.6), the function F is expressed as

$$ F = \frac{F({}^{1}S_{IJ}) - H({}^{1}E_{IJ}^{VP})}{H({}^{1}E_{IJ}^{VP})} = \frac{f}{H} \tag{3.36} $$

The expression for the viscoplastic strain rate, Eq. (3.35), assumes that the material obeys the von Mises yield criterion with isotropic hardening and the associated flow rule for static deformations, and Eq. (3.36) implies that the viscoplastic strain rate depends on the amount by which the static loading surface is exceeded. The notation < > in Eq. (3.35) means that

$$ < \Phi\ (F) > = \begin{cases} \Phi\ (F) & \text{when } \Phi\ (F) > 0 \\ 0 & \text{when } \Phi\ (F) \leq 0 \end{cases} \tag{3.37} $$

In other words, viscoplastic deformation occurs only when $\Phi(F)$ exceeds zero. Different functional forms have been proposed for Φ [87] to describe the process and the simplest form is chosen in this study,

$$\Phi(F) = F \tag{3.38}$$

It should be noted that $F > 0$ constitutes an inadmissible state in the theory of inviscid plasticity, the plastic state being identified by $F = 0$, but in viscoplasticity $F > 0$ is admissible and indicates viscoplastic flow. Using Eqs. (3.28, 36, 38) in Eq. (3.35), one obtains

$$\overset{1}{E}{}^{VP}_{IJ} = \bar{\gamma}\left(\frac{\sqrt{3J_2} - H}{H}\right)\frac{3\ \overset{1}{S}_{IJ}}{2\sqrt{3J_2}}$$

$$= \frac{\sqrt{3}}{2}\ \frac{\bar{\gamma}}{H/\sqrt{3}}\ \left(\frac{\sqrt{3J_2} - H}{\sqrt{3J_2}}\right)\ \overset{1}{S}_{IJ}$$

or,

$$\overset{1}{E}{}^{VP}_{IJ} = \begin{cases} \dfrac{\gamma}{H/\sqrt{3}}\left(1 - \dfrac{H}{\sqrt{3J_2}}\right)\overset{1}{S}_{IJ} & \text{when } \dfrac{\sqrt{3J_2}}{H} - 1 > 0 \\ 0 \quad \text{when } \dfrac{\sqrt{3J_2}}{H} - 1 \leq 0 \end{cases} \tag{3.39}$$

where $\gamma = \dfrac{\sqrt{3}}{2}\bar{\gamma}$

A dynamic yield criterion can be obtained by squaring both sides of Eq. (3.39).

$$ {}^{1}\dot{E}^{VP}_{IJ}\ {}^{1}\dot{E}^{VP}_{IJ} = \frac{\gamma^2}{H^2/3}\left(1 - \frac{H}{\sqrt{3J_2}}\right)^2 {}^{1}\bar{S}_{IJ}\ {}^{1}\bar{S}_{IJ} $$

or,

$$ I_2 = \frac{\gamma^2}{H^2/3}\left(1 - \frac{H}{\sqrt{3J_2}}\right)^2 J_2 $$

or,

$$ \sqrt{I_2} = \frac{\gamma}{H/\sqrt{3}}\left(1 - \frac{H}{\sqrt{3J_2}}\right)\sqrt{J_2} $$

$$ \sqrt{I_2} = \frac{\gamma}{H}\left(\sqrt{3J_2} - H\right) = F\gamma \qquad (3.40) $$

$$ \therefore \quad \sqrt{3J_2} = \frac{H}{\gamma}\sqrt{I_2} + H = H\left(\frac{\sqrt{I_2}}{\gamma} + 1\right) \qquad (3.41) $$

where I_2 is the second invariant of the viscoplastic strain rate tensor, and Eq. (3.41) represents an expanded yield condition for rate-sensitive materials. It is clear that as $\gamma \to \infty$ Eq. (3.41) reverts back to the static von Mises yield condition. Eq. (3.39) can now be written as

$$ {}^{1}\dot{E}^{VP}_{IJ} = \frac{\gamma}{H/\sqrt{3}}\left(1 - \frac{H}{H\left(\frac{\sqrt{I_2}}{\gamma} + 1\right)}\right){}^{1}\bar{S}_{IJ} $$

or,

$$ {}^{1}\dot{E}^{VP}_{IJ} = \frac{\gamma}{H/\sqrt{3}}\left(\frac{\sqrt{I_2}/\gamma}{1 + \sqrt{I_2}/\gamma}\right){}^{1}\bar{S}_{IJ} \qquad (3.42) $$

Since $\sqrt{I_2} = F\gamma$ from Eq. (3.40), one gets

$$ {}^{1}\dot{E}_{IJ}^{VP} = \frac{\gamma}{H/\sqrt{3}} \left(\frac{F}{1+F}\right) {}^{1}\bar{S}_{IJ} \qquad (3.43) $$

Again, it is seen from Eq. (3.42) that as $\gamma \to \infty$ these equations represent inviscid plasticity:

$$ {}^{1}\dot{E}_{IJ}^{VP} = \frac{\sqrt{I_2}}{H/\sqrt{3}} {}^{1}\bar{S}_{IJ} = \dot{\lambda}\, {}^{1}\bar{S}_{IJ} \qquad (3.44) $$

The computational scheme for viscoplastic analyses can now be described. Each load increment applied on the body produces an instantaneous elastic strain and the corresponding stress increment can be computed as

$$ S_{IJ}^{I} = S_{IJ}^{E} = C_{IJKL}\, E_{KL} = E_{IJKL}\, E_{KL} \qquad (3.45) $$

This increment is added to the total stress and the scalar function F is computed. If $F \leq 0$ no viscoplastic deformations occur. If $F > 0$ the viscoplastic strain rates are computed as per Eq. (3.43) and the increments in viscoplastic strains are simply

$$ E_{IJ}^{VP} = {}^{1}\dot{E}_{IJ}^{VP}\, dt \qquad (3.46) $$

for sufficiently small time increments. The total equivalent viscoplastic strain is computed and the new value of H', the hardening parameter, evaluated using the uniaxial static stress-strain curve. The "viscoplastic" stresses are computed as

$$S^{VP}_{IJ} = E_{IJKL}\, E^{VP}_{KL} \tag{3.47}$$

and the stress increments can be written as (see section 2.6)

$$S_{IJ} = S^{I}_{IJ} - S^{VP}_{IJ} = S^{E}_{IJ} - S^{VP}_{IJ} \tag{3.48}$$

and the total stresses are

$$^{2}S_{IJ} = {}^{1}S_{IJ} + S_{IJ} \tag{3.49}$$

The viscoplastic strain increments are then treated as initial strains as discussed in section 2.6.

3.2.3 Use of Viscoplasticity for Plasticity Solutions

It was shown in the previous section that the viscoplasticity equations degenerate to give inviscid plasticity results as the material parameter γ tends to infinity. An alternative approach is to use any arbitrary value of γ but make use of time as an artifice and let an equilibrium plastic state, $F = 0$, be attained as a result of "viscoplastic" deformations. The instantaneous response in this procedure is purely elastic and the resulting state of stress might fall outside the static yield surface, see Fig. 3.3. This creates the situation where $F > 0$ which is inadmissible in classical plasticity but not so in viscoplasticity. Now, "viscoplastic" deformations are allowed to take place with time and gradually the stresses are redistributed until the state of stress at no point exceeds the yield surface, i.e. $F = 0$, Fig. 3.3.

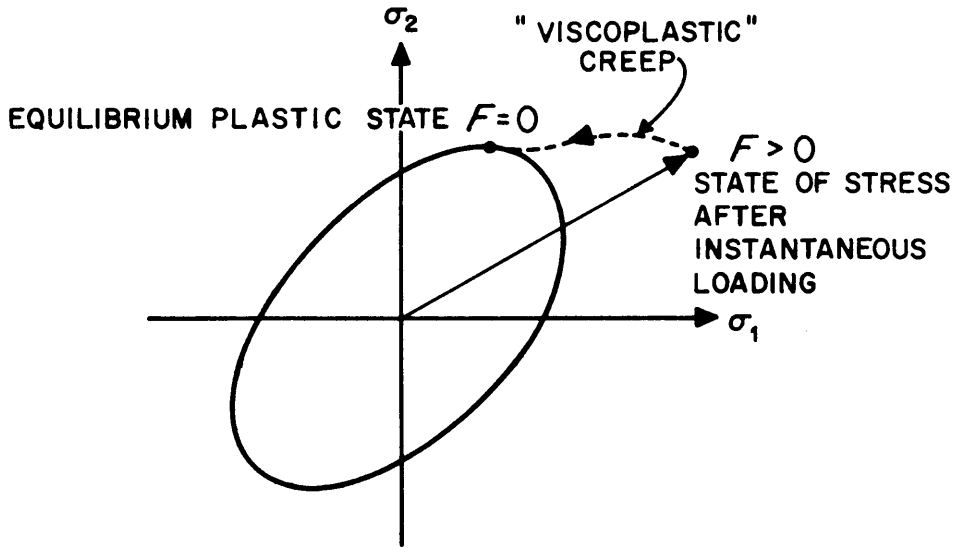

FIG.3.3 "VISCOPLASTIC" DEFORMATIONS LEADING TO A STEADY STATE PLASTICITY SOLUTION

The resulting equilibrium state is them the rate-independent elastic-plastic solution for the given problem.

3.3 Generalized Plane Stress

The stress-strain transformation matrix given by E_{IJKL} for elastic and C_{IJKL} for elastic-plastic deformations must be condensed to the generalized plane stress case for thin or moderately thick shell applications. For axisymmetric deformations, one can assume

$$\begin{aligned} {}^1S_{12} &= {}^1S_{23} = {}^1S_{33} = 0 \\ S_{12} &= S_{23} = S_{33} = 0 \qquad \text{(a)} \\ E_{12} &= E_{23} = 0 \end{aligned}$$

The stress-strain relation can then be written as

$$S_{IJ} = C_{IJKL}\, E_{KL} + C_{IJ33}\, E_{33} \qquad (3.50)$$

and

$$S_{33} = C_{33KL}\, E_{KL} + C_{3333}\, E_{33} = 0 \qquad (3.51)$$

Solving for E_{33} and substituting into Eq. (3.50) gives

$$S_{IJ} = \overline{C}_{IJKL}\, E_{KL}$$

where

$$\overline{C}_{IJKL} = C_{IJKL} - C_{IJ33}\,\frac{C_{33KL}}{C_{3333}} \qquad (3.52)$$

This modified stress-strain matrix can be obtained using Gaussian elimination technique. For plane stress problems, in addition to the conditions (a) one can assume

$$^{1}S_{22} = S_{22} = 0 \qquad \text{(b)}$$

Then the equations for $S_{22} = 0$ and $S_{33} = 0$ can be solved simultaneously to give E_{22} and E_{33} which can be substituted in

$$S_{IJ} = C_{IJKL}\, E_{KL} + C_{IJ22}\, E_{22} + C_{IJ33}\, E_{33} \qquad (3.53)$$

to give a modified stress-strain relation for plane stress problems,

$$S_{IJ} = \overline{\overline{C}}_{IJKL}\, E_{KL} \qquad (3.54)$$

where $\overline{\overline{C}}_{IJKL}$ can be obtained in the calculations using Gaussian elimination.

4. NUMERICAL ANALYSIS OF NONLINEAR PROBLEMS

4.1 Sources of Nonlinearities in Structural Systems

The nonlinearities in the behavior of a structure may be due to physical or geometrical causes. These are referred to as physical or material nonlinearities and geometrical nonlinearities. The material nonlinearities are caused by the use of materials that are characterized by nonlinear constitutive laws. Modern design methods, which make use of materials well beyond their elastic limits, make the consideration of this type of nonlinearity essential in most structural problems. The geometric nonlinearities, on the other hand, are due to finite deformations of the structure. Large deformations of bars, plates and shells are typical cases in which this type of nonlinearity must be considered. Two separate aspects of geometric nonlinearity may be recognized:

i) the use of the complete kinematic expression for finite strains, i.e. inclusion of nonlinear terms in the strain-displacement relations, and

ii) the use of deformed configuration to obtain the equations of motion which, as a consequence, become dependent on the total deformations.

For many structural problems it is essential to consider both physical and geometrical nonlinearities. The equations of motion for these problems are in the form of nonlinear differential or integro-differential equations depending on whether differential or integral forms are used to describe material behavior. These equations are quite complex for most practical problems and necessitate the use of numerical solution techniques.

4.2 Solution Methods

Efficient solution methods are required for the numerical analysis of nonlinear structural systems. A great number of methods have been proposed in recent years due to the surge of activity in this field and many survey papers [32, 88, 89, 90] have dealt with them in detail. These methods fall into one of the following three classes [42]:

Class I - Incremental methods (no equilibrium checks).

Class II - Direct or iterative methods.

Class III - Modified incremental methods (with equilibrium checks).

I. Incremental methods. In these methods the load is applied in small increments and a sequence of linear analyses are carried out. For each step the increments in displacements, strains and stresses are computed and the information is used for the next step. Several variants are possible depending upon the scheme used for estimating the stiffness of the structure at any step. These methods are extremely fast but they all suffer from the disadvantage that, in general, equilibrium at any particular load level is not satisfied and the solutions tend to drift away from the true solution unless very small load steps are taken.

II. Direct methods. The total load on the structure is applied and the response is computed by using any one or a combination of several known iterative techniques. Although many efficient procedures can be obtained, the major drawback of this class of methods is that they cannot be applied to problems that are path-dependent, such as plastic deformations using flow theories of plasticity.

III. Modified incremental methods. These methods involve the combined use of the methods of Classes I and II. As in Class I the total load is applied in a series of load steps but the equilibrium is checked at each load level and iterative methods of Class II are applied repeatedly until the desired degree of accuracy is achieved for the equilibrium convergence. Many computational schemes are possible in this class. One particular scheme called the residual load method or one-step iteration method [26] involves the calculation of the unbalanced forces at the end of each load increment and their application as additional pseudo-loads in the next increment. Computationally this is equivalent to the Class I methods and requires no significant increase in computation time over the conventional pure incremental method. The application of the unbalanced forces helps in reducing the drift and results in substantially improved results. This residual load method has been used in the present study.

4.3 Linearized Incremental Equations of Motion

The incremental equations of motion are obtained by equating the incremental virtual work done by the internal stress fields to the incremental virtual work done by the external loads. The required virtual work expressions were derived in Chapter 2. The case of non-conservative loading using the residual load approach is considered in this section. Equating the expressions for incremental virtual work given in Eqs. (2.73, 81), one obtains

$$\int_{B_o} [\rho_o \ddot{u}^I \delta u_I + (S^{IJ} \delta E_{IJ} + {}^1S^{IJ} \delta \eta_{IJ})] dV - \int_{\partial B_o} {}^2p \frac{\rho_o}{\rho} N^J X^J|_K X^M|_I u^K|_M \delta u_I dA$$

$$= -\int_{\partial B_0} {}^2p\frac{\rho_0}{\rho} N^J X^J|_I \, \delta u_I dA + \int_{B_0} \rho_0 \, {}^2f^I \delta u_I \, dV - \int_{B_0} (\rho_0 \, {}^1\ddot{u}^I \delta u_I + {}^1S^{IJ} \delta e_{IJ}) dV \tag{4.1}$$

The second integral on the left hand side of this equation is linear in displacement increment $\underset{\sim}{u}$ and hence has the form of a stiffness term, and is present only for nonconservative loading. This is a nonsymmetric term and can be neglected for most engineering applications, as discussed in section 2.4. Deleting this term and using the constitutive equation

$$S^{IJ} = C^{IJKL} E_{KL} \tag{3.26}$$

one can rewrite Eq. (4.1) as

$$\int_{B_0} [\rho_0 \ddot{u}^I \delta u_I + (C^{IJKL} E_{KL} \, \delta E_{IJ} + {}^1S^{IJ} \delta \eta_{IJ})] dV = -\int_{\partial B_0} {}^2p\frac{\rho_0}{\rho} N^J X^J|_I \, \delta u_I dA$$

$$+\int_{B_0} \rho_0 \, {}^2f^I \delta u_I dV - \int_{B_0} (\rho_0 \, {}^1\ddot{u}^I \delta u_I + {}^1S^{IJ} \delta e_{IJ}) dV \tag{4.2}$$

Recalling that

$$E_{IJ} = e_{IJ} + \eta_{IJ} \tag{2.20}$$

where e_{IJ} is linear in $\underset{\sim}{u}$, and η_{IJ} quadratic in $\underset{\sim}{u}$, Eq. (4.2) can be written as

$$\delta \underset{\sim}{u} \cdot [\underset{\sim}{M} \cdot \ddot{\underset{\sim}{u}} + \{\underset{\sim}{K}_o + \underset{\sim}{K}_1(u_I) + \underset{\sim}{K}_2(u_I, u_J) + K_G\} \cdot \underset{\sim}{u}]$$

$$= \delta \underset{\sim}{u} \cdot [{}^2\underset{\sim}{R} - \underset{\sim}{M} \cdot {}^1\ddot{\underset{\sim}{u}} - {}^1\underset{\sim}{F}^R] \tag{4.3}$$

where

$$\delta \underset{\sim}{u} \cdot \underset{\sim}{M} \cdot \ddot{\underset{\sim}{u}} = \int_{B_0} \rho_0 \, \ddot{u}^I \, \delta u_I \, dV \tag{a}$$

$$\delta \underset{\sim}{u} \cdot \underset{\sim}{K}_0 \cdot \underset{\sim}{u} = \int_{B_0} C^{IJKL}\, e_{KL}\, \delta e_{IJ}\, dV \qquad (b)$$

$$\delta \underset{\sim}{u} \cdot \underset{\sim}{K}_1 (u_I) \cdot \underset{\sim}{u} = \int_{B_0} C^{IJKL} (e_{KL}\, \delta \eta_{IJ} + \eta_{KL}\, \delta e_{IJ})\, dV \qquad (c)$$

$$\delta \underset{\sim}{u} \cdot \underset{\sim}{K}_2 (u_I, u_J) \cdot \underset{\sim}{u} = \int_{B_0} C^{IJKL}\, \eta_{KL}\, \delta \eta_{IJ}\, dV \qquad (d)$$

$$\delta \underset{\sim}{u} \cdot \underset{\sim}{K}_G \cdot \underset{\sim}{u} = \int_{B_0} {}^1S^{IJ}\, \delta \eta_{IJ}\, dV \qquad (e)$$

$$\delta \underset{\sim}{u} \cdot {}^2\underset{\sim}{R} = -\int_{\partial B_0} {}^2p\, \frac{\rho}{\rho}\, N^J\, X^J|_I\, \delta u_I\, dA + \int_{B_0} \rho_0\, {}^2f^I\, \delta u_I\, dV \qquad (f)$$

$$\delta \underset{\sim}{u} \cdot \underset{\sim}{M} \cdot {}^1\ddot{\underset{\sim}{u}} = \int_{B_0} \rho_0\, {}^1\ddot{u}^I\, \delta u_I\, dV \qquad (g)$$

and finally, the internal resisting force, ${}^1\underset{\sim}{F}^R$, is given by

$$\delta \underset{\sim}{u} \cdot {}^1\underset{\sim}{F}^R = \int_{B_0} {}^1S^{IJ}\, \delta\, e_{IJ}\, dV \qquad (h)$$

Defining the total loading term including out-of-balance forces as $\bar{\underset{\sim}{R}}$, i.e.,

$$\bar{\underset{\sim}{R}} = {}^2\underset{\sim}{R} - \underset{\sim}{M} \cdot {}^1\ddot{\underset{\sim}{u}} - {}^1\underset{\sim}{F}^R \qquad (4.4)$$

one obtains the incremental equations of motion as

$$\delta \underset{\sim}{u} \cdot [\underset{\sim}{M} \cdot \ddot{\underset{\sim}{u}} + \{\underset{\sim}{K}_0 + \underset{\sim}{K}_1 + \underset{\sim}{K}_2 + \underset{\sim}{K}_G\} \cdot \underset{\sim}{u}] = \delta \underset{\sim}{u} \cdot \bar{\underset{\sim}{R}} \qquad (4.5)$$

Inspection of Eqs. (a) through (h) shows that the nonlinearities in Eq. (4.5) arise from the presence of the stiffness terms $\underset{\sim}{K}_1$ and $\underset{\sim}{K}_2$ which depend on the displacement increment $\underset{\sim}{u}$ itself. The terms $\underset{\sim}{K}_0$ and $\underset{\sim}{K}_G$, the incremental and geometric stiffnesses, respectively, are independent of $\underset{\sim}{u}$ and constant for a given increment. Assuming the displacement increments $\underset{\sim}{u}$ to be small, $\underset{\sim}{K}_1$ and $\underset{\sim}{K}_2$ can be neglected since their contributions, $\underset{\sim}{K}_1 \cdot \underset{\sim}{u}$ and

$\underset{\sim}{K}_2 \cdot \underset{\sim}{u}$, are of quadratic and cubic orders in $\underset{\sim}{u}$ and likely to be small compared to $\underset{\sim}{K}_0 \cdot \underset{\sim}{u}$ and $\underset{\sim}{K}_G \cdot \underset{\sim}{u}$ which are linear in $\underset{\sim}{u}$. Furthermore, accuracy in the evaluation of the incremental tangent stiffness for any step is less critical than the need to satisfy the equilibrium requirements in order to avoid excessive drift in solutions obtained using the methods discussed in section 4.2. Hence, linearization of Eq. (4.5) is achieved here by elimination of $\underset{\sim}{K}_1$ and $\underset{\sim}{K}_2$. The linearized incremental equations of motion are then given by

$$\delta\underset{\sim}{u} \cdot [\underset{\sim}{M} \cdot \ddot{\underset{\sim}{u}} + (\underset{\sim}{K}_0 + \underset{\sim}{K}_G) \cdot \underset{\sim}{u}] = \delta\underset{\sim}{u} \cdot \bar{\underset{\sim}{R}} \tag{4.6}$$

Finally, the correct expressions for $\underset{\sim}{K}_0$, $\underset{\sim}{K}_G$ and ${}^1\underset{\sim}{F}^R$ (part of $\bar{\underset{\sim}{R}}$) can be obtained from Eqs. (b, e and h) by the use of strain-displacement relations:

$$2e_{IJ} = u_{I|J} + u_{J|I} + {}^1u_{K|I}\, u^K{}_{|J} + u_{K|I}\, u^K{}_{|J} \tag{2.19}$$

and $$2\eta_{IJ} = u_{K|I}\, u^K{}_{|J}$$

Damping forces

The incremental equations of motion given by Eq. (4.6) do not include the effect of damping forces but may be extended to include them in a straightforward manner for the case of viscous damping forces which are proportional to velocity. Eq. (4.6) is modified to

$$\delta\underset{\sim}{u} \cdot [\underset{\sim}{M} \cdot \ddot{\underset{\sim}{u}} + \underset{\sim}{C} \cdot \dot{\underset{\sim}{u}} + (\underset{\sim}{K}_0 + \underset{\sim}{K}_G) \cdot \underset{\sim}{u}] = \delta\underset{\sim}{u} \cdot \bar{\underset{\sim}{R}} - \delta\underset{\sim}{u} \cdot \underset{\sim}{C} \cdot {}^1\dot{\underset{\sim}{u}} \tag{4.7}$$

Defining $\hat{\underset{\sim}{R}} = \bar{\underset{\sim}{R}} - \underset{\sim}{C} \cdot {}^{1}\dot{\underset{\sim}{u}} = {}^{2}\underset{\sim}{R} - \underset{\sim}{M} \cdot {}^{1}\ddot{\underset{\sim}{u}} - \underset{\sim}{C} \cdot {}^{1}\dot{\underset{\sim}{u}} - {}^{1}F^{R}$ (4.8)

one gets

$$\delta\underset{\sim}{u} \cdot [\underset{\sim}{M} \cdot \ddot{\underset{\sim}{u}} + \underset{\sim}{C} \cdot \dot{\underset{\sim}{u}} + (\underset{\sim}{K}_0 + \underset{\sim}{K}_G) \cdot \underset{\sim}{u}] = \delta\underset{\sim}{u} \cdot \hat{\underset{\sim}{R}} \qquad (4.9)$$

The damping coefficient $\underset{\sim}{C}$ may be taken as a combination of mass proportional and stiffness proportional damping. This is known as Rayleigh damping which is the same as the two-term approximation to the Caughey series [91]. This damping coefficient can be written as

$$\underset{\sim}{C} = \alpha \underset{\sim}{M} + \beta(\underset{\sim}{K}_0)_{t=0} \qquad (4.10)$$

where

α and β are the mass proportional and stiffness proportional damping factors, respectively, and $(\underset{\sim}{K}_0)_{t=0}$ is the incremental stiffness for the first time step, i.e. at time t=0. For convenience of notation, let

$$(\underset{\sim}{K}_0)_{t=0} = {}^{0}\underset{\sim}{K}_0 \; ; \quad \underset{\sim}{C} = \alpha\underset{\sim}{M} + \beta\,{}^{0}\underset{\sim}{K}_0 \qquad (4.11)$$

$\underset{\sim}{C}$ then remains constant for the structure throughout the analysis. This assumption is made because the damping mechanism in any structure is really quite complex, and it is difficult to justify the use of anything but the simplest idealizations.

It is worth noting that mass proportional damping causes negligible damping in higher modes whereas stiffness proportional damping has the tendency to suppress them. This property might be used to advantage in problems wherein undesirable higher modes need to be eliminated. Certain numerical integration schemes, like the Houbolt or Wilson-Farhoomand, introduce artificial

viscosity to achieve this effect but the use of stiffness proportional damping may provide better means of suppressing unwanted modes.

4.4 Numerical Integration of Equations of Motion

The normal mode superposition procedure for the solution of the equations of motion is applicable only for linear dynamic analysis. Even in the case of linear problems, however, it may be more advantageous to use the so-called step-by-step or direct integration when analyzing large systems subjected to short duration loads where a large number of modes may be excited. Blast or impact problems are generally solved using such direct integration methods. For problems involving physical and/or geometrical nonlinearities the only feasible approach is through the use of direct integration operators.

The direct integration of the governming equations of motion involves the determination of the approximate solution at any time $t + \Delta t$ from the known solution for displacements, velocities and accelerations at time t. The initial data at time $t=0$ are sufficient to initiate such "single-step" methods. There are also some methods which require the knowledge about the state of motion prior to time t (i.e. at $t-\Delta t$, $t-2\Delta t$, etc.) in order to advance the solution from t to $t + \Delta t$. These are termed "multi-step" methods [97] and require special starting procedures.

Several step-by-step methods have been introduced and discussed in the literature [49, 92-99]. Their properties with

regard to accuracy and stability have been studied extensively for linear dynamic analysis, but much work remains to be done pertaining to their application to nonlinear problems. The choice of the integration method for nonlinear dynamic analysis has been found to depend on the formulation used to set up the equations of motion. The Newmark method [92], for instance, has been reported by Stricklin, et al [48] to degenerate, leading to unstable solutions, when applied to problems wherein the non-linearities are treated as pseudo-forces in the formulation. This formulation gives rise to spurious oscillations which are left uncontrolled by the standard Newmark method, but may be damped out by the use of integration operators, such as the one due to Houbolt [95], that possess inherent artificial viscosity.

The discretized form of the linearized incremental equations of motion, Eq. (4.9), may be written as

$$[M]\{\ddot{u}\} + [C]\{\dot{u}\} + [K_0 + K_G]\{u\} = \{\hat{R}\} \tag{4.12}$$

Defining the tangent stiffness at time t as

$$[K_t] = [K_0 + K_G] \tag{4.13}$$

one gets

$$[M]\{\ddot{u}\} + [C]\{\dot{u}\} + [K_t]\{u\} = \{\hat{R}\} \tag{4.14}$$

The Newmark and Wilson-Farhoomand methods are used in this study to solve Eq. (4.14), and are discussed briefly in the following sections.

4.4.1 Newmark Generalized Acceleration Method

A family of step-by-step methods was presented by Newmark [92] for the solution of problems in structural dynamics. The solution at the end of a time step is expressed in terms of a Taylor series with the remainder given by quadrature formulas. Two free parameters of integration, γ and β, indicate how much of the acceleration at the end of the interval enters into the relations for velocity and displacement at the end of the interval. A number of different methods may be obtained by varying the values of γ and β. The value of $\gamma = 0.5$ insures that no spurious damping forces arise. γ greater than 0.5 introduces artificial damping while γ less than 0.5 gives rise to negative damping, involving self-excited vibrations solely due to the numerical procedure. Although no direct physical interpretation of β is possible, it was pointed out in [92] that certain values of β correspond to specific ways of acceleration variation over each time interval --e.g. $\beta = \frac{1}{6}$ corresponds to a linear acceleration assumption while $\beta = \frac{1}{4}$ corresponds to a constant average acceleration.

For undamped vibrations, the choice of $\beta = 0$ leads to an explicit solution algorithm, provided the mass of the structure is approximated by a diagonal lumped mass matrix. The use of any other value for β or the inclusion of damping forces or nondiagonal mass matrix leads to implicit integration methods that require the solution of a system of equations at each step to advance the solution. The method obtained using $\gamma = 0.5$ and $\beta = 0.25$ is known to be unconditionally stable for linear problems

and stability limits can be estabished for other values of these parameters.

Following [92],

$$\{\dot{u}\} = \gamma\ \Delta t\ \{{}^{2}\ddot{u}\} + (1 - \gamma)\ \Delta t\ \{{}^{1}\ddot{u}\} \tag{4.15}$$

$$\{u\} = \beta\ \Delta t^{2}\ \{{}^{2}\ddot{u}\} + (\tfrac{1}{2} - \beta)\ \Delta t^{2}\ \{{}^{1}\ddot{u}\} + \Delta t\ \{{}^{1}\dot{u}\} \tag{4.16}$$

Solving for $\{{}^{2}\ddot{u}\}$,

$$\{{}^{2}\ddot{u}\} = \frac{1}{\beta\ \Delta t^{2}}\ \{u\} - \frac{1}{\beta\ \Delta t}\ \{{}^{1}\dot{u}\} - \frac{1}{2\beta}\ \{{}^{1}\ddot{u}\} + \{{}^{1}\ddot{u}\} \tag{4.17}$$

Hence,

$$\{\ddot{u}\} = \frac{1}{\beta\ \Delta t^{2}}\ \{u\} - \frac{1}{\beta\ \Delta t}\ \{{}^{1}\dot{u}\} - \frac{1}{2\beta}\ \{{}^{1}\ddot{u}\} \tag{4.18}$$

Substituting Eq. (4.17) into Eq. (4.15),

$$\{\dot{u}\} = \frac{\gamma}{\beta\ \Delta t}\ \{u\} - \frac{\gamma}{\beta}\ \{{}^{1}\dot{u}\} - (\frac{\gamma}{2\beta} - 1)\ \Delta t\ \{{}^{1}\ddot{u}\} \tag{4.19}$$

Eqs. (4.18, 19) may be rewritten as

$$\{\ddot{u}\} = \frac{1}{\beta\ \Delta t^{2}}\ \{u\} - \{A\};\quad \{A\} = \frac{1}{\beta\ \Delta t}\ \{{}^{1}\dot{u}\} + \frac{1}{2\beta}\ \{{}^{1}\ddot{u}\} \tag{4.20}$$

$$\{\dot{u}\} = \frac{\gamma}{\beta\ \Delta t}\ \{u\} - \{B\}\ ;\quad \{B\} = \frac{\gamma}{\beta}\ \{{}^{1}\dot{u}\} + (\frac{\gamma}{2\beta} - 1)\ \Delta t\ \{{}^{1}\ddot{u}\} \tag{4.21}$$

Substituting Eqs. (4.20, 21) into Eq. (4.14) and recalling the definition of $\{\hat{R}\}$ from Eq. (4.8), one gets

$$([K_t] + \frac{1}{\beta\ \Delta t^{2}}\ [M] + \frac{\gamma}{\beta\ \Delta t}\ [C])\ \{u\} = \{{}^{2}R\} - [M]\{{}^{1}\ddot{u}\} - [C]\{{}^{1}\dot{u}\} - \{{}^{1}F^{R}\} + [M]\{A\} + [C]\{B\} \tag{4.22}$$

The equations for the Newmark method may be summarized as shown in Table 4-1. Note that the left superscripts ^{1} and ^{2} refer to configurations B_1 and B_2 at times t and $t + \Delta t$, respectively.

Table 4-1. Newmark Method of Direct Integration

$$a_0 = \frac{1}{\beta\,\Delta t^2} \qquad b_1 = \frac{1}{\beta\,\Delta t^2} = a_0$$

$$a_1 = \frac{\gamma}{\beta\,\Delta t} = a_0\gamma \qquad b_2 = -\frac{1}{\beta\,\Delta t} = -a_2$$

$$a_2 = \frac{1}{\beta\,\Delta t} = a_0\,\Delta t \qquad b_3 = -\frac{1}{2\beta} = -(a_3 + 1)$$

$$a_3 = \frac{1}{2\beta} - 1 \qquad b_4 = \frac{\gamma}{\beta\,\Delta t} = a_1$$

$$a_4 = \frac{\gamma}{\beta} - 1 \qquad b_5 = -\frac{\gamma}{\beta} = -(a_4 + 1)$$

$$a_5 = \left(\frac{\gamma}{2\beta} - 1\right)\Delta t \qquad b_6 = \left(1 - \frac{\gamma}{2\beta}\right)\Delta t = -a_5$$

$$[K_t + a_0\,M + a_1\,C]\,\{u\} = \{{}^2R\} - \{{}^1F^R\} + [M]\,\{a_2\,{}^1\dot{u} + a_3\,{}^1\ddot{u}\} + [C]\,\{a_4\,{}^1\dot{u} + a_5\,{}^1\ddot{u}\}$$

or,

$$[K^*]\,\{u\} = \{R^*\}$$

Solve for the incremental displacements $\{u\}$. Then,

$$\{{}^2\ddot{u}\} = \{{}^1\ddot{u}\} + b_1\,\{u\} + b_2\,\{{}^1\dot{u}\} + b_3\,\{{}^1\ddot{u}\}$$

$$\{{}^2\dot{u}\} = \{{}^1\dot{u}\} + b_4\,\{u\} + b_5\,\{{}^1\dot{u}\} + b_6\,\{{}^1\ddot{u}\}$$

$$\{{}^2u\} = \{{}^1u\} + \{u\}$$

4.4.2 Wilson - Farhoomand θ-Method

The linear acceleration method belonging to the Newmark family of step-by-step procedures ($\gamma = \frac{1}{2}$, $\beta = \frac{1}{6}$) was modified by Wilson [49] in order to obtain an unconditionally stable algorithm. The acceleration was assumed to vary linear over an interval $\tau = 2\,\Delta t$ where Δt is the time increment. After solving for the pseudo-displacement increments between t and $t + \tau$, the complete solution at $t + \Delta t$ is obtained using linear interpolation for acceleration and consistent kinematic relations for velocities and displacements, i.e. quadratic and cubic variations, respectively. This method was shown to be unconditionally stable for linear systems but possessed considerable amount of artificial damping, more than sufficient to suppress the spurious oscillations of discretized systems.

A further extension of this method was made by Farhoomand [93] to reduce the integration errors and obtain an optimal value of τ. The acceleration was assumed to vary linearly during the time interval $\tau = \theta\,\Delta t$, where the parameter θ must be chosen with regard to the accuracy and stability of integration. The value of $\theta = 1$ represents the linear acceleration method, and $\theta = 2$ the modified "averaging" method of Wilson. It was shown by Bathe and Wilson [94] that θ must be chosen greater than 1.37 for unconditional stability. It can also be seen from [94] that, although strong damping of the higher modes is retained, the integration accuracy of the lower modes is much improved by choosing $\theta = 1.4$ instead of 2.

The details of derivation of the θ-method may be found

in [45, 93], and only a summary of the equations useful for the computer coding is presented in Table 4.2.

Table 4-2. Wilson - Farhoomand θ-Method of Direct Integration

$$\tau = \theta \, \Delta t$$

$$a_0 = \frac{6}{\tau^2} \qquad b_1 = \frac{6}{\theta \, \tau^2} = \frac{a_0}{\theta}$$

$$a_1 = \frac{3}{\tau} \qquad b_2 = -\frac{6}{\theta\tau} = -\frac{a_2}{\theta}$$

$$a_2 = \frac{6}{\tau} = 2 \, a_1 \qquad b_3 = 1 - \frac{3}{\theta}$$

$$a_3 = a_4 = 2 \qquad b_4 = \frac{\Delta t}{2}$$

$$a_5 = \frac{\tau}{2} \qquad b_5 = \frac{\Delta t^2}{3} \qquad b_6 = \frac{b_5}{2}$$

Load extrapolation $\{R_{t+\tau}\} = \{{}^1R\} + \theta \{{}^2R - {}^1R\}$

Let $\{u^*\}$ represent pseudo-displacement increments during the time interval t to $t + \tau$

$$[K_t + a_0 M + a_1 C] \{u^*\} = \{R_{t+\tau}\} - \{{}^1F^R\} + [M] \{a_2 \, {}^1\dot{u} + a_3 \, {}^1\ddot{u}\} + [C] \{a_4 \, {}^1\dot{u} + a_5 \, {}^1\ddot{u}\}$$

or,

$$[K^*] \{u^*\} = \{R^*\}$$

Solve for the pseudo-displacement increments $\{u^*\}$

Then,

$$\{{}^2\ddot{u}\} = b_1 \{u^*\} + b_2 \{{}^1\dot{u}\} + b_3 \{{}^1\ddot{u}\}$$

$$\{{}^2\dot{u}\} = \{{}^1\dot{u}\} + b_4 \{{}^1\ddot{u} + {}^2\ddot{u}\}$$

$$\{{}^2u\} = \{{}^1u\} + \Delta t \{{}^1\dot{u}\} + b_5 \{{}^1\ddot{u}\} + b_6 \{{}^2\ddot{u}\}$$

4.4.3 Algorithmic Damping and the Use of δ Control in Newmark Method

The frequency spectrum of a continuous system is truncated when the system is idealized by a discrete model as in the finite element methods. The number of modes in the discrete system is limited by the finite number of degrees of freedom associated with it and the maximum frequency is termed the cut-off frequency. While the lower frequencies may be approximated quite well, the higher frequencies of the discretized system are in considerable error compared to those of the continuous system. The use of direct integration procedures implies a common value of the time step, Δt, for all the modes. The integration errors in the period and/or response amplitude depend on the values of $\Delta t/T_i$ where T_i is the period of vibration for mode i. Choice of a Δt small enough to integrate the highest modes accurately requires the use of excessive computing effort. Indeed, there is the question of whether such an approach is justifiable in view of the statement above regarding the large errors in the discrete high frequencies. The methods of Houbolt, Wilson, etc., possess inherent artificial viscosity which causes the higher modes to be damped out when the Δt is chosen to insure accuracy in the response of lower modes. This might be justified and indeed necessary in problems where the lower modes dominate the response, as is the case in most structural vibration problems.

The widely used constant average acceleration method of Newmark ($\gamma = \frac{1}{2}$, $\beta = \frac{1}{4}$), on the other hand, introduces no artificial viscosity into the solution procedure, and will preserve the

undesirable higher modes. These higher modes will have large errors in their time periods due to the discretization as well as the integration procedures. The inability of this Newmark method to suppress undesirable higher modes may be rectified by taking advantage of the property of the integration parameter γ mentioned earlier in section 4.4.1, i.e. artificial damping may be introduced by choosing $\gamma > 0.5$.

Letting

$$\gamma = 0.5 + \delta \tag{4.23}$$

where δ is a positive value, artificial viscosity can be introduced into the solution to any desired degree. Use of this δ control requires modification in the value of β, and Goudreau [98] has shown that β must be greater than 0.25 to preserve unconditional stability for linear systems. The relationship between β and δ is given as [98]

$$\beta \geq 0.25\,(1 + \delta)^2 \tag{4.24}$$

The advantage of using δ control with the Newmark family of β methods over methods possessing inherent artifical viscosity is that the amount of damping introduced may be controlled by an independent parameter δ instead of being fixed by the choice of the time step for integration of the incremental equations of motion.

In the case of impact problems, the response is not dominated by a few low frequency modes, and as $\Delta t \to 0$, any stable integration procedure can be made convergent to the exact solution of the discrete system. However, this may be hardly worthwhile

due to the spurious high frequency oscillations of the discrete system and it may be preferable to introduce artificial damping into the solution procedure. Nevertheless, there are certain structures so sensitive to even small amounts of damping that no algorithmic damping may be tolerated and in such cases the Newmark β methods with $\delta = 0$ must be used. Also, it is recommended to use the Newmark methods over the Wilson-Farhoomand Θ-method when considering suddenly applied loads, discontinuous load history or if the system is released suddenly from a deflected position as the Θ-method has been shown in such cases to magnify rather than suppress the response of the inaccurate higher modes [98, 99].

4.5 Numerical Example of the Solution Procedure

A numerical example is presented in this section to illustrate the accuracy of the solution procedure for dynamic analysis of shells of revolution. The transient response of a shallow, spherical, thin cap was studied by Klein and Sylvester [44] and Stricklin, et al [48]. The geometry, material properties and load history of this cap are given in Fig. 6.8. A suddenly applied uniform external pressure of 100 psi was applied to this cap and the finite element analysis was carried out using the Newmark method ($\gamma = 0.5$, $\beta = 0.25$) with a time step of 10×10^{-6} seconds. The discretization was achieved by the use of five degenerate isoparametric elements (see Chapter 5) from the apex to the boundary and the mass distribution was approximated by a diagonal lumped mass matrix.

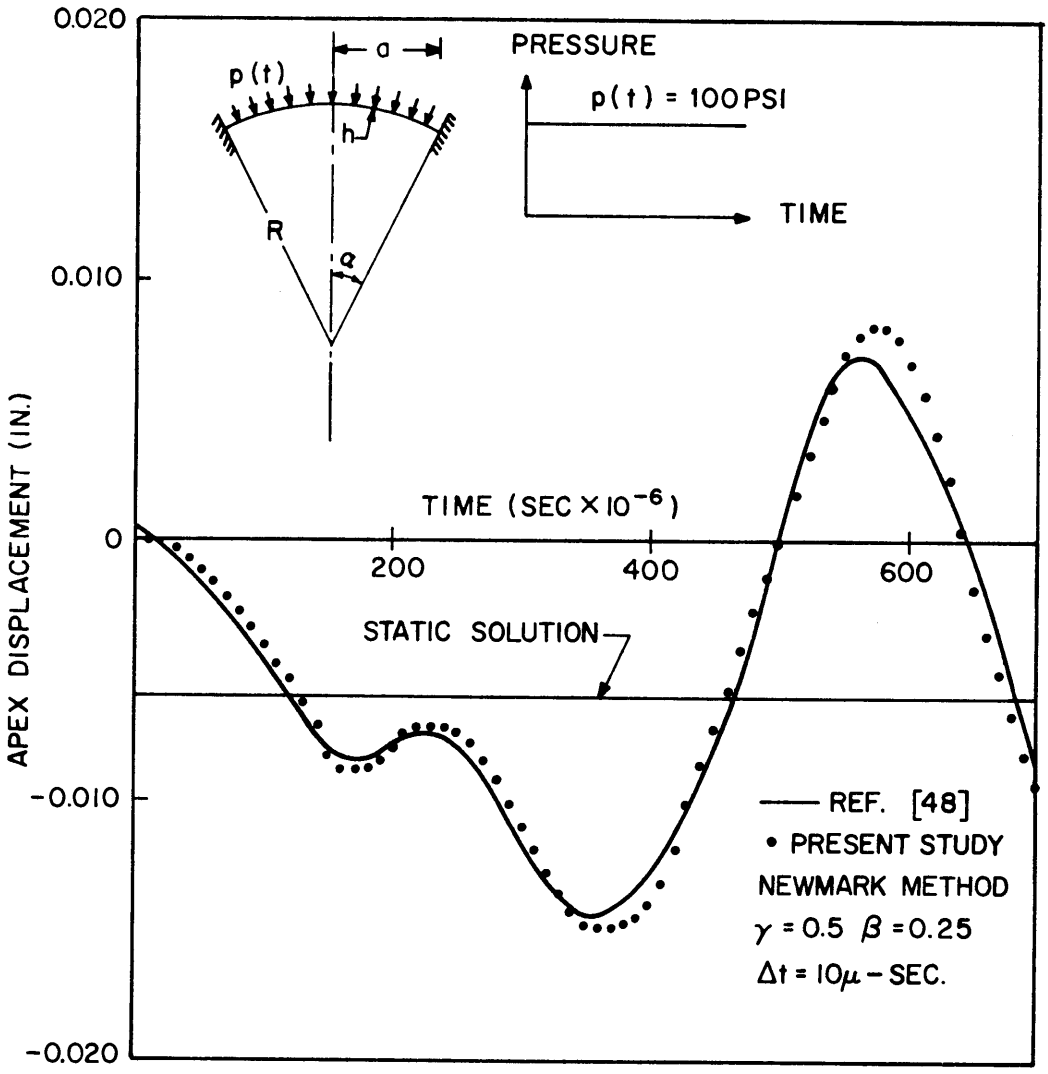

FIG. 4.1 DYNAMIC RESPONSE OF SHALLOW SPHERICAL CAP UNIFORM EXTERNAL STEP PRESSURE OF 100 PSI

The time variation of the apex displacement is plotted in Fig. 4.1 and agrees very closely with the results of Stricklin, et al [48]. The period of vibration is also in excellent agreement with the theoretical result of 493 μ-sec. computed using the chart for shallow caps presented in Fig. 8.5 of the book by Kraus [100]. The peak amplitudes are slightly greater in the present study because the Newmark method with no artificial damping has been employed, whereas Stricklin used the Houbolt method which introduces damping into the solution.

Further examples illustrating the efficacy of the computer programs developed for elastic, elastic-plastic and elastic-viscoplastic analyses are deferred until Chapter 6.

5. FINITE ELEMENT FORMULATION

The finite element method is used for the numerical solution of the linearized incremental equations of motion derived in section 4.3. This method was first introduced by Turner et al [14] and is basically an extension of the Ritz method, with the field variables being expanded over a series of subdomains instead of over the total region. Interpolation polynominals are used to describe these variables within a subregion or finite element in terms of their values at selected nodal points of the element. Using the direct stiffness method of displacement formulation, the discretized equations of motion are obtained for the total region. The displacements at nodal points are then obtained by numerical solution of these algebraic simultaneous equations. Several excellent treatises have been published that give detailed discussions of the finite element method as well as its mathematical background [18-21, 101, 102].

A great variety of elements have been developed over the years for use in the analysis of linear as well as nonlinear problems. The isoparametric family of elements [103] uses the same interpolation formula to describe the geometry as well as the displacement field. Although successfully used in both static and dynamic elastic-plastic analyses of axisymmetric shells, the use of these elements is computationally inefficient for inelastic analysis of moderately thick shells. This is due to the excessive number of degrees of freedom employed (at least a quadratic displacement variation across the thickness is required to insure convergence [104]), and the fact that integration across the thickness cannot be made separately.

Incompatable displacement modes that are condensed before solution [104, 106] may be used to reduce the number of degrees of freedom and thus improve the efficiency of these elements.

Construction of discrete models to represent thick shells or shells with sharp discontinuities in their geometry like cut-outs or stiffeners may necessitate the use of one or more of the elements belonging to the isoparametric family. However, in problems involving thin or moderately thick shells, considerable economy in computational effort may be achieved by the use of degenerate isoparametric elements [107], Fig. 5.1. Different parametric representations are used to describe the geometry and displacement fields of these elements. Relaxation of the classical Kirchhoff-Love hypothesis of thin shell theories permits shear deformations to be included, thus enabling moderately thick shells to be represented by such elements. Although excellent results are obtained for moderately thick shells, it was found [108, 109] that significant errors arise when these elements are employed in the analysis of thin shells due to shear deformations being allowed in a pure bending mode as a result of the relaxation of Kirchhoff-Love hypothesis. Larsen [43] used the cubic element, see Fig. 5.1, for most applications since the excessive strain energy due to shear was most dominant in the case of elements with linear and quadratic displacement variations. The same cubic element is also used in the numerical examples presented in this report. The finite element formulation outlined in this chapter follows along the same line of development presented by Larsen [43].

5.1 Geometric Representation

The geometry of a shell element is described in a global

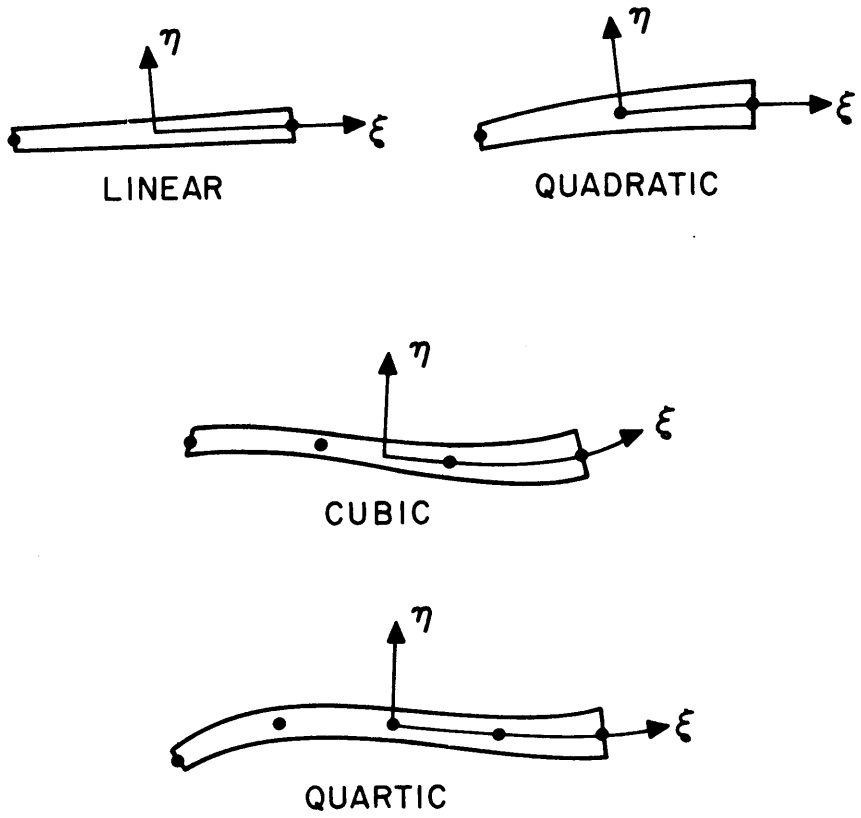

FIG. 5.1 DEGENERATE ISOPARAMETRIC FINITE ELEMENTS

Cartesian system (r, z) and a local natural system (ξ, η). The local system is, in general, curvilinear and any point within an element has its coordinates such that

$$-1 \leq \xi \leq +1 \qquad -1 \leq \eta \leq +1 \tag{5.1}$$

The ξ - axis bisects the shell thickness and describes the middle surface while the η - axis is simply defined as an axis along which $\xi = 0$ and not necessarily as the normal to the middle surface. The inner and outer faces of the shell are represented by $\eta = -1$ and $\eta = +1$, respectively. The "normal" angle θ is defined as the angle between the r - and η - axis, see Fig. 5.2. In addition, an auxiliary orthogonal system (s, t) is also introduced with the s - axis coinciding with the ξ - axis of the local natural system, Fig. 5.2.

The global and natural coordinates of any point are related by means of a transformation in terms of interpolation polynominals and nodal point coordinates. For any point (ξ, η) within an element, the global coordinates (r, z) can be written following [107], as

$$\begin{Bmatrix} r \\ z \end{Bmatrix} = \sum_{i=1}^{M} \phi_i(\xi) \begin{Bmatrix} r_i \\ z_i \end{Bmatrix} + \eta \sum_{i=1}^{M} \frac{1}{2} \phi_i(\xi) h_i \begin{Bmatrix} \cos \theta_i \\ \sin \theta_i \end{Bmatrix} \tag{5.2}$$

where $\phi_i(\xi)$ are interpolation polynomials,

h_i = thickness at node i,

θ_i = "normal" angle at node i, and

(r_i, z_i) = global coordinates of node i.

The number of nodal points M, and hence the order of the polynomials, is determined by the element type used. The interpolation polynomials for linear, quadratic, cubic and quartic elements are given

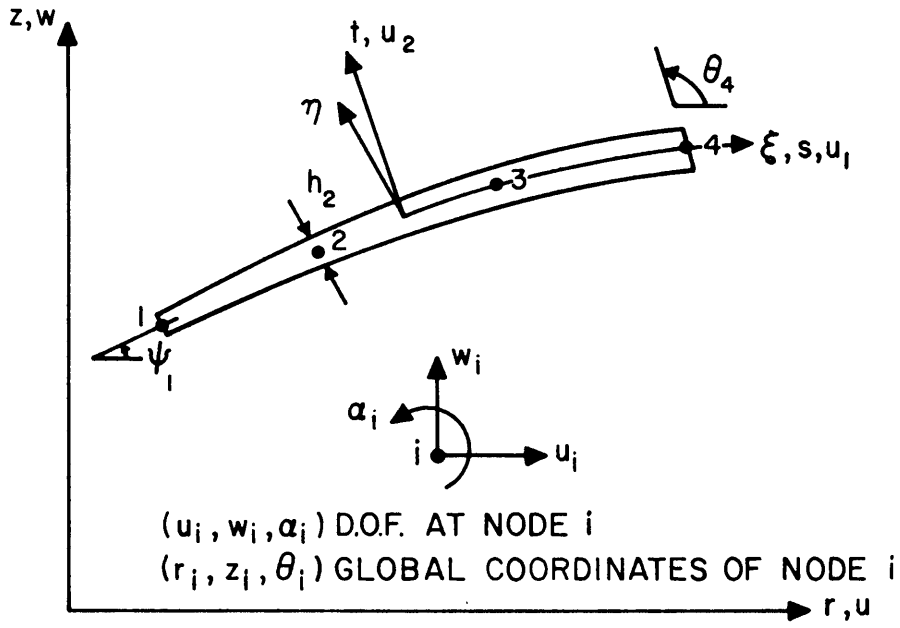

FIG. 5.2 GEOMETRY OF CUBIC ELEMENT, COORDINATE SYSTEMS, AND DEGREES OF FREEDOM

in Appendix A.

5.2 Displacement Field

The basic assumptions in describing the kinematics of the element are:

i) plane sections initially normal to the middle surface remain plane, but not necessarily normal to the middle surface after deformation, and

ii) displacement normal to the middle surface is constant through the thickness.

The classical Kirchhoff-Love hypothesis used in thin shell theories is relaxed. This permits shear deformations and hence moderately thick shells may be considered.

For any point (ξ, η) within an element, the global displacements (u, w) are then given by the following displacement field:

$$\begin{Bmatrix} u \\ w \end{Bmatrix} = \sum_{i=1}^{N} \phi_i(\xi) \begin{Bmatrix} u_i \\ w_i \end{Bmatrix} + \eta \sum_{i=1}^{N} \frac{1}{2} \phi_i(\xi) h_i \begin{Bmatrix} -\sin\theta_i \\ \cos\theta_i \end{Bmatrix} \alpha_i \qquad (5.3)$$

where

(u_i, w_i) = global displacements of node i, and

α_i = rotation of the normal at node i,

are the three degrees of freedom (DOF) at each node, Fig. 5.2. The first term in Eq. (5.3) represents the middle surface displacements and the second term, the effect of the rotation of the normal.

The same displacement field is assumed for both the incremental displacements, $\underset{\sim}{u}$, and the total displacements, ${}^{1}\underset{\sim}{u}$. The order of the interpolation polynomials should be equal to or greater than the order of the polynomials used in describing the geometry of the element, i.e. $N \geq M$, and $M = N$ has been chosen for simplicity

in this study.

If the vector of nodal point displacements and rotations is denoted by $\{\hat{u}\}$, the Eq. (5.3) may be written in the symbolic form

$$\{u\} = [\phi_u]\ \{\hat{u}\} \tag{5.4}$$

Finally, the displacements can be transformed from the global to the auxilary coordinate system (s, t) by the relation

$$\begin{Bmatrix} u_1 \\ u_2 \end{Bmatrix} = \begin{bmatrix} \cos\psi & \sin\psi \\ -\sin\psi & \cos\psi \end{bmatrix} \begin{Bmatrix} u \\ w \end{Bmatrix} \tag{5.5}$$

where the angle $\psi(\xi)$ is defined in Fig. 5.2.

5.3 Strain-Displacement Matrices

The increment in Lagrangian strain between configurations B_1 and B_2, referred to B_0, is decomposed into linear and nonlinear parts by

$$E_{IJ} = e_{IJ} + \eta_{IJ} \tag{2.20}$$

where

$$\begin{aligned} 2\, e_{IJ} &= u_{I|J} + u_{J|I} + {}^1u^K{}_{|I}\, u_{K|J} + {}^1u^K{}_{|J}\, u_{K|I} \\ 2\, \eta_{IJ} &= u^K{}_{|I}\ u^K{}_{|J} \end{aligned} \tag{2.19}$$

The linear part may be rewritten as

$$2\, e_{IJ} = (\delta^K{}_I + {}^1u^K{}_{|I})u_{K|J} + (\delta^K{}_J + {}^1u^K{}_{|J})u_{K|I} \tag{5.6a}$$

or

$$2\, e_{IJ} = {}^1F^K_{\cdot I}\, u_{K|J} + {}^1F^K_{\cdot J}\, u_{K|I} \tag{5.6b}$$

For axisymmetric deformations, the three coordinate axes are identified with the meridional (s), hoop, and transverse normal (t) directions, respectively.

Hence,

$$u^1|_2 = u^2|_1 = u^2|_3 = u^3|_2 = 0$$

$$^1u^1|_2 = {}^1u^2|_1 = {}^1u^2|_3 = {}^1u^3|_2 = 0 \tag{5.7}$$

$$^1F^1_{\cdot 2} = {}^1F^2_{\cdot 1} = {}^1F^2_{\cdot 3} = {}^1F^3_{\cdot 2} = 0$$

Love's first thin shell approximation postulates that the transverse normal stresses are negligible, i.e.

$$S^{33} = {}^1S^{33} = 0 \tag{5.8}$$

and this postulate is also retained for moderately thick shells in order to avoid the constraints imposed on the transverse direction by the assumed displacement field. However, the second assumption in section 5.2 implies that

$$u^3|_3 = {}^1u^3|_3 = 0 \ , \ {}^1F^3_{\cdot 3} = 1 \tag{5.9}$$

An inconsistency arises from the mutually exclusive nature of the two conditions, $U^3|_3 = 0$ and $S^{33} = 0$, and the generalized plane stress approach is used to remove the inconsistency. The following approximations are then made:

$$(u^3|_3)^* = (E_{33})^* \tag{5.10}$$

and

$$({}^1F^3_{\cdot 3})^* = 1 + ({}^1E_{33})^* \tag{5.11}$$

where the asteriks indicate physical components. The condensation of the constitutive relations for the generalized plane stress, using Eq. (5.10), was described in section 3.3. If $E_{33} << 1$, $^1E_{33} << 1$, the deformation gradient $^1F^3_{\cdot 3}$ may be approximated by

unity, but Eq. (5.11) must be used in problems where thickness changes are significant. The strains E_{33} and ${}^1E_{33}$ are evaluated using constitutive relations and not from kinematics. The constitutive relations themselves are given in terms of physical components and as such no distinction is made between physical and tensor components in the following development.

The linear part of the strain increment is related to the displacement gradients by means of a deformation gradient matrix, i.e.

$$\{e\} = [\Lambda] \quad \{u_\partial\} \tag{5.12}$$

where

$$\langle e \rangle = \langle e_{11} \; e_{22} \; 2e_{13} \rangle \tag{5.13}$$

$$\langle u_\partial \rangle = \langle \frac{\partial u_1}{\partial s} \; \frac{u}{r} \; \frac{\partial u_1}{\partial t} \; \frac{\partial u_2}{\partial s} \rangle \tag{5.14}$$

and $[\Lambda]$ is a deformation gradient matrix which can be obtained using Eq. (5.6b). This gives

$$\begin{Bmatrix} e_{11} \\ e_{22} \\ 2e_{13} \end{Bmatrix} = \begin{bmatrix} {}^1F^1_{:1} & 0 & 0 & {}^1F^3_{:1} \\ 0 & {}^1F^2_{:2} & 0 & 0 \\ {}^1F^1_{:3} & 0 & {}^1F^1_{:1} & {}^1F^3_{:3} \end{bmatrix} \begin{Bmatrix} \frac{\partial u_1}{\partial s} \\ \frac{u}{r} \\ \frac{\partial u_1}{\partial t} \\ \frac{\partial u_2}{\partial s} \end{Bmatrix} \tag{5.15}$$

Using Eq. (5.6a) the transformation $[\Lambda]$ between the strain increments and the displacement gradients can be rewritten as

$$[\Lambda] = \begin{bmatrix} 1 + \frac{\partial {}^1u_1}{\partial s} & 0 & 0 & \frac{\partial {}^1u_2}{\partial s} \\ 0 & 1 + \frac{{}^1u}{r} & 0 & 0 \\ \frac{\partial {}^1u_1}{\partial t} & 0 & 1 + \frac{\partial {}^1u_1}{\partial s} & 1 + {}^1E_{33} \end{bmatrix} \tag{5.16}$$

This transformation has to be recomputed at each step, but the transformation matrix [B], which relates the displacement gradients $\{u_\partial\}$ to the vector of incremental nodal point displacements and rotations $\{\hat{u}\}$, depends only on the undeformed configuration and the interpolation polynomials, and consequently remains unchanged throughout the analysis. The relationship is given as

$$\{u_\partial\} = [B]\ \{\hat{u}\} \tag{5.17}$$

and a similar transformation also relates $\{{}^1u_\partial\}$ to $\{{}^1\hat{u}\}$,

$$\{{}^1u_\partial\} = [B]\ \{{}^1\hat{u}\} \tag{5.18}$$

The matrix [B] may be decomposed into

$$[B(\xi,\eta)] = [B_1(\xi)] + \eta\,[B_2(\xi)] \tag{5.19}$$

where both $[B_1]$ and $[B_2]$ depend only on ξ and the dependence of [B] on η is kept as a multiplying factor outside the matrix $[B_2]$. Derivation of these displacement gradient matrices was given by Larsen [43] and is presented here in Appendix B. Combining Eqs. (5.12, 17) the linear part of the strain increment is obtained as

$$\begin{Bmatrix} \eta_{11} \\ \eta_{22} \\ \eta_{33} \end{Bmatrix} = \frac{1}{2} \begin{Bmatrix} \left(\frac{\partial u_1}{\partial s}\right)^2 + \left(\frac{\partial u_2}{\partial s}\right)^2 \\ \left(\frac{u}{r}\right)^2 \\ \frac{\partial u_1}{\partial s}\ \ \frac{\partial u_1}{\partial t} \end{Bmatrix} \tag{5.21}$$

The right hand side of this equation can be obtained easily once the displacement gradients $\{u_\partial\}$ are obtained using Eq. (5.17). However, an explicit nonlinear strain - displacement relation will be needed in the development of the geometric stiffness matrix and can be written as

$$\begin{Bmatrix} \eta_{11} \\ \eta_{22} \\ \eta_{13} \end{Bmatrix} = \frac{1}{2} \begin{Bmatrix} \langle \hat{u} \rangle [H_{11}] \{\hat{u}\} \\ \langle \hat{u} \rangle [H_{22}] \{\hat{u}\} \\ \langle \hat{u} \rangle [H_{13}] \{\hat{u}\} \end{Bmatrix} \tag{5.22}$$

If $\langle b_1 \rangle_i$ and $\langle b_2 \rangle_i$ denote the i^{th} row of $[B_1]$ and $[B_2]$, respectively, the submatrices $[H_{11}]$, $[H_{22}]$ and $[H_{13}]$ can be written in the form [43] :

$$\begin{aligned} [H_{11}] &= [\Gamma]_1 + \eta\,[\pi]_1 + \eta^2\,[\Omega]_1 \\ [H_{22}] &= [\Gamma]_2 + \eta\,[\pi]_2 + \eta^2\,[\Omega]_2 \\ [H_{13}] &= [\Gamma]_3 + \eta\,[\pi]_3 + \eta^2\,[\Omega]_3 \end{aligned} \tag{5.23}$$

where

$$\begin{aligned} [\Gamma]_1 &= \{b_1\}_1 \langle b_1 \rangle_1 + \{b_1\}_4 \langle b_1 \rangle_4 \\ [\Gamma]_2 &= \{b_1\}_2 \langle b_1 \rangle_2 \\ [\Gamma]_3 &= \{b_1\}_1 \langle b_1 \rangle_3 \\ [\pi]_1 &= \{b_1\}_1 \langle b_2 \rangle_1 + \{b_2\}_1 \langle b_1 \rangle_1 + \{b_1\}_4 \langle b_2 \rangle_4 \\ &\quad + \{b_2\}_4 \langle b_1 \rangle_4 \\ [\pi]_2 &= \{b_1\}_2 \langle b_2 \rangle_2 + \{b_2\}_2 \langle b_1 \rangle_2 \\ [\pi]_3 &= \{b_1\}_1 \langle b_2 \rangle_3 + \{b_2\}_1 \langle b_1 \rangle_3 \\ [\Omega]_1 &= \{b_2\}_1 \langle b_2 \rangle_1 + \{b_2\}_4 \langle b_2 \rangle_4 \\ [\Omega]_2 &= \{b_2\}_2 \langle b_2 \rangle_2 \\ [\Omega]_3 &= \{b_2\}_1 \langle b_2 \rangle_3 \end{aligned}$$

These submatrices can be computed at each integration point within an element. They depend only on ξ and again the dependence on η is merely in the form of multiplying factors. As is the case with $[B_1]$ and $[B_2]$, these submatrices also remain constant throughout the analysis since they are obtained directly from $[B_1]$ and $[B_2]$.

A final point to be noted with regard to the strain-displacement relations concerns the singularity in hoop strains at the apex. This may be removed by the application of L' Hospital's rule. If the tangent to the middle surface at the apex is horizontal, the hoop and meridional strains are set equal.

5.4 Element Stiffness Matrices

The incremental stiffness matrix $[K_o]$ and the geometric stiffness matrix $[K_G]$ are considered in this section. These element stiffness matrices that are present in the statement of linearized incremental equations of motion, Eq.(4.9), are obtained using Eqs. (4.3b, e) together with the expressions derived in section 5.3 for the strain - displacement matrices. The volume integrals are evaluated using numerical quadrature. While integration along the meridional direction is performed using Gaussian quadrature, an option has been provided to use either Gaussian or Simpson integration in the transverse direction. In the case of elastic - plastic deformation, the onset of yielding (at the extreme fibers) in an element can be detected promptly if Simpson integration is used in the transverse direction, whereas there may be a delay if Gaussian quadrature is used since the monitoring stations associated with the latter are all placed in the interior of the element.

The element stiffness matrix is the sum of $[K_o]$ and $[K_G]$. The stiffness matrix for the entire structure is obtained by the standard assembly process of the direct stiffness method.

5.4.1 Incremental Stiffness $[K_o]$

This matrix may be obtained using Eq. (4.3b) together with the linear strain - displacement expression in Eq. (5.20)

$$\delta\hat{\underset{\sim}{u}}^T \cdot \underset{\sim}{K}_0 \cdot \hat{\underset{\sim}{u}} = \int_{B_0} C^{IJKL}\, e_{KL}\, \delta e_{KL}\, dV \tag{4.3b}$$

since

$$\{e\} = [\Lambda]\,[B]\,\{\hat{u}\}$$

$$\{\delta e\} = [\Lambda]\,[B]\,\{\delta\hat{u}\}$$

and

$$dV = 2\pi r\, dr dz = 2\pi r|J|\, d\eta d\xi$$

one can obtain

$$[K_0] = 2\pi \int_{-1}^{1}\int_{-1}^{1} [B]^T\,[\Lambda]^T\,[C]\,[\Lambda]\,[B]\, r\,|J|\, d\eta d\xi \tag{5.24}$$

Defining

$$[D] = [\Lambda]^T\,[C]\,[\Lambda] \tag{5.25}$$

$$[K_0] = 2\pi \int_{-1}^{1}\int_{1}^{1} [B]^T\,[D]\,[B]\, r\,|J|\, d\eta d\xi \tag{5.26}$$

Since

$$[B(\xi,\eta)] = [B_1(\xi)] + \eta\,[B_2(\xi)] \tag{5.19}$$

one can rewrite $[K_0]$ as

$$[K_0] = 2\pi \int_{-1}^{1} ([B_1]^T\,[D_1]\,[B_1] + [B_1]^T\,[D_2]\,[B_1] + [B_2]^T\,[D_2][B_1] + [B_2]^T\,[D_3]\,[B_2])\, d\xi \tag{5.27}$$

where $[D_1(\xi)]$, $[D_2(\xi)]$ and $[D_3(\xi)]$ are obtained by integrating across the thickness, i.e.

$$\begin{aligned}
[D_1(\xi)] &= \int_{-1}^{1} [D]\, r(\xi,\eta)\, |J(\xi,\eta)|\, d\eta \\
[D_2(\xi)] &= \int_{-1}^{1} \eta[D]\, r(\xi,\eta)\, |J(\xi,\eta)|\, d\eta \\
[D_3(\xi)] &= \int_{-1}^{1} \eta^2 [D]\, r(\xi,\eta)\, |J(\xi,\eta)|\, d\eta
\end{aligned} \tag{5.28}$$

These integrations are performed rather easily by using the expressions derived in Appendix B for r and $|J|$. The abcissas and weights for quadrature formulas can be obtained from standard mathematical tables [110].

The matrix $[K_0]$ is seen to consist of four terms, Eq. (5.27). The first term accounts for membrane action alone, and the last term for bending alone. The second and third terms represent the coupling between membrane and bending which vanishes in the case of flat plates or shallow shells undergoing small elastic deformations.

5.4.2 Geometric Stiffness $[K_G]$

The nonlinear strain - displacement relation of Eq. (5.22) is substituted into Eq. (4.3e) for the evaluation of this part of the element stiffness

$$\delta\hat{\underset{\sim}{u}}^T \cdot \underset{\sim}{K}_G \cdot \hat{\underset{\sim}{u}} = \int_{B_0} {}^1S^{IJ}\, \delta\eta_{IJ}\, dV \qquad (4.3e)$$

$$= \int_{B_0} \langle\delta\eta\rangle \{{}^1S\}\, dV$$

where

$$\langle\delta\eta\rangle = \langle\delta\eta_{11} \quad \delta\eta_{22} \quad \delta\eta_{13}\rangle$$

and

$$\{{}^1S\}^T = \langle {}^1S^{11} \quad {}^1S^{22} \quad 2\,{}^1S^{13}\rangle$$

Taking the variation of Eq. (5.22), one gets

$$\delta\eta_{11} = \langle\delta\hat{u}\rangle\ [H_{11}]\ \{\hat{u}\}$$

$$\delta\eta_{22} = \langle\delta\hat{u}\rangle\ [H_{22}]\ \{\hat{u}\} \qquad (5.29)$$

$$\delta\eta_{13} = \langle\delta\hat{u}\rangle\tfrac{1}{2}([H_{13}]^T + [H_{13}])\ \{\hat{u}\}$$

where $[H_{11}]$, $[H_{22}]$ and $[H_{13}]$ are defined in section 5.3. Upon substitution of these expressions into Eq. (4.3e) one gets

$$\langle\delta\hat{u}\rangle\ [K_G]\ \{\hat{u}\} = \langle\delta\hat{u}\rangle \int_{B_0} ({}^1S^{11}[H_{11}] + {}^1S^{22}[H_{22}] + 2\ {}^1S^{13}\ \tfrac{1}{2}\ ([H_{13}]^T + [H_{13}])\ dV\ \{\hat{u}\} \qquad (5.30)$$

or,

$$[K_G] = 2\pi \int_{-1}^{1}\int_{-1}^{1} \langle {}^1S\rangle \begin{bmatrix} [H_{11}] \\ [H_{12}] \\ \tfrac{1}{2}([H_{13}]^T + [H_{13}]) \end{bmatrix} r\,|J|\ d\eta d\xi$$

$$= 2\pi \int_{-1}^{1}\int_{-1}^{1} \langle {}^1S\rangle \begin{bmatrix} [\Gamma]_1^* + \eta\,[\pi]_1^* + \eta^2\,[\Omega]_1^* \\ [\Gamma]_2^* + \eta\,[\pi]_2^* + \eta^2\,[\Omega]_2^* \\ [\Gamma]_3^* + \eta\,[\pi]_3^* + \eta^2\,[\Omega]_3^* \end{bmatrix} r\ |J| d\eta d\xi \qquad (5.31)$$

where

$$[\Gamma]_i^* = [\Gamma]_i \text{ for } i = 1,2$$
$$[\Gamma]_3^* = \tfrac{1}{2}([\Gamma]_3^T + [\Gamma]_3)$$

and similar definitions hold for $[\pi]_i^*$ and $[\Omega]_i^*$.

Define the following row vectors:

$$\langle M_0(\xi)\rangle = \int_{-1}^{1} \langle {}^1S\rangle\, r(\xi,\eta)|J(\xi,\eta)|\, d\eta$$

$$\langle M_1(\xi)\rangle = \int_{-1}^{1} \eta\, \langle {}^1S\rangle\, r(\xi,\eta)\, |J(\xi,\eta)|\, d\eta \qquad (5.32)$$

$$\langle M_2(\xi)\rangle = \int_{-1}^{1} \eta^2\, \langle {}^1S\rangle\, r(\xi,\eta)\, |J(\xi,\eta)|\, d\eta$$

Eq. (5.31) can then be simplified to

$$[K_G] = 2\pi \int_{-1}^{1} \sum_{i=1}^{3} (M_{0i}\, [\Gamma]_i^* + M_{1i}\, [\pi]_i^* + M_{2i}\, [\Omega]_i^*)\, d\xi \qquad (5.33)$$

where M_{0i}, M_{1i} and M_{2i} represent the i^{th} elements of the vectors defined in Eq. (5.32).

Note that the stress vector $\langle {}^1S\rangle$ in Eq. (5.32) must be post-multiplied by

$$\begin{bmatrix} \frac{1}{|J|^2} & & \\ & \frac{1}{r^2} & \\ & & \frac{1}{|J|^2} \end{bmatrix}$$

The integrations across the η - direction are again simplified by the use of expressions obtained in Appendix B for $r(\xi,\eta)$ and $|J(\xi,\eta)|$.

5.5 Element Mass Matrix

The use of the same displacement field assumptions that are used for element stiffness evaluation leads to a consistent mass matrix formulation and can be obtained from Eq. (4.3a). The advantage of using such a mass matrix is the existence of upper bounds when used in conjunction with a dis-

placement compatible finite element [46,47], but this advantage is lost if incompatible displacement modes are added to an element. The primary disadvantage lies in the greater computational effort involved compared to the physical lumped mass procedure. As also pointed out in [47], computations required for evaluation of consistent mass matrix involve functions of higher order than those that occur in stiffness computations and a larger number of integration points within the element may be needed to avoid problems in numerical sensitivity.

Whereas derivatives of the displacement field are involved in the integrals for evaluation of stiffness, the expressions for mass matrix are only in terms of the polynomials assumed in the displacement field and not their derivatives. Since the accuracy in polynomial representation of a field variable is always superior to that of the derivatives (obtained from differentiation of the polynomials), it is justifiable to use an independent lower order displacement field assumption to approximate the inertia forces. The simplest form is obtained when the total mass of an element is taken into account by means of physical lumped masses assigned to the element nodal points, resulting in a diagonal lumped mass matrix. Lumping the masses at the nodes is quite straightforward for simple elements but may present some difficulties in the case of more complex elements for which special procedures may have to be devised. Appendix C presents the procedure used in the case of the four nodal point degenerate isoparametric element used in this study and is similar to the procedure presented in [105] for isoparametric elements except for the addition of rotatory inertia terms.

5.6 Element Damping Matrix

The effect of damping forces on the structure are included in the incremental equations of motion as discussed in section 4.3. Once the mass and incremental stiffness matrices have been evaluated for an element, the damping matrix is obtained, following Eq. (4.10), as

$$[C] = \alpha\,[M] + \beta[{}^{0}K_{0}] \tag{5.34}$$

where

$[{}^{0}K_{0}]$ is the incremental element stiffness at zero time

and

α,β are the mass and stiffness proportional damping factors, respectively.

5.7 Consistent Nodal Forces

5.7.1 Internal Resting Forces

The internal resisting forces acting at the nodal points of an element are obtained using the virtual work expression

$$\delta\hat{\underset{\sim}{u}} \cdot {}^{1}\underset{\sim}{F}^{R} = \int_{B_0} {}^{1}S^{IJ}\,\delta e_{IJ}\,dV \tag{4.3h}$$

$$= \int_{B_0} \langle\delta e\rangle\,\{{}^{1}S\}\,dV$$

Since

$$\{e\} = [\Lambda]\,[B]\,\{\hat{u}\},$$

$$\{\delta e\} = [\Lambda]\,[B]\,\{\delta\hat{u}\}$$

and Eq. (4.3h) can be rewritten as

$$\hat{\delta u} \cdot {}^{1}F^{R} = \langle \hat{\delta u} \rangle \int_{B_0} [B]^T [\Lambda]^T \{{}^{1}S\} \, dV$$

or

$$\{{}^{1}F^{R}\} = 2\pi \int_{-1}^{1} \int_{-1}^{1} [B]^T [\Lambda]^T \{{}^{1}S\} \, r \, |J| \, d\eta d\xi \tag{5.35}$$

Recalling that

$$[B] = [B_1(\xi)] + \eta \, [B_2(\xi)] \tag{5.19}$$

and defining

$$\{N_0(\xi)\} = \int_{-1}^{1} [\Lambda]^T \{{}^{1}S\} \, r(\xi,\eta) \, |J(\xi,\eta)| \, d\eta$$

$$\{N_1(\xi)\} = \int_{-1}^{1} \eta \, [\Lambda]^T \{{}^{1}S\} \, r(\xi,\eta) \, |J(\xi,\eta)| \, d\eta$$

one obtains the internal resisting forces in an element as

$$\{{}^{1}F^{R}\} = 2\pi \int_{-1}^{1} ([B_1]^T \{N_0\} + [B_1]^T \{N_1\}) \, d\xi \tag{5.37}$$

Numerical integration is used in both the ξ- and η- directions and a direct assembly of element force vectors gives the internal resisting force vector for the entire structure.

5.7.2 Viscoplastic Pseudo - Loading

The last term in the virtual work expression of Eq. (2.93) gives rise to the viscoplastic pseudo - loading which can be evaluated for each element in a manner analogous to that used for the internal resisting forces,

$$\hat{\delta u} \cdot R^{VP} = \int_{B_0} \langle \delta e \rangle \{S^{VP}\} \, dV \tag{5.38}$$

$$= \langle \hat{\delta u} \rangle \int_{B_0} [B]^T [\Lambda]^T \{S^{VP}\} \, dV$$

or,

$$\{R^{VP}\} = \int_{B_0} [B]^T [\Lambda]^T \{S^{VP}\} \, dV \tag{5.39}$$

where S^{VP} is the time dependent viscoplastic Piola - Kirchhoff stress increment between B_1 and B_2 and is given by Eq. (2.92).

Let $\{S^{VP}\}^T = \langle S_{11}^{VP} \; S_{22}^{VP} \; 2S_{13}^{VP} \rangle$

and define

$$\{Q_0(\xi)\} = \int_{-1}^{1} [\Lambda]^T \{S^{VP}\} \, r(\xi,\eta) \, |J(\xi,\eta)| \, d\eta$$

and (5.40)

$$\{Q_1(\xi)\} = \int_{-1}^{1} \eta \, [\Lambda]^T \{S^{VP}\} \, r(\xi,\eta) \, |J(\xi,\eta)| \, d\eta$$

Proceeding as in section 5.7.1, the viscoplastic pseudo - loading can be obtained as

$$\{R^{VP}\} = 2\pi \int_{-1}^{1} ([B_1]^T \{Q_0\} + [B_2]^T \{Q_1\}) \, d\xi \tag{5.41}$$

5.7.3 Externally Applied Loading

The element nodal force vectors, $\{^2R\}$, due to traction type loading can be obtained using the virtual work expressions derived in section 2.4 for the nonconservative and conservative loads.

Nonconservative Loading

For a pressure type nonconservative loading, the nodal load vector is given by

$$\delta\hat{\underset{\sim}{u}} \cdot {}^2\underset{\sim}{R} = -\int_{\partial B_0} \{\delta u\}^T \frac{\rho_0}{\rho} \, {}^2p[{}^1F^{-1}]^T \{N\} \, dA \tag{4.3f}$$

From Eq. (5.4) one has

$$\begin{Bmatrix} u \\ w \end{Bmatrix} = [\phi_u] \{\hat{u}\}$$

In order to make the matrix multiplications in Eq. (4.3f) consistent, $\{\delta u\}^T$ must have three components, δu, δu_θ and δw. The displacement in the circumferential direction vanishes for axisymmetric deformations; $\delta u_\theta = 0$. Hence, addition of a row filled with zeroes to the matrix $[\phi_u]$ is made to get a new transformation matrix $[\overline{\phi}_u]$, and

$$\begin{Bmatrix} u \\ u_\theta = 0 \\ w \end{Bmatrix} = [\overline{\phi}_u] \{\hat{u}\} \tag{5.42}$$

which gives

$$\{\delta u\}^T = \{\delta \hat{u}\}^T [\overline{\phi}_u]^T \tag{5.43}$$

Substituting this into Eq. (4.3f) one gets

$$\delta \hat{\underset{\sim}{u}} \cdot {}^2\underset{\sim}{R} = - \langle \delta \hat{u} \rangle \int_{\partial B_0} \frac{\rho_0}{\rho} [\overline{\phi}_u]^T \, {}^2p \, [{}^1F^{-1}]^T \{N\} \, dA \tag{5.44}$$

From the requirement of conservation of mass

$$\frac{\rho_0}{\rho} = \det [{}^1F] \tag{5.45}$$

The unit normal to the middle surface may be decomposed as,

Fig. 5.2,

$$\langle N \rangle = \langle -\sin\psi \quad 0 \quad \cos\psi \rangle \tag{5.46}$$

Finally, if $\{^2p\}$ is the vector of hydrostatic pressure magnitudes at the nodal points,

$$^2p = \langle \phi \rangle \{^2p\} \tag{5.47}$$

where $\langle \phi \rangle$ is the vector of interpolation polynomials.

Defining

$$\beta = \left[\left(\frac{\partial r}{\partial \xi}\right)^2 + \left(\frac{\partial z}{\partial \eta}\right)^2\right]^{\frac{1}{2}} \tag{5.48}$$

the differential surface area is given as

$$dA = 2\pi r(\xi)\ \beta(\xi)\ d\xi \tag{5.49}$$

The element load vector is then given by

$$\{^2R\} = -2\pi \int_{-1}^{1} [\bar{\phi}_u]^T \langle \phi \rangle \{^2p\}\ [^1F^{-1}]^T \{N\}\ r(\xi)\ \beta(\xi)\ \det [^1F] d\xi \tag{5.50}$$

Conservative Loading

In the case of conservative loading the element nodal force vector for surface traction can be obtained starting from the virtual work expression of Eq. (2.84)

$$\delta\hat{\underset{\sim}{u}} \cdot {}^2\underset{\sim}{R} = \int_{\partial B_0} \delta u_I\ (^1F^{-1})^I_{\cdot J}\ {}^2\bar{t}^J\ dA$$

The load intensity at any point on the loading surface is given by

$$\begin{Bmatrix} {}^2p_1 \\ \\ {}^2p_2 \end{Bmatrix} = \begin{bmatrix} \langle\phi\rangle & \vdots & \\ \cdots\cdots & \vdots & \cdots\cdots \\ & \vdots & \langle\phi\rangle \end{bmatrix} \begin{Bmatrix} {}^2\hat{p}_1 \\ \\ {}^2\hat{p}_2 \end{Bmatrix} \tag{5.51}$$

with ${}^2p_1$ and ${}^2p_2$ being the load intensities in the r- and z- directions, respectively, in configuration B_2. $\langle\phi\rangle$ is a vector consisting of interpolation polynomials $\phi_i(\xi)$ and ${}^2\hat{p}_1$ and ${}^2\hat{p}_2$ are vectors of load intensities at nodal points. As discussed in section 2.4, the load intensities ${}^2p_1$ and ${}^2p_2$ must then be expressed in terms components ${}^2p_1^c$, 0, ${}^2p_2^c$ along the convected base vectors ${}^2\underset{\sim}{G}_I$. As in the case of non-conservative loads, one can also write

$$\langle\delta u\rangle = \langle\delta\hat{u}\rangle\, [\overline{\phi}_u]^T \tag{5.43}$$

and

$$dA = 2\pi\, r(\xi)\, \beta(\xi)\, d\xi \tag{5.49}$$

which, when substituted into the virtual work expression, have

$$\delta\underset{\sim}{u} \cdot {}^2\underset{\sim}{R} = \langle\delta\hat{u}\rangle\, 2\pi \int_{-1}^{1} [\overline{\phi}_u]^T\, [{}^1F^{-1}] \begin{Bmatrix} {}^2p_1^c \\ 0 \\ {}^2p_2^c \end{Bmatrix} r(\xi)\, \beta(\xi)\, d\xi$$

or,

$$\{{}^2R\} = 2\pi \int_{-1}^{1} [\bar{\Phi}_u]^T \, [{}^1F^{-1}] \begin{Bmatrix} {}^2p_1^c \\ 0 \\ {}^2p_2^c \end{Bmatrix} r(\xi)\, \beta(\xi)\, d\xi \qquad (5.52)$$

The inverse of the deformation gradient is obtained numerically and Eq. (5.50) or (5.52) is integrated using Gaussian guadrature. The load vector for the entire structure is obtained by direct assembly of the element nodal force vectors.

6. NUMERICAL EXAMPLES

6.1 Description of Computer Programs

Two separate programs have been written using the formulation presented in the foregoing sections for the nonlinear static and dynamic analysis of shells of revolution under axisymmetric loading. The coding is in Fortran IV for use on CDC 6400.

The programs use basically high speed, in-core storage, except small segments where low speed, tape-simulated disc storage is used for displacement gradient and stress-strain matrices. Dynamic storage allocation is utilized whereby the total core storage requirements are separated into fixed and variable parts. The fixed part consists of instructions, non-subscripted variables, and arrays independent of the size of each individual problem. The variable part consists of an array A that appears in the blank COMMON.

The fixed storage requirement for the binary versions of the programs is approximately 56000 (octal). The variable requirement is calculated within the programs for any given problem (depending on the number of elements, nodal points, etc.). The field length required for execution is reset within the programs using system function LOCF and system subroutine MEMORY which are available on the CDC 6400 computer at the University of California, Berkeley.

PROGRAM NLAXDP: This is the program for nonlinear analysis of elastic-plastic shells of revolution under axisym-

metric static and/or dynamic loads. The von Mises yield criterion, and isotropic hardening laws are used in the flow theory of plasticity. The program consists of:

MAIN program computes the variable storage requirements, dynamically assigns the needed storage and drives the major subroutines.

INPUTD subroutine reads and echos the geometric and material data and initializes all matrices.

STIFFNS. The displacement gradient matrices are computed during the first increment at integration and nodal points and stored on discs for use during subsequent increments. The stress-strain matrix is read from a tape and numerical integration is used for evaluation of element stiffness matrices with four or six Gaussian integration points in the meridional direction and two to seventeen Gaussian or Simpson stations over the thickness (the minimum of two Gaussian points is sufficent for elastic problems). The element mass and damping matrices remain constant for the entire analysis. They are computed during the first increment and stored on a disc along with the linear elastic element stiffnesses. These matrices can be recovered from the disc for use in the subsequent increments. Recomputation of incremental element stiffnesses can then be avoided for those elements which are found to be in the elastic loading or unloading range. The stress-strain matrix is transformed according to the deformation gradients, and incremental and geometric stiffnesses are assembled for the entire system. The equilibrium modal forces are also computed from the stress

field.

DISPL. This subroutine imposes the boundary conditions, triangularizes the system stiffness matrix and also drives the load generating subroutines NODLOD and DYNLOD, and the equation solver NUMSYM. The incremental and total nodal displacements are computed and, in the case of dynamic analyses, the accelerations and velocities at the nodal points are also computed.

STRESS computes the strains and Piola-Kirchhoff stresses at integration and nodal points, and also transforms these stresses to Cauchy stresses. The plastic strain increments are computed and the MATP subroutine is called which checks the loading criterion, interpolates material properties given in discrete form and determines the stress-strain relationship for elastic-plastic deformations. All stress-strain matrices are stored on disc and all the required stress results are printed out.

PROGRAM VISPAX: This program treats large displacement static and/or dynamic analysis of shells of revolution made of elastic-viscoplastic materials. It can also be used to obtain elastic-plastic solutions when the time parameter is used as an artifice. This program is very similar to the elastic version of the previous program. The main difference is in the STIFFNS subroutine where pseudo-loading due to viscoplastic strains is computed.

VISPL subroutine computes the equivalent viscoplastic strain rates, increments of viscoplastic strains and stresses,

and also interpolates material property data given in discrete form to obtain the new values of static loading surface.

These programs have been provided with restart capability. An external magnetic tape is supplied by the user and an index array in the data deck specifies the steps at the end of which the requisite restart information is to be placed on this tape. The solution can then be restarted at any step N in a new run if the required information at the end of step N-1 is available on the tape.

This restart provision is extremely useful from many viewpoints. It enables the analyst to carry out a solution in a truly incremental manner in that he can apply a certain number of load or time steps, study the results obtained, and decide on the next series of steps to be applied or even go back to some previous stage of computation if he judges it necessary to alter the load increments or time steps.

6.2 Elastic and Elastic-Plastic Analyses

Several examples will be presented in this section to illustrate the capability of Program NLAXDP in solving static and dynamic problems for elastic and elastic-plastic material behavior.

6.2.1 Static Analyses

An example of shallow spherical cap was presented in section 5.5 to illustrate the capability of the program to perform linear dynamic analyses using lumped mass idealization and step-by-step time integration. Before proceeding further with

large displacement dynamic analyses problems, the accuracy of the program for highly nonlinear analysis is demonstrated in the case of two static problems.

6.2.1 (a) Elastic Shallow Spherical Cap

The theoretical as well as numerical analysis of the nonlinear behavior of spherical caps have been pursued by a great many investigators. Yaghmai [36] gave an exhaustive review of these works and presented a bibliography of this field including experimental investigations.

The deformation mode depends on characteristic geometric properties of the shell. One such parameter is defined by Kornishin [111] as

$$\bar{\kappa} = a^2/Rh \tag{6.1}$$

where R is the radius of the middle surface, h is the shell thickness and a is the radius of the horizontal projection of the shell. Another commonly used parameter is

$$\lambda^2 = \sqrt{12(1 - \nu^2)}\, R \tag{6.2}$$

where ν is the Poisson's ratio for the material. The parameter introduced by Weinitschke [112, 113],

$$\mu^2 = \sqrt{12(1 - \nu^2)}\, R\alpha^2/h \tag{6.3}$$

where α is the half angle of the opening of the shell, is only a slight variation of Eq. (6.2), and for small values of α both λ and μ will be identical. For clamped shells with uniformly distributed pressure, axisymmetric deformation mode prevails for

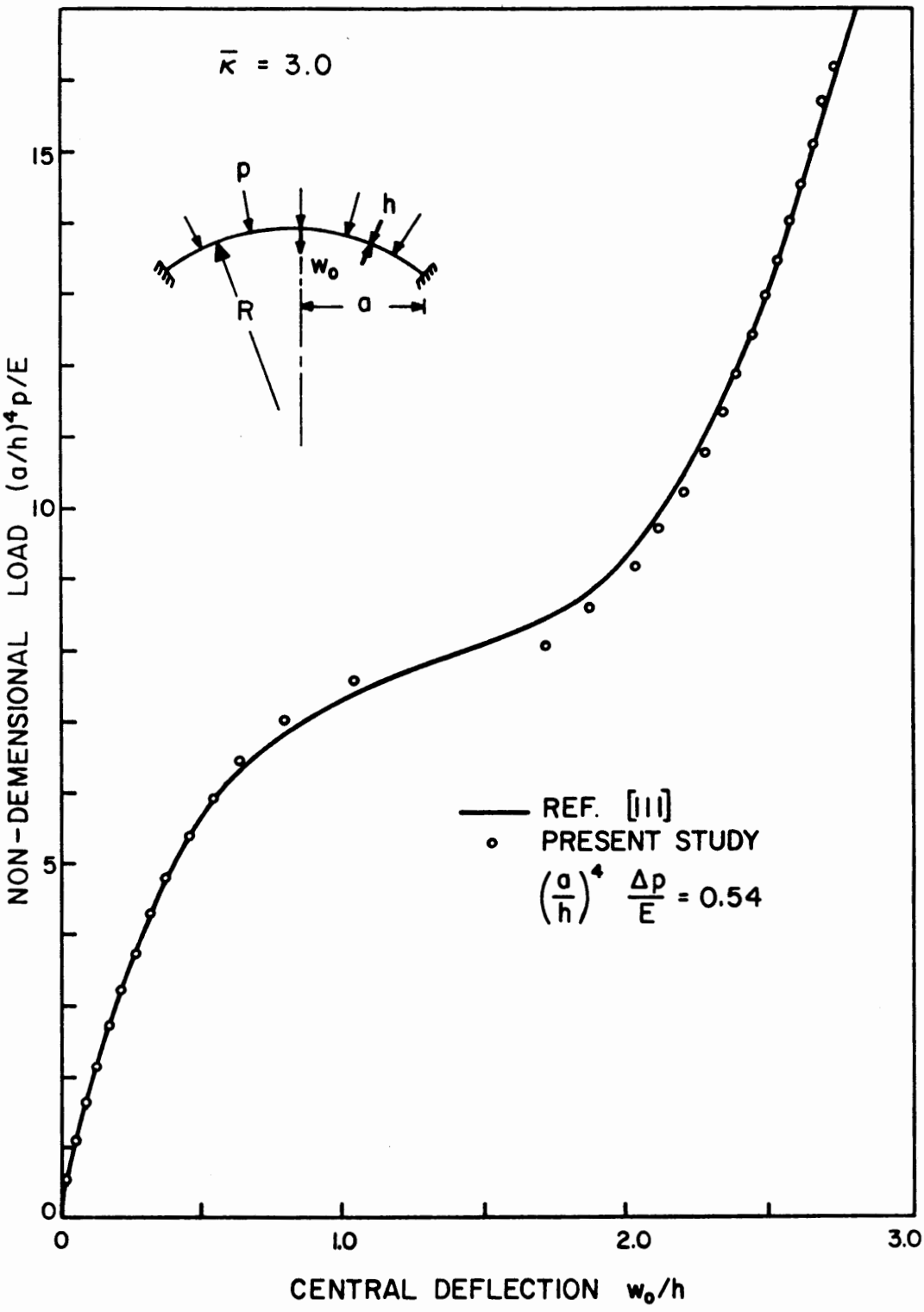

FIG. 6.1 LARGE DISPLACEMENT ELASTIC ANALYSIS OF SHALLOW SPHERICAL SHELL

$\mu \leq 5.5$.

A clamped shallow spherical cap with the parameter $\bar{\kappa} = 3$ is considered as an example problem. The non-dimensional load-deflection curve shown in Fig. 6.1 is obtained from the tabulated values of the power series solution given by Kornishin [111], and is valid for any thin shell for which $\bar{\kappa} = 3$ and Poisson's ratio $\nu = 0.3$. The results of finite element analysis, carried out using the incremental solution procedure together with an equilibrium correction at each step, is also shown in Fig. 6.1 and shows excellent agreement with Kornishin's solution. Seven elements were used to discretize the shell from the apex to the support and a nondimensional load increment of 0.54 was used throughout. It is interesting to note that the apex deflection is overestimated in the region where the slope of the curve is small but the solution is quickly brought back toward the theoretical solution because of the use of equilibrium correction.

6.2.1 (b) Elastic-Plastic Torispherical Pressure Head

The static analysis of a torispherical pressure head under internal pressure, including the effects of both material and geometric nonlinearities, is taken up as the next example. The shell is shown as an insert in Fig. 6.2 and has the following dimensions:

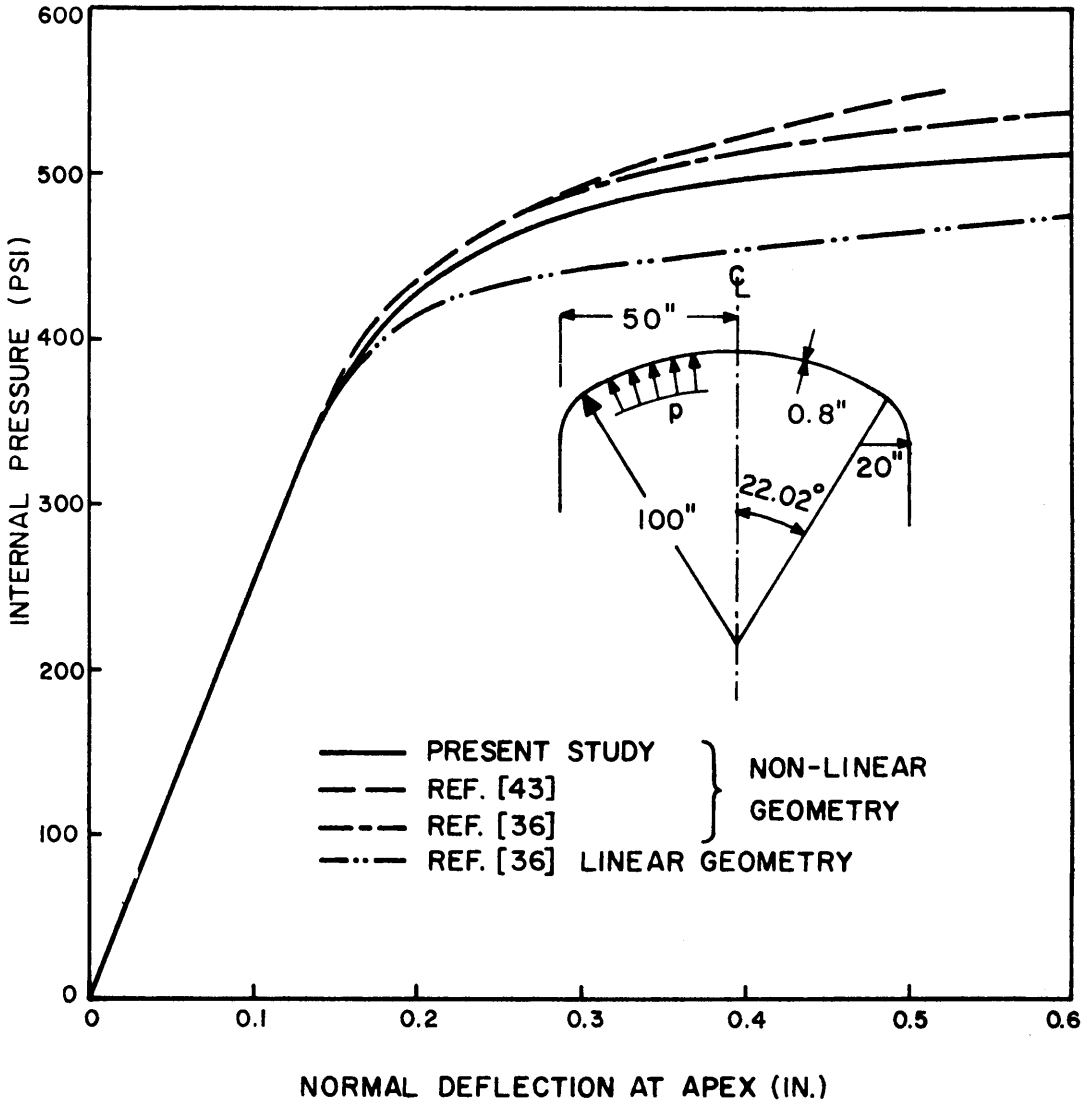

FIG. 6.2 ELASTIC-PLASTIC ANALYSIS OF TORISPHERICAL PRESSURE HEAD

D = 100 in. R = 100 in.

r = 20 in. h = 0.8 in.

The material is assumed to be elastic-perfectly plastic and to have the following properties:

Young's modulus, $E = 30 \times 10^6$ psi

Poisson's ratio, $\nu = 0.3$

Yield stress, $\sigma_y = 30{,}000$ psi

A total of 20 finite elements were used to discretize the shell from the apex to the support. Eight equal elements were used over the sphere, eight equal elements over the torus and four elements over the cylindrical portion. Four Gaussian integration points were used in the meridional direction and eleven Simpson points across the shell thickness. Very refined load increments of 5 psi were applied in order to obtain accurate solution in the nonlinear range.

This shell was studied earlier by Yaghmai [36] using the incremental formulation based on moving reference configuration and by Larsen [43] who used a Lagrangian formulation. The load-deflection curve for the apex displacement is plotted in Fig. 6.2 and compared with the results of Yaghmai (Δp=7.5 psi) and Larsen (Δp=10 psi). The linear solution given by Yaghmai is also plotted in the same figure. The present results indicate that the nonlinear behavior of the shell is much softer than predicted in

the earlier works. However, the load-carrying capacity is still considerably higher than in the linear analysis and can be taken advantage of in the design of such structures.

6.2.2 Dynamic Analysis

Examples presented in this section are:

(a) undamped forced vibrations of an elastic cantilever (linear geometry),

(b) elastic-plastic response of a simply supported beam (linear geometry), and

(c) elastic and elastic-plastic dynamic response of a shallow spherical thin cap (linear and nonlinear geometry).

6.2.2 (a) Linear Forced Vibrations of Cantilever

The geometry and material properties of an elastic cantilever beam and time history of the load to which it is subjected are shown in Fig. 6.3. The undamped forced vibration analysis of this beam was carried out as a trial problem. Both the Newmark ($\gamma = 0.5$, $\beta = 0.25$) and Wilson ($\theta = 1.4$) methods were used and the results compared with the known exact solution. The time increment used in the analysis is 0.004 sec. and the results for the cantilever tip deflection normalized with respect to the static solution are plotted in Fig. 6.4.

The effect of damping inherent in the Wilson θ method is to reduce the value of the peak amplitude compared with the Newmark method and this can be observed in Fig. 6.4. Even the Newmark method which does not introduce any artificial viscosity into the numerical integration is seen to have reduced the peak amplitude to slightly below 2.0 but this can be attributed to the discretization error

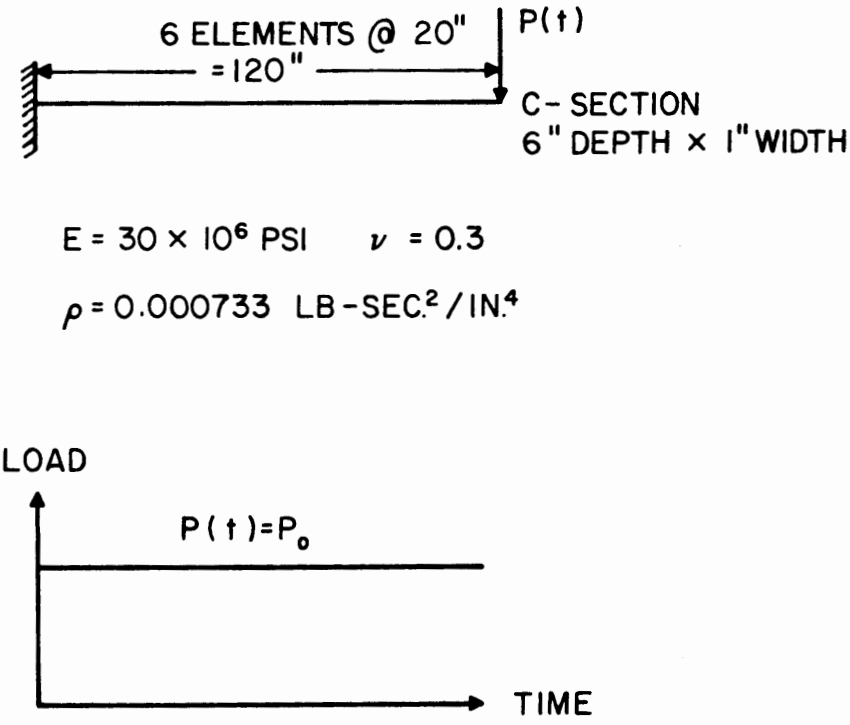

FIG. 6.3 LOAD-TIME VARIATION FOR DYNAMIC ANALYSIS OF CANTILEVER BEAM

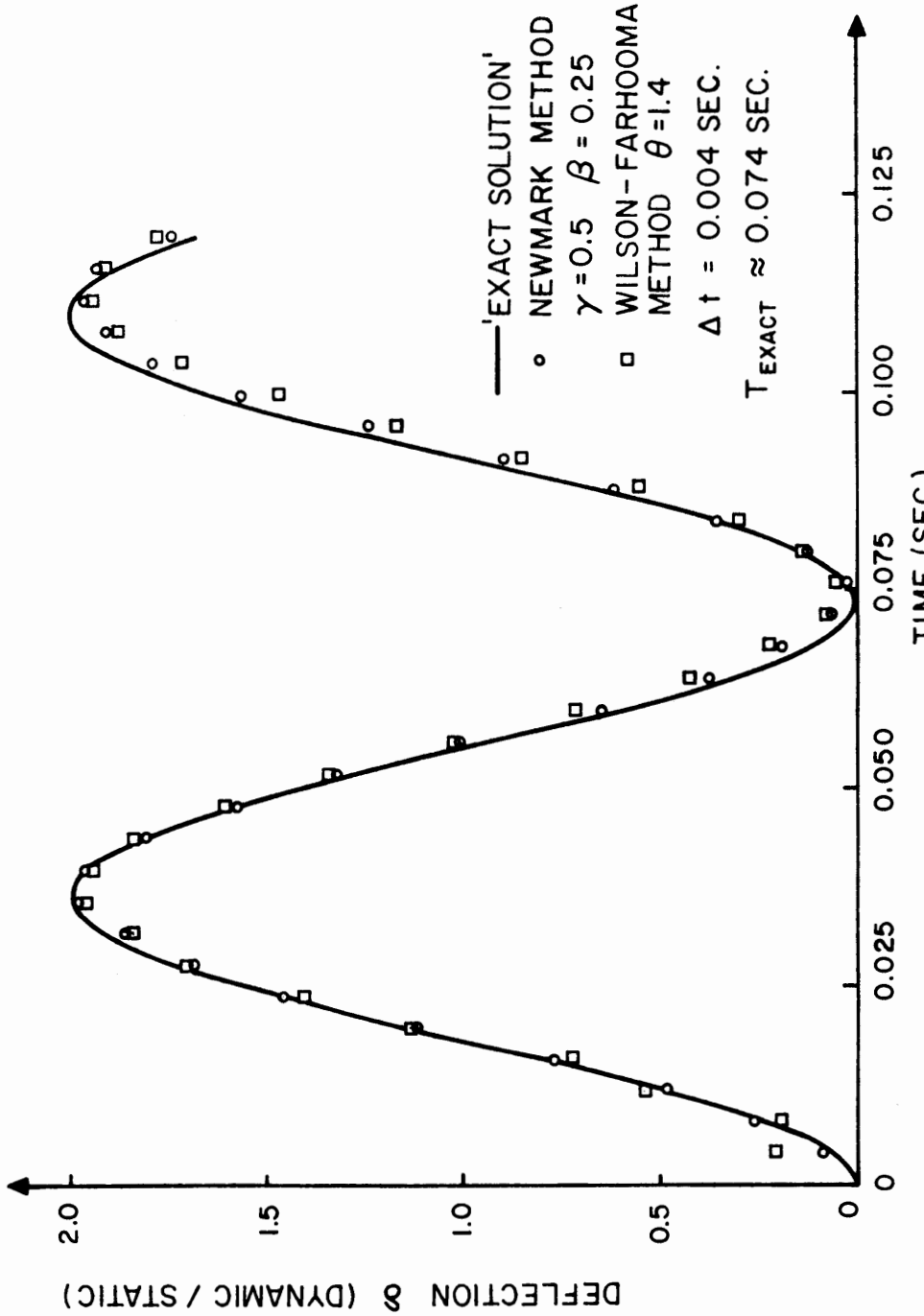

FIG.6.4 DEFLECTION OF A CANTILEVER BEAM

involved and not to the solution procedure itself. The elongation in time period is a function of the ratio $\Delta t/T$ and can be reduced if shorter time increments are used in the analysis. It has been pointed out by Goudreau and Taylor [114] that the Wilson θ method exhibits very poor behavior for suddenly applied loads or if the system is suddenly released from a deflected position, and the initial inaccuracies in the solution in this example may be due to the nature of the algorithm itself.

6.2.2 (b) Elastic-Plastic Response of Simply Supported Beam

A simply supported beam is subjected to uniformly distributed pressure $p(t)$ and the results are compared to some nondimensional peak values reported by Baron et al [115] and by Nagarajan and Popov [105]. The material is assumed to be elastic-perfectly plastic and Fig. 6.5 shows the geometry and material properties of the beam. Taking advantage of symmetry about the midspan, one half of the beam was considered in the finite element analysis and five equal elements were used for the discretization. Two types of load-time variation were considered as shown in Fig 6.5: step pressure loading and a suddenly applied load which decays exponentially.

The peak elastic-plastic response of the beam was determined for $p(t) = 0.75\ p_o$ in the case of step pressure loading, and for $p(t) = 2\ p_o e^{-t/t_o}$ in the case of esponentially decaying load. Here p_o is the value of the static collapse load and $t_o = T/2$, T being the fundamental period of the beam.

The midspan deflection, δ, is normalized with respect to Δ, the static elastic deflection corresponding to the load p_o. Fig. 6.6 shows the variation of δ/Δ with time for the step pressure

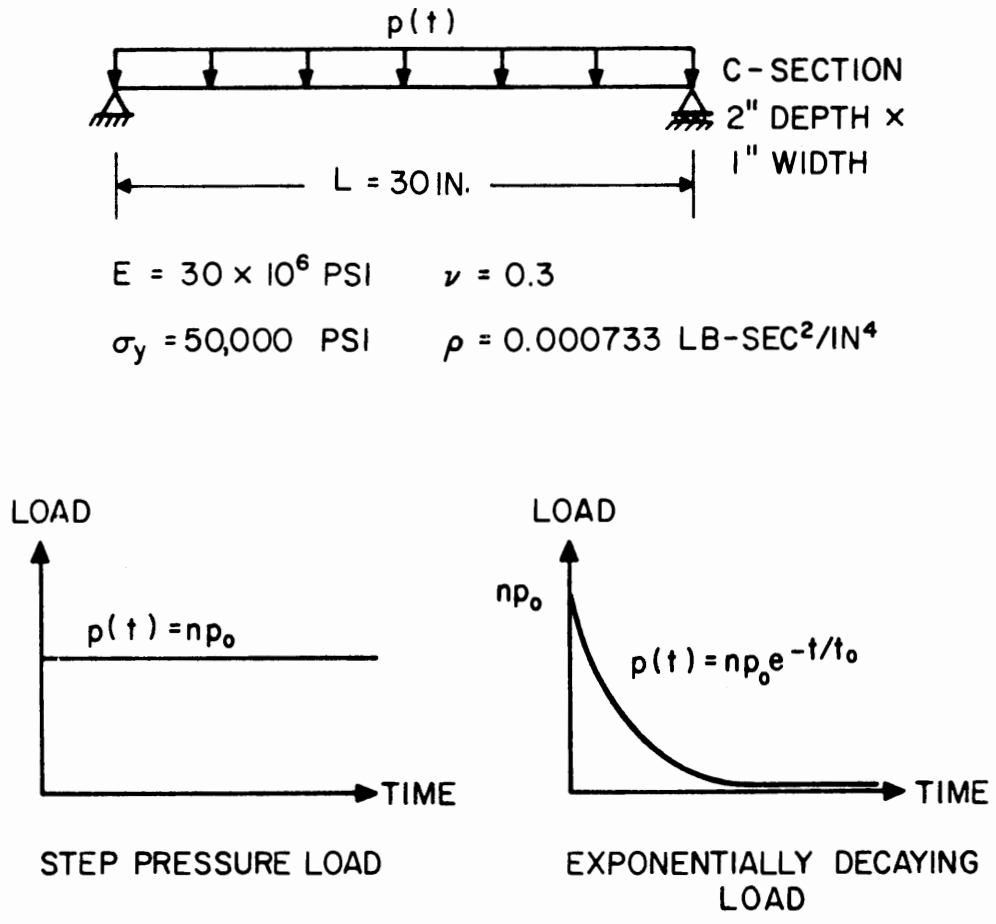

FIG. 6.5 SIMPLY SUPPORTED BEAM AND LOAD-TIME VARIATIONS

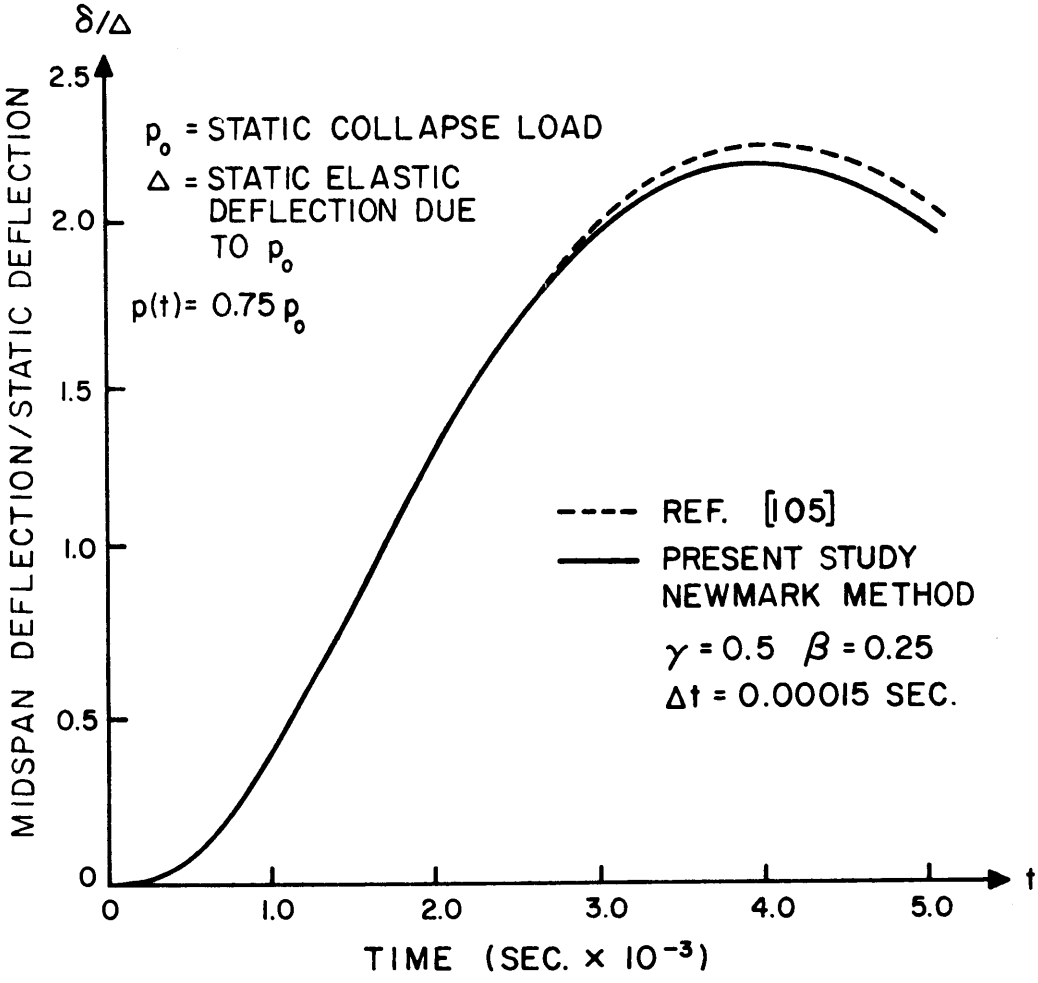

FIG.6.6 DYNAMIC ANALYSIS OF A SIMPLY SUPPORTED BEAM SUBJECTED TO A UNIFORM STEP PRESSURE

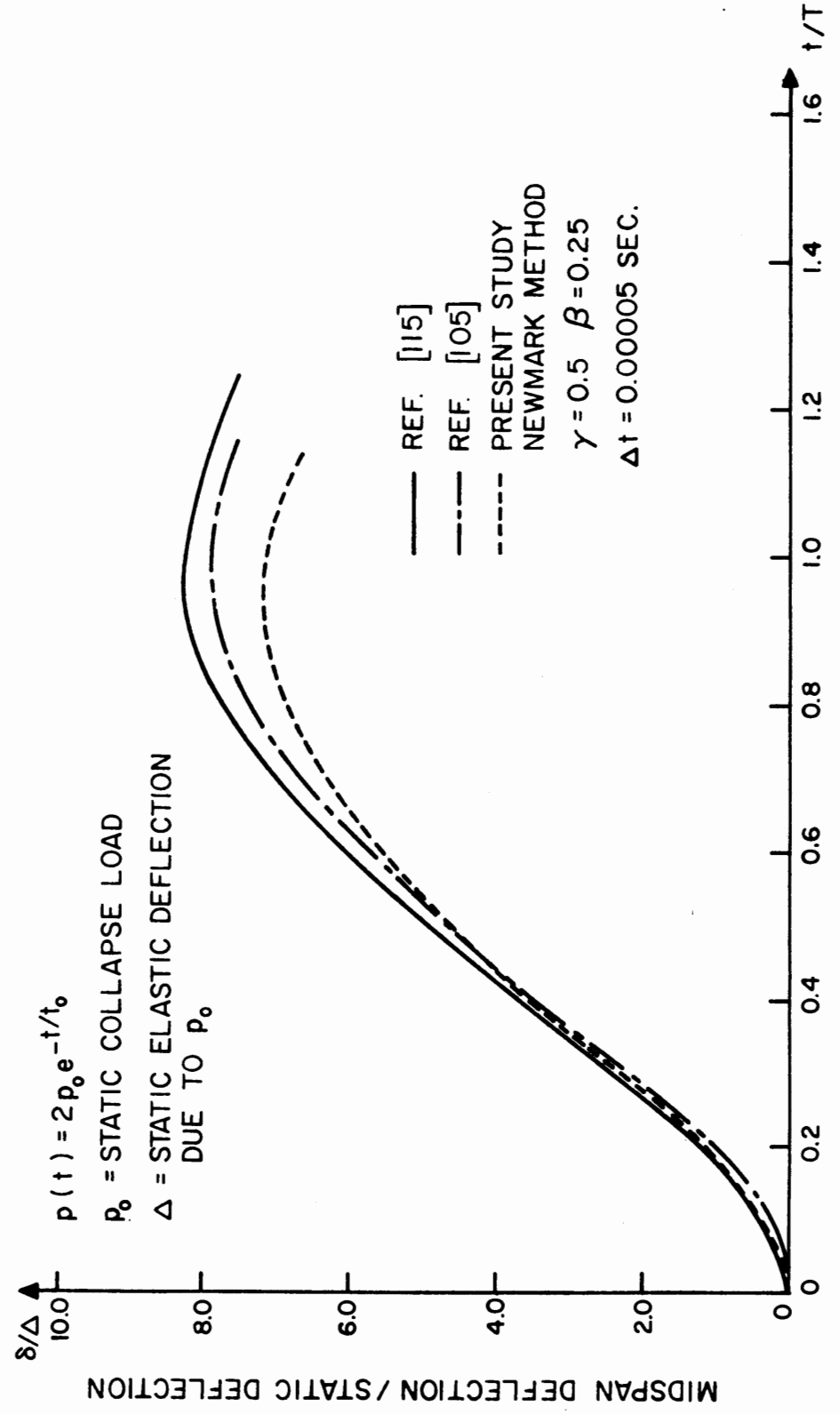

FIG. 6.7 DYNAMIC ANALYSIS OF A SIMPLY SUPPORTED BEAM SUBJECTED TO A UNIFORM EXPONENTIALLY DECAYING PRESSURE

load and also shows the curve given in Ref. [105]. The peak value of 2.17 compares well with the value of 2.22 of Ref. [105] and 2.28 of ref. [115].

The fundamental period of this beam is 0.0049 sec. for linear elastic undamped vibration and the maximum value of δ/Δ for such vibrations would be 1.5. As can be seen from Fig. 6.6, in the case of elastic-plastic analysis the peak value is greater and the time period elongated due to the plastic deformations which cause softening of the system.

Fig. 6.7 shows the variation of δ/Δ with t/T and also the curves given in Refs. [105, 115]. The time increment has to be chosen much smaller for this problem because the exponentially decaying load is more complex than the step function, and its Fourier components range over the entire frequency spectrum, thus exciting several modes of vibration in the beam.

6.2.2 (c) Shallow Spherical Cap

The shallow sperical cap shown in Fig. 6.8 has been studied by many authors, most extensively by Stricklin et al [116] and more recently by Nagarajan and Popov [105]. A linear elastic dynamic analysis of this cap with a 100 psi step pressure was studied in Sec. 4.5 as a trial problem.

The geometry, material properties and the load-time history are given in Fig. 6.8. Because of the symmetry of the structure, only one half of it needed to be studied and a total of five elements were employed to discretize the shell cap from the apex to the support. The Newmark ($\gamma = 0.5$, $\beta = 0.25$) method was used with a time step of 10×10^{-6} sec. Uniform external step pressures of 445 and 600 psi were applied on the cap and dynamic analyses were carried out for

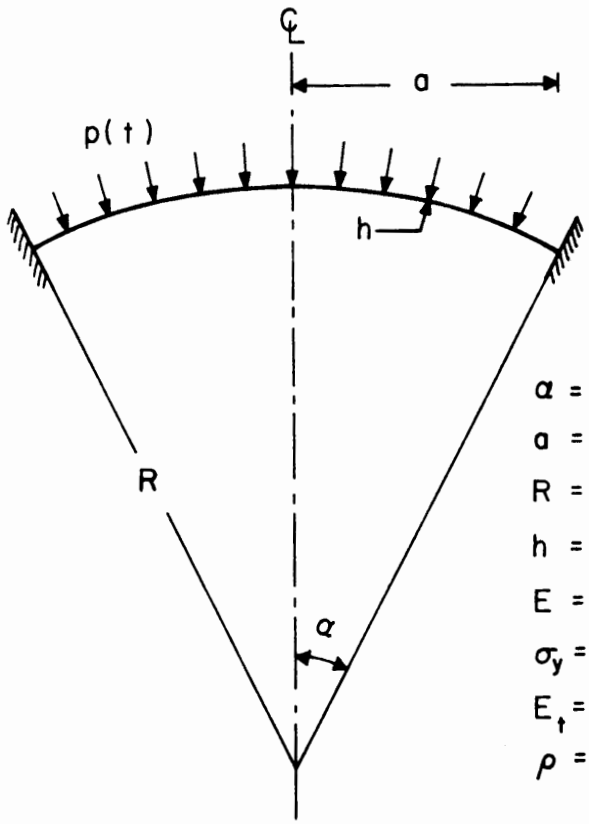

$\alpha = 26 \cdot 67°$
$a = 10$ IN.
$R = 22 \cdot 27$ IN.
$h = 0.41$ IN.
$E = 10.5 \times 10^6$ PSI $\quad \nu = 0.3$
$\sigma_y = 24{,}000$ PSI
$E_t = 210{,}000$ PSI
$\rho = 0.000245$ LB-SEC^2/IN^4

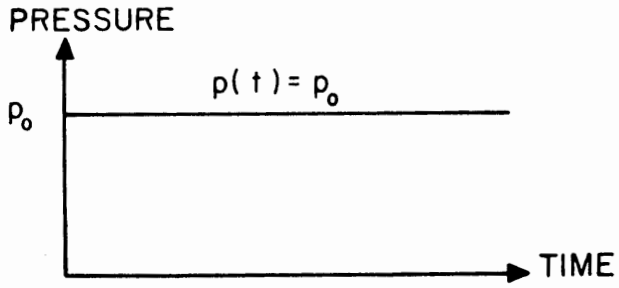

FIG.6.8 SHALLOW SPHERICAL SHELL CAP AND PRESSURE-TIME HISTORY

elastic and elastic-plastic cases, assuming linear as well as non-linear geometry.

(i) 445 psi Step Pressure

The apex displacement of the cap vs. time is plotted in Fig. 6.9 for the different cases. Comparing the linear and nonlinear elastic responses, it can be seen that the period of vibration is greater for the nonlinear response. The inward radial motion gives rise to a softening system whereas the outward motion causes the system to stiffen and the effect of this is that the absolute peak displacement of the apex is greater for the nonlinear analysis during the inward motion and lower during the outward motion. In the case of the plastic analysis, although the plastic yielding during inward radial motion causes a softening of the system, the peak amplitudes are lower than in the elastic responses. The frequencies of the first several modes of vibration of a shell cap are clustered rather close to the fundamental frequency and have a significant effect on the response. This causes a number of minor oscillations which result in repeated elastic unloading and plastic yielding, and the damping introduced thereby lowers the peak amplitude of motion.

The nonlinear elastic-plastic response of the cap bears a similar comparison with the linear solution as the comparison between the nonlinear and linear elastic responses. All the curves indicate that the vibration occurs about the static solution.

The linear elastic-plastic response is compared in Fig. 6.10 with the solution given in Ref. [105]. It can be noted that, except for the initial peak amplitudes, the two results show excellent agreement. Isoparametric finite elements are used in Ref. [105] while degenerate isoparametric elements are employed in this study.

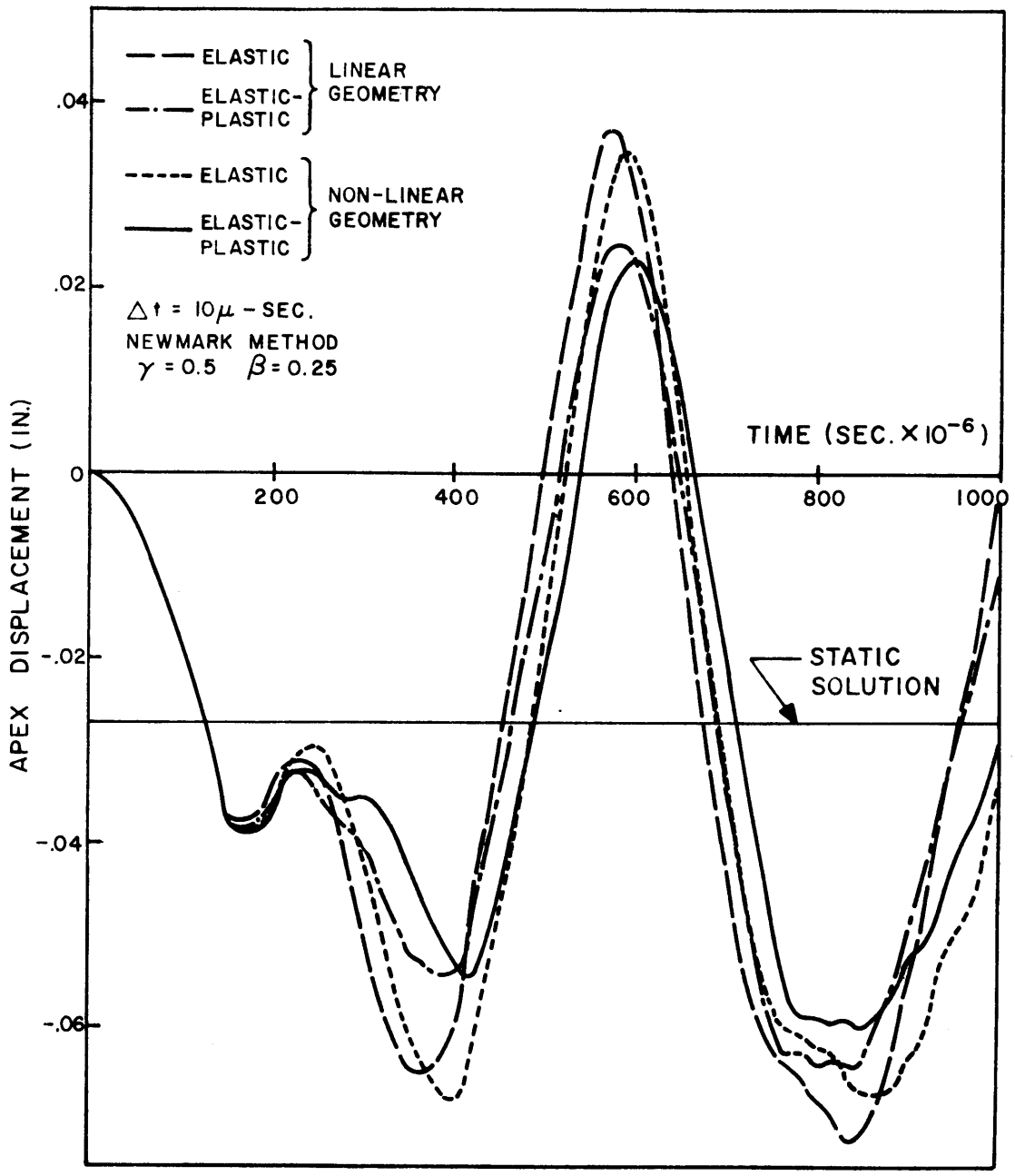

FIG.6.9 DYNAMIC RESPONSE OF SHALLOW SPHERICAL CAP UNDER UNIFORM EXTERNAL STEP PRESSURE OF 445 PSI

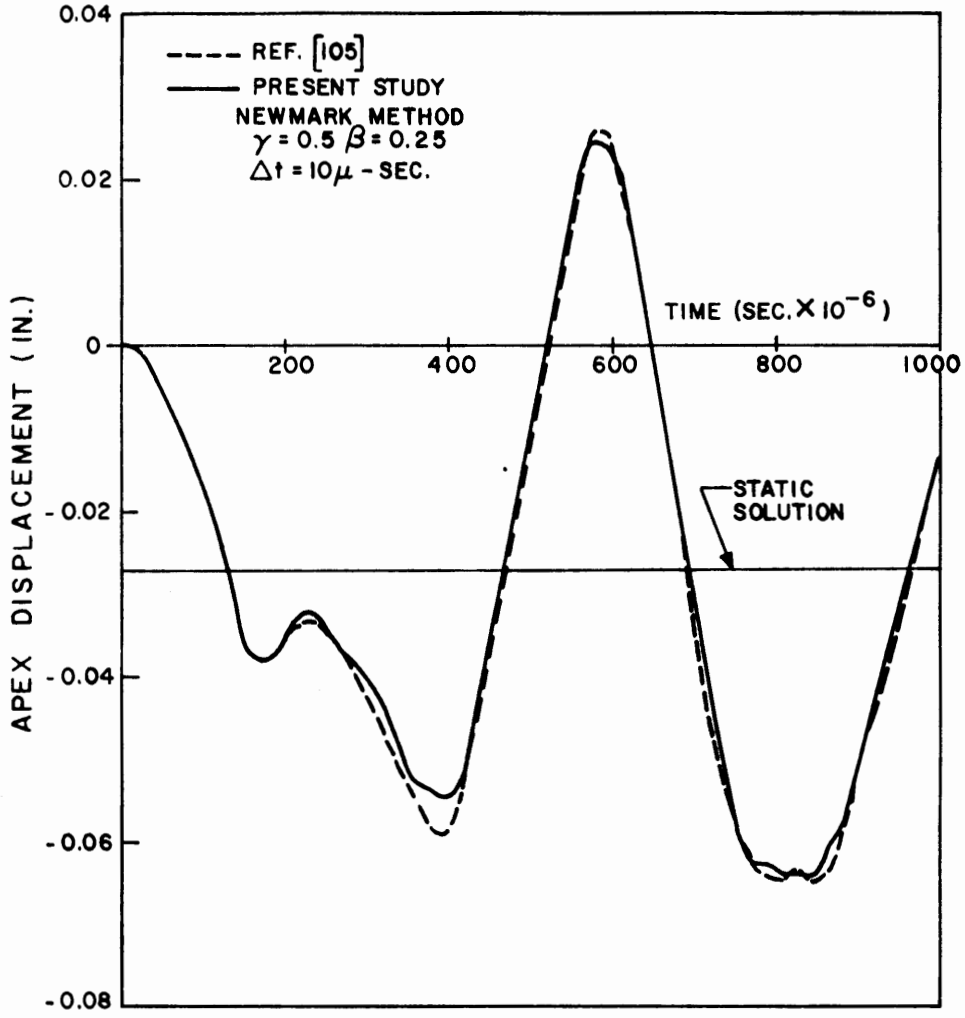

FIG. 6.10 SHALLOW SPHERICAL CAP UNDER UNIFORM EXTERNAL STEP PRESSURE OF 445 PSI — ELASTIC-PLASTIC, GEOMETRICALLY LINEAR ANALYSIS

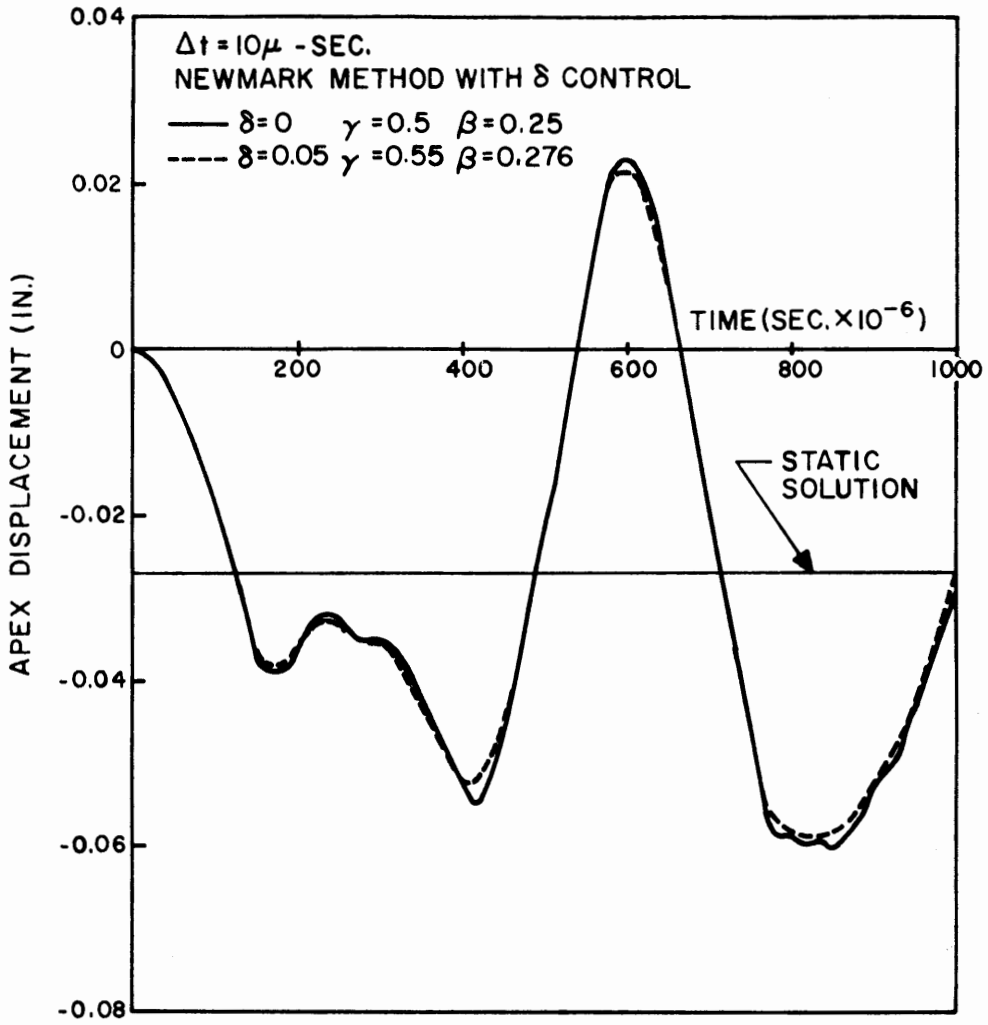

FIG. 6.11 EFFECT OF USING NEWMARK METHOD WITH δ CONTROL— ELASTIC-PLASTIC, GEOMETRICALLY NONLINEAR ANALYSIS OF SHALLOW SPHERICAL CAP UNDER UNIFORM EXTERNAL STEP PRESSURE OF 445 PSI

While the transverse normal stresses are retained in the former, the latter formulation assumes that these stresses are negligibly small. This affects the effective stress patterns which control the plastic loading and contributes to the differences between the two solutions.

Finally, the effect of using the δ control in Newmark's method is demonstrated in Fig. 6.11 for the geometrically nonlinear, elastic-plastic analysis of this cap for 445 psi step pressure. The apex displacement-time graph from Fig. 6.9, using the standard Newmark method, is replotted in Fig. 6.11 along with the solution obtained using $\delta = 0.05$ in Newmark's method. As can be seen from this figure, the primary effect of this δ control is to smooth out the roughness in the response and is the result of the damping introduced in the higher modes. A small amount of damping is also presented in the lower modes as a result of which the amplitude peaks are slightly damped as may be seen in Fig. 6.11.

(ii) 600 psi Step Pressure

In order to illustrate more clearly the effect of the nonlinearities on the response, a higher magnitude of pressure, a 600 psi uniform external step pressure was applied on the cap. Fig. 6.12 shows the apex displacement as a function of time for the different cases. The damping of the peaks, period elongation and phase shift are now much more pronounced for the nonlinear analyses. It is also apparent that the mean value about which the cap vibrates is greater in the elastic-plastic cases than in the elastic cases where vibration takes place about the static solution. This indicates a greater permanent deflection in the elastic-plastic cases, even though the static solutions are almost identical for elastic and elastic-plastic analyses since this system is only mildly nonlinear when a pressure-type loading is applied statically.

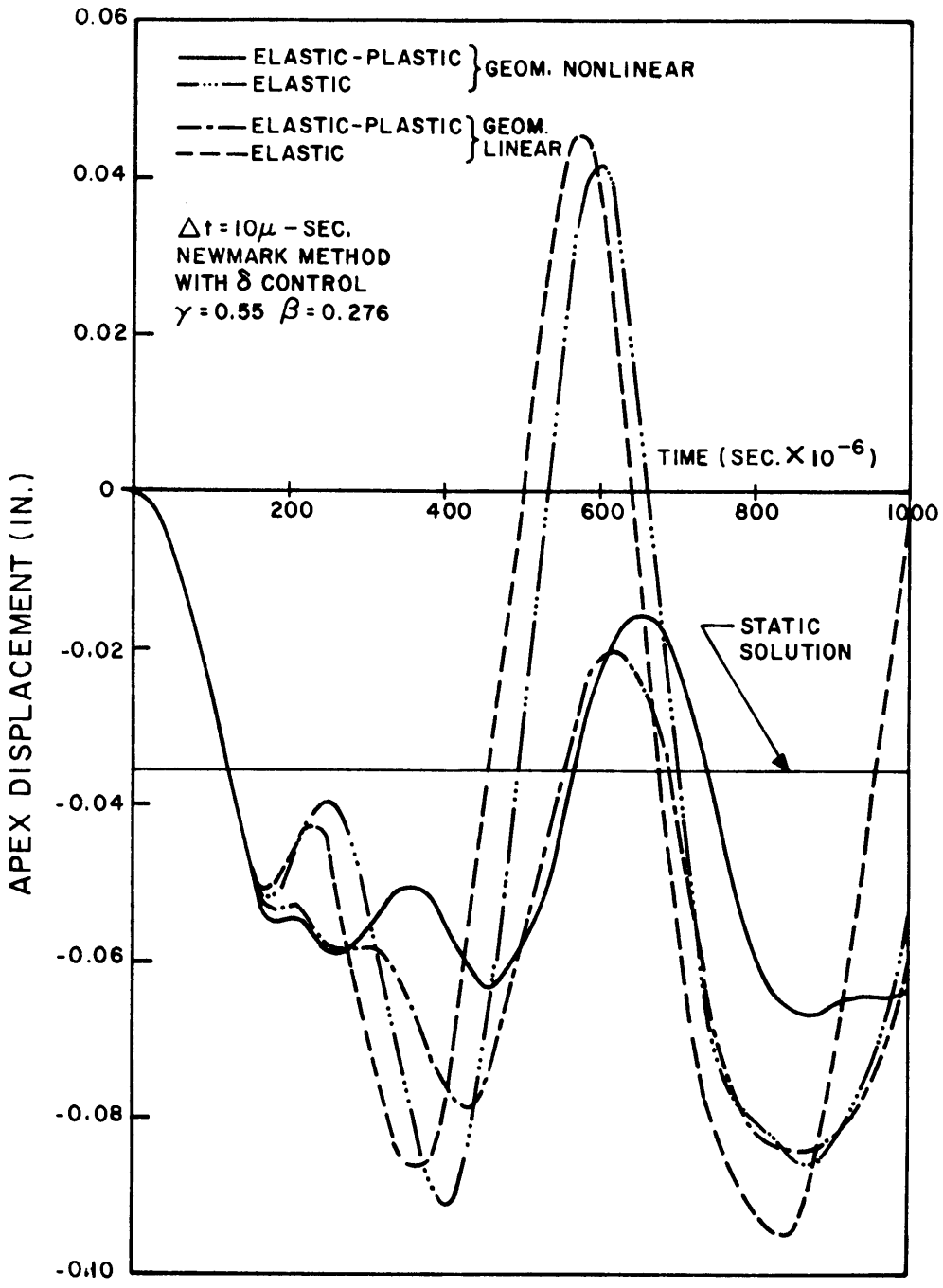

FIG. 6.12 SHALLOW SPHERICAL CAP UNDER UNIFORM EXTERNAL STEP PRESSURE OF 600 PSI

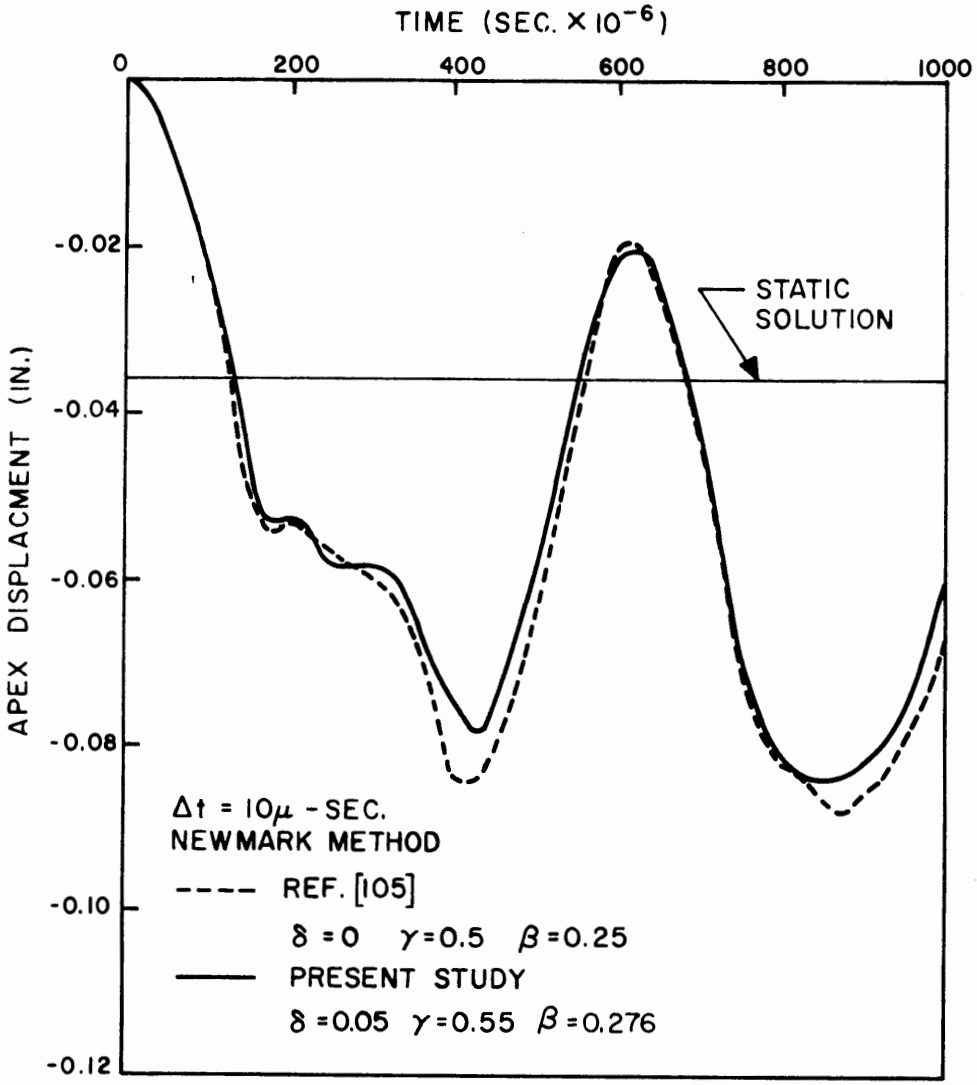

FIG. 6.13 SHALLOW SPHERICAL CAP UNDER UNIFORM EXTERNAL STEP PRESSURE OF 600 PSI — ELASTIC-PLASTIC, GEOMETRICALLY LINEAR ANALYSIS

The geometrically linear, elastic-plastic analysis of this study is compared once again (Fig. 6.13) with the results given in Ref. [105]. The agreement is very good except for the initial peak value and the same discussion holds as in the case of 445 psi. In addition, the use of $\delta = 0.05$ in the present analysis introduces a slight damping of the peaks and smooths out some minor oscillations in the response.

6.3 Elastic - Viscoplastic Analyses

The examples in this section demonstrate the capability of Program VISPAX for solving problems in which the material is assumed to behave in an elastic-viscoplastic manner. In addition, elastic-plastic solutions are also obtained using this program following two different approaches:

(a) Obtain viscoplastic solutions for several values of the material viscosity parameter γ and extrapolate for $\gamma \to \infty$ (theoretically, elastic-plastic solutions are obtained as $\gamma = \infty$).

(b) Use time as an artifice to let the system reach equilibrium states (i.e. the effective stresses at all points in the structure are either on or inside the static loading surface).

6.3.1 Simply Supported Beam

A simply supported beam shown in Fig. 6.14 is considered as the first example for elastic-viscoplastic analysis. The nondimensional load defined in Fig. 6.14 is applied at a rate of 2×10^4 sec.$^{-1}$ The static stress-strain curve is assumed to be elastic-perfectly plastic. Two values of the viscosity coefficient are considered in the analysis and inertia forces are neglected. Four elements are used to discretize half the span and a 6 X 13 integration scheme is

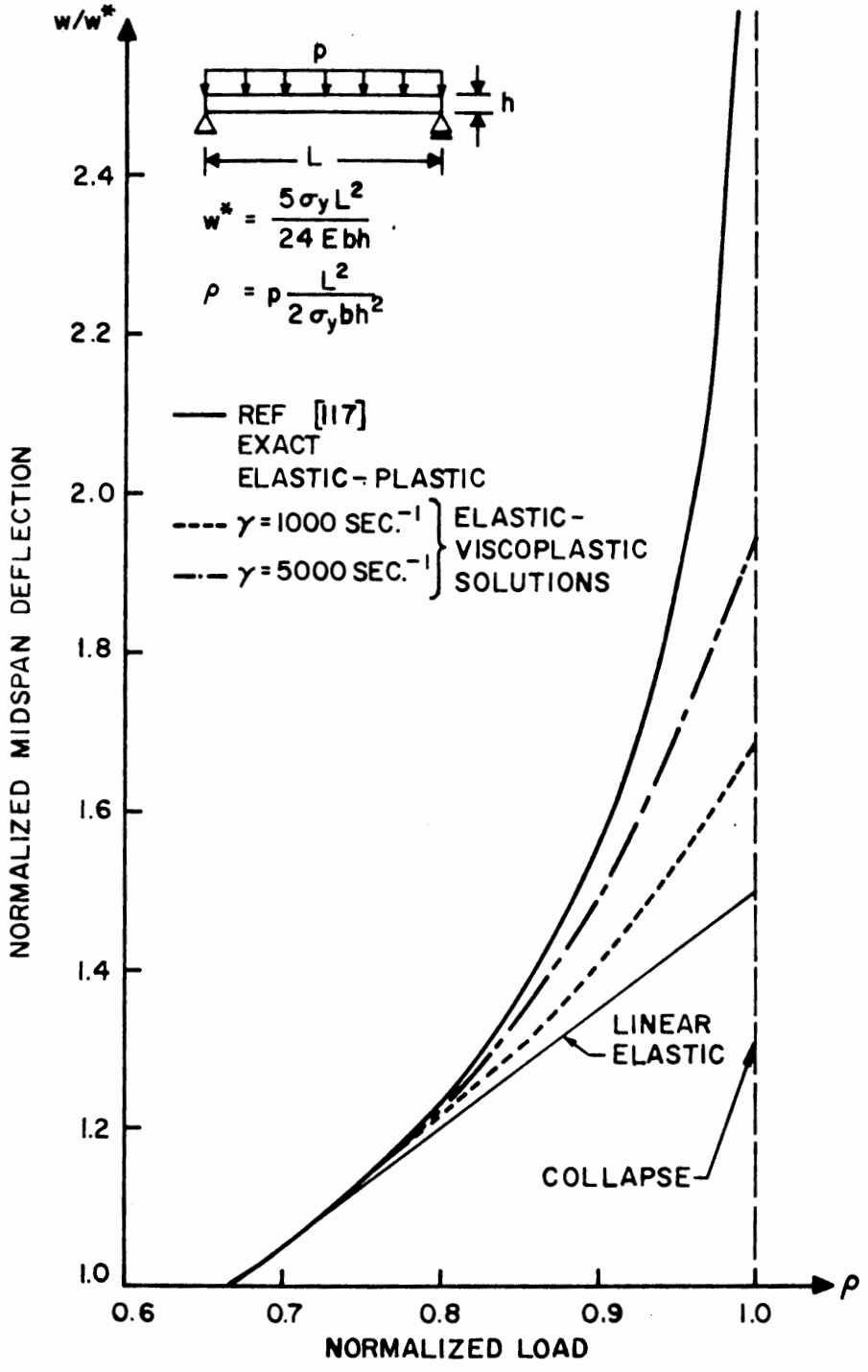

FIG. 6.14 VISCOPLASTIC ANALYSIS OF SIMPLY SUPPORTED BEAM

used for each element.

The normalized load-displacement curves are given in Fig. 6.14 up to a value of $\rho = 1.0$ which would be the collapse value were the load to be applied in a quasi-static manner. Fig. 6.14 also shows the theoretical elastic-plastic curve given by Prager and Hodge [17] for quasi-static loading and it is instructive to compare it with the results of the present study. As expected the curve for the lower value of γ is closer to linear elastic behavior while the higher value of γ corresponds closer to the elastic-plastic solution. The elastic-perfectly plastic solution can be achieved in the limit as γ tends to infinity as discussed in section 3.2.3, and pursued further in the examples of a fixed end beam and torispherical pressure head.

6.3.2 Fixed End Beam

The elastic-plastic analysis of a fixed end beam using viscoplasticity formulation is considered next. The geometry of the beam is shown as an insert in Fig. 6.15. The static stress-strain curve is elastic-perfectly plastic and the material has the following properties:

$$E = 30 \times 10^6 \text{ psi} \qquad \nu = 0.3 \qquad \sigma_y = 50{,}000 \text{ psi}$$

The beam is discretized using seven elements from a fixed end to the midspan - two elements of 1.5 in. length near the fixed end, three elements of 3 in. length and again two 1.5 in. long elements near the midspan. The integration is performed using 4 X 11 scheme for each element.

The normalized load-deflection for the midspan is presented in Fig. 6.15, and Fig. 6.16 shows the midspan deflection as a function of a normalized time parameter. Fig. 6.15 also shows the result

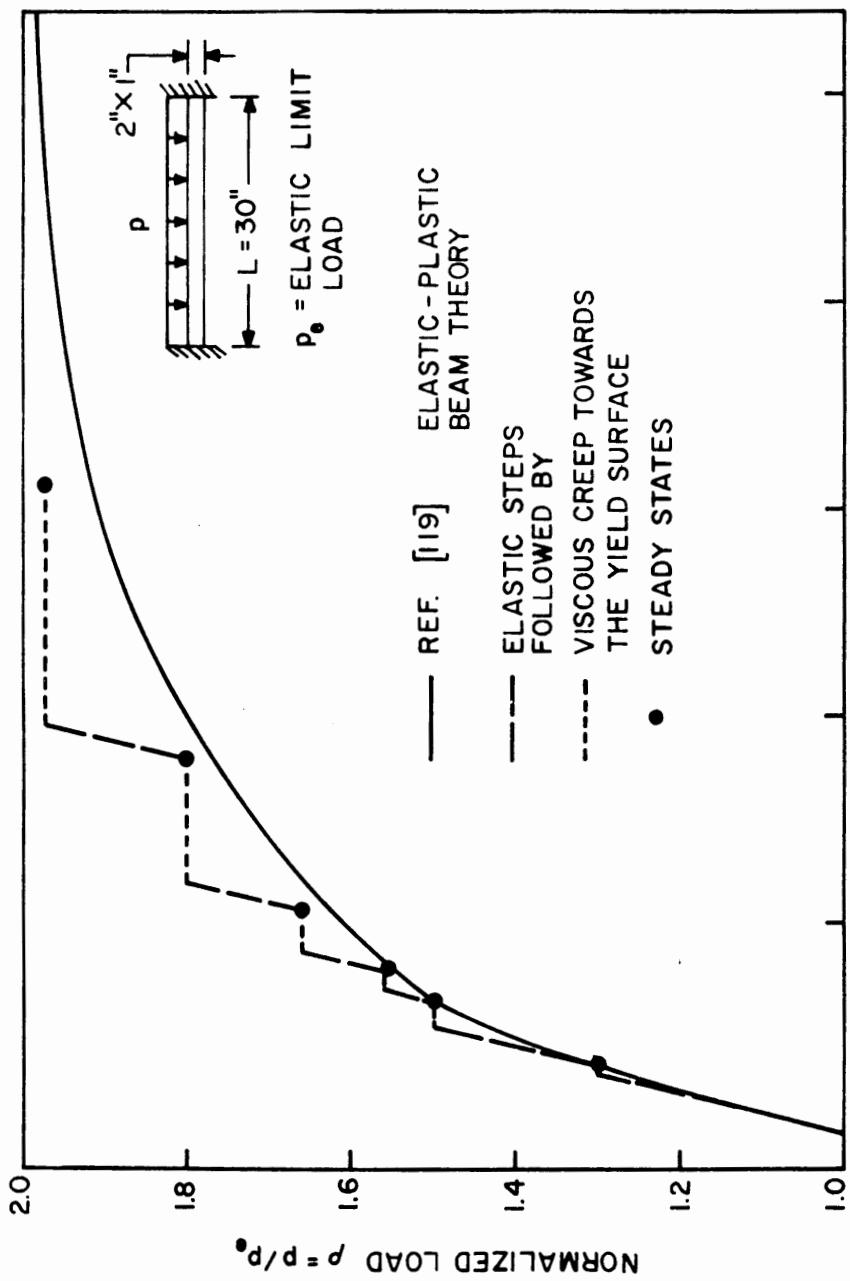

FIG. 6.15 ELASTIC-PLASTIC ANALYSIS OF A FIXED END BEAM USING VISCOPLASTICITY FORMULATION

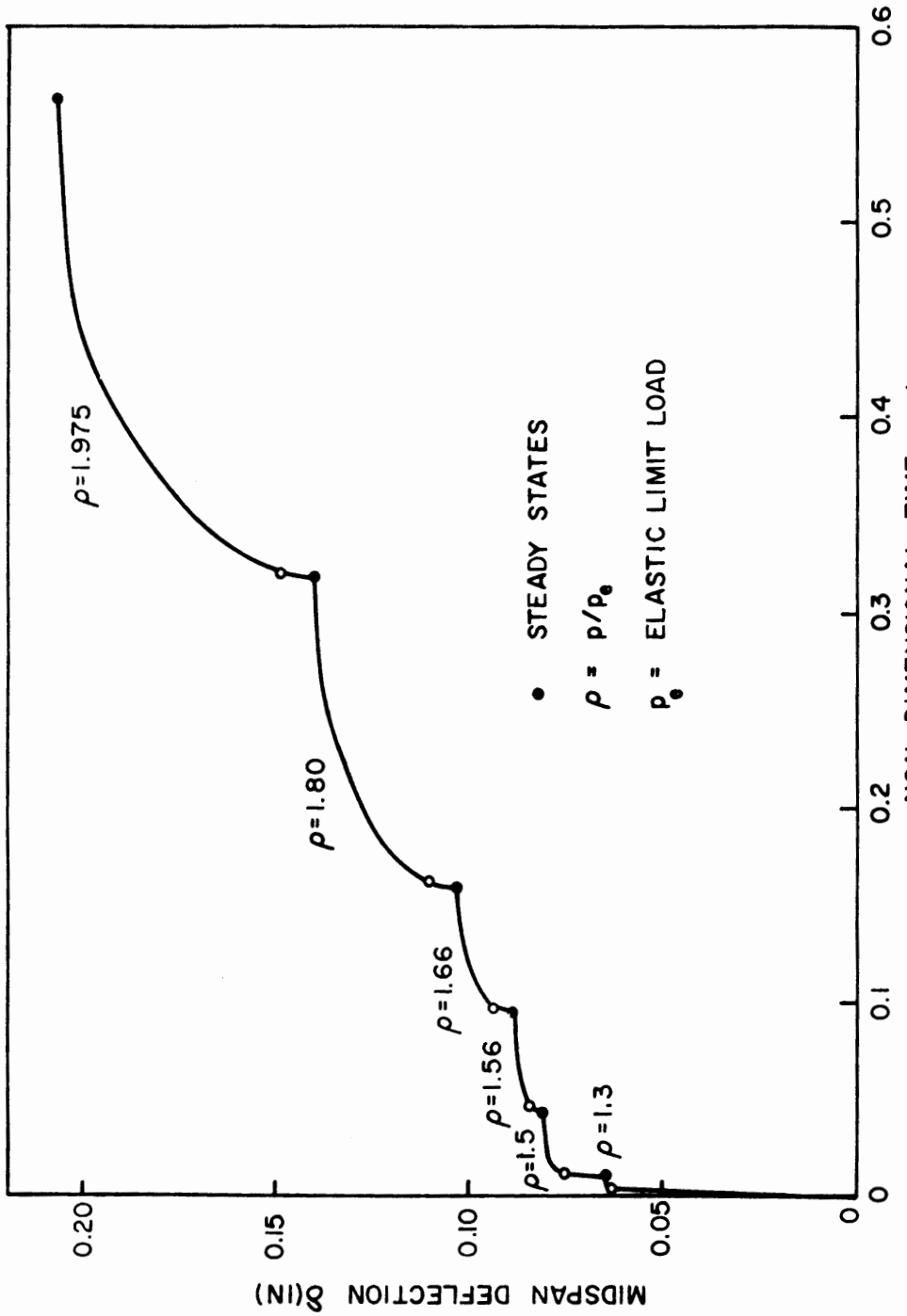

FIG. 6.16 MIDSPAN DEFLECTION VS. TIME ELASTIC-PLASTIC ANALYSIS OF A FIXED END BEAM USING VISCOPLASTICITY FORMULATION

obtained by using an elasto-plastic beam theory which accounts for the gradual growth and propagation of plastic zones [118, 119]. Each increment of load is applied elastically and then viscoplastic effect is introduced because the stresses exceed the static yield surface. This artifically induced effect continues until steady state elastic-plastic solution is obtained. This is observed in Fig. 6.16 which shows the displacement-time curves for each of the increments of load application. The load-displacement progression towards the theoretical elastic-plastic solution can be seen in Fig. 6.15. As the load level increases, the steady state solutions show lack of convergence to the theoretical curve and is quite characteristic of numerical solutions to problems involving asymptotic behavior. It would be necessary to make further refinements in discretization of the beam to obtain better convergence.

6.3.3 Torispherical Pressure Head

The elastic-plastic behavior of a torispherical pressure head was studied in section 6.2.1(b). The elastic-viscoplastic behavior of the same is studied here and elastic-plastic solutions are also obtained using viscoplasticity approach. The geometry of the pressure head is identical to that analyzed in section 6.2.1(b)

D = 100 in. R = 100 in.

r = 20 in. h = 0.8 in.

The static stress-strain curve is elastic-perfectly plastic, with yield stress σ_y = 30,000 psi, Young's modulus E = 30 X 10^6 psi and Poisson's ratio ν = 0.3.

A total of 20 finite elements were used to describe the shell from the apex to the support. Eight equal elements were used

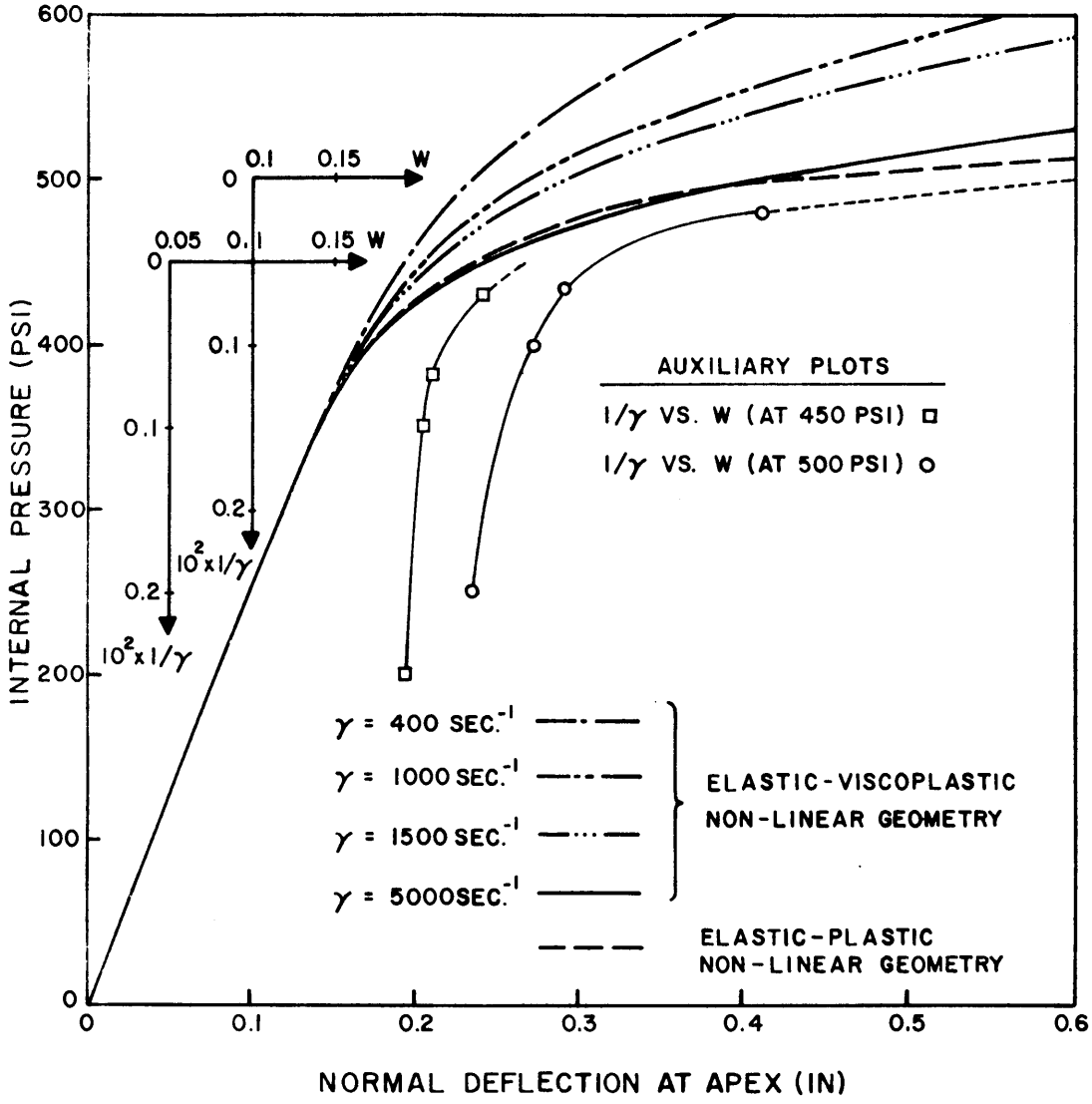

FIG. 6.17 NONLINEAR ANALYSIS OF TORISPHERICAL PRESSURE VESSEL UNDER INTERNAL PRESSURE

over the sphere, another eight equal elements over the torus and the remaining four elements for the cylinder. Four Gaussian integration points were used in the meridonal direction and eleven Simpson points across the thickness.

The viscoplastic solution was studied for four different values of the material viscosity coefficient, γ, from 400 sec.$^{-1}$ to 5000 sec.$^{-1}$, and the internal pressure was applied at the rate of 10 X 10^6 psi/sec. Inertia effects were neglected but geometric non-linearities were included in the analyses. Fig. 6.17 shows the plots of internal pressure vs. apex deflection for these viscoplastic analyses and also the elastic-plastic solution obtained in section 6.2.1(b). It can be seen that the viscoplastic solutions are stiffer and predict higher load carrying capacity for the lower values of γ, but as γ increases the solution comes very close to the elastic-plastic solution. Since elastic-plastic solution is expected as $\gamma \to \infty$, a simple extrapolation procedure is used as shown in the auxiliary plots in Fig. 6.17. The apex displacement, w, is plotted as a function of $1/\gamma$ at two selected levels of internal pressure, 450 and 500 psi. For instance, the deflection at 450 psi for the four different values of γ are plotted and joined by a curve which can then be extrapolated for $1/\gamma = 0$, i.e. $\gamma = \infty$. In this case, the extrapolated curve indicates that the apex displacement at 450 psi internal pressure should be about 0.265 in. for an elastic-plastic solution. Similarly, an apex displacement of about 0.6 in. is predicted at 500 psi for an elastic-plastic pressure head. This pressure head was also analyzed for elastic-plastic behavior using the second method mentioned in section 6.3 in which time is used as an artifice in the viscoplasticity solution. The elastic-viscoplastic solution for γ = 400 sec.$^{-1}$ given

in Fig. 6.17 was carried out until the internal pressure reached the value of 450 psi. Then the solution was allowed to progress with time towards a steady state elastic-plastic solution. Fig. 6.19 shows the displacement-time curve reaching a steady state at about 0.265 in. and this is also shown in the load-displacement graph in Fig. 6.18. The elastic-plastic solution of section 6.2.1(b) is also plotted in Fig. 6.18. The pressure was then increased to 500 psi using 10 psi increments in the viscoplastic analysis. Once again, displacement was allowed to increase with time in an artifical viscoplasticity solution. The solution reaches a steady state at about 0.61 in. as can be seen from Fig. 6.19. It may be observed now that these steady state elastic-plastic displacements compare excellently with the results obtained by extrapolating for γ tending to infinity in the viscoplastic analyses.

Comparing these results with the elastic-plastic solution taken from section 6.2.1(b) it appears that this pressure vessel has an even softer behavior and lower collapse load than indicated by the extremely refined elastic-plastic solution obtained earlier, and caution must be exercised before accepting such analyses to have converged if the results therefrom are to be used for design purposes.

This example clearly demonstrates the capability of the viscoplastic analysis program to arrive at elastic-plastic solutions. The approach using a large value of γ in the viscoplastic analysis appears to be more economical than the other in which stress redistribution leads to steady states. This is due to the well known disadvantage of the initial strain formulation which requires the latter scheme to use a large number of pseudo-time steps or iterations, especially as the stiffness becomes very small. The direct application of elastic-plastic analysis with refined load steps might require less

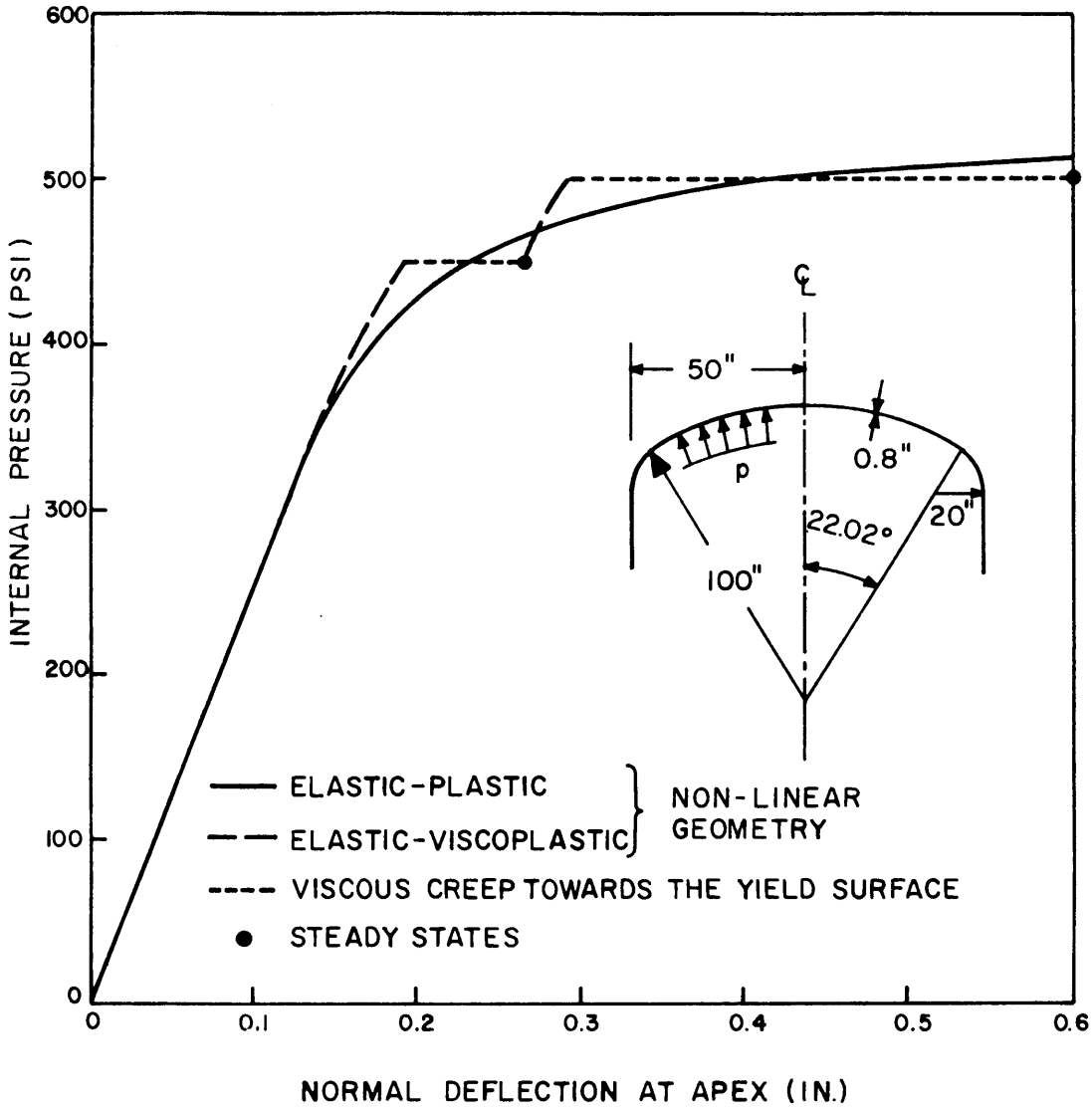

FIG. 6.18 INTERNAL PRESSURE VS. APEX DEFLECTION ELASTIC-PLASTIC ANALYSIS OF TORI-SPHERICAL HEAD USING VISCOPLASTICITY FORMULATION

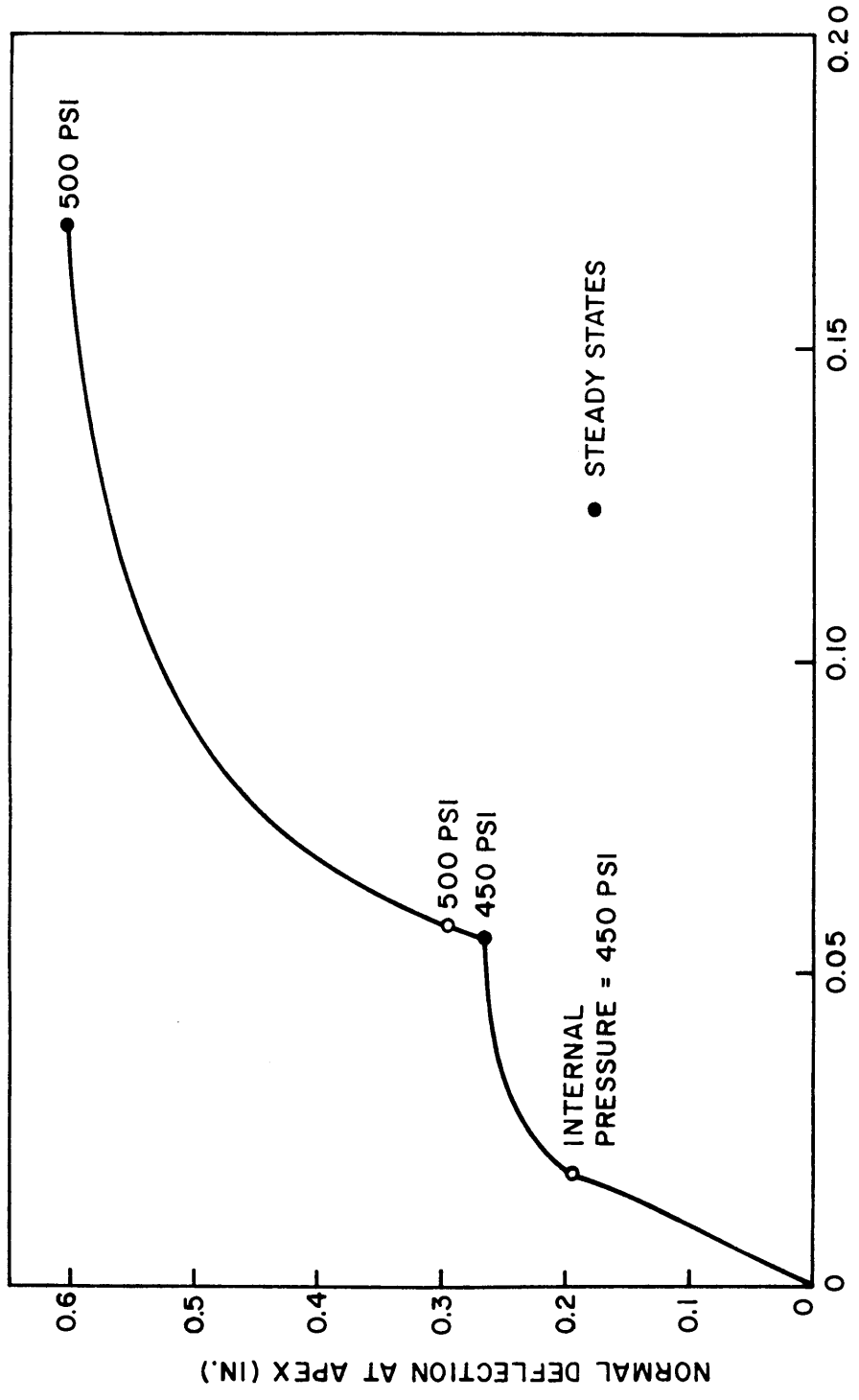

FIG.6.19 APEX DEFLECTION VS. TIME ELASTIC-PLASTIC ANALYSIS OF TORISPHERICAL HEAD USING VISCOPLASTICITY FORMULATION

computational effort than either of the two viscoplasticity schemes; however, in the case of important and sensitive structures, it is desirable to have independent alternate methods which can be used to verify the accuracy and reliability of any one analysis.

6.3.4 Dynamic Analysis of Shallow Spherical Cap

Elastic-viscoplastic dynamic response analysis was conducted for the same shallow spherical thin cap studied in section 6.2.2(c). The dimensions of the cap are given in Fig. 6.8. The static stress-strain curve was assumed to be elastic-plastic with linear strain hardening and the material properties corresponding to this are also given in Fig. 6.8. The viscosity coefficient, γ, of the material was assumed to be 400 $sec.^{-1}$

A total of five finite elements were used to discretize the shell cap from the apex to the clamped support. The Newmark method with δ control ($\delta = 0.05$, $\gamma = 0.55$, $\beta = 0.276$) was used with a time step of 10×10^{-6} sec. Uniform external step pressure of 600 psi was applied on the cap and dynamic analyses were carried out assuming both linear and nonlinear geometry.

The apex displacement of the cap vs. time is plotted in Fig. 6.20. The results of the elastic analyses given earlier in Fig. 6.12 are also repeated in the figure to facilitate comparison.

The viscoplastic responses exhibit lower peak values, elongated time periods and phase shifts compared to the elastic analyses. Also, the viscoplastic vibrations take place about a greater permanent displacement than the elastic vibrations which occur about the static solution. It may be noted that the visco-plastic responses obtained here are, in fact, very similar to the results of the elastic-plastic analyses in section 6.2.2(c), and

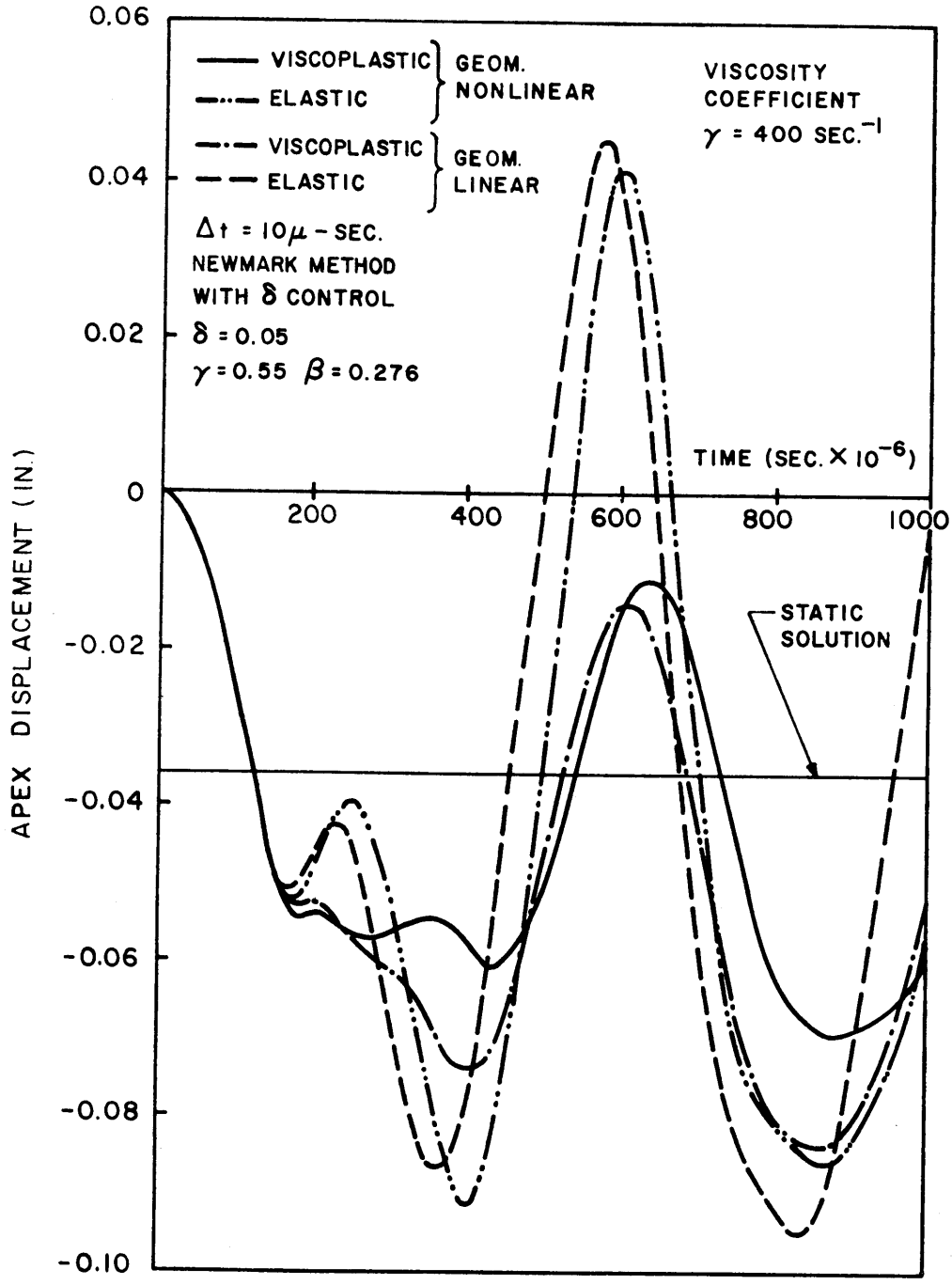

FIG. 6.20 SHALLOW SPHERICAL CAP UNDER UNIFORM EXTERNAL STEP PRESSURE OF 600 PSI

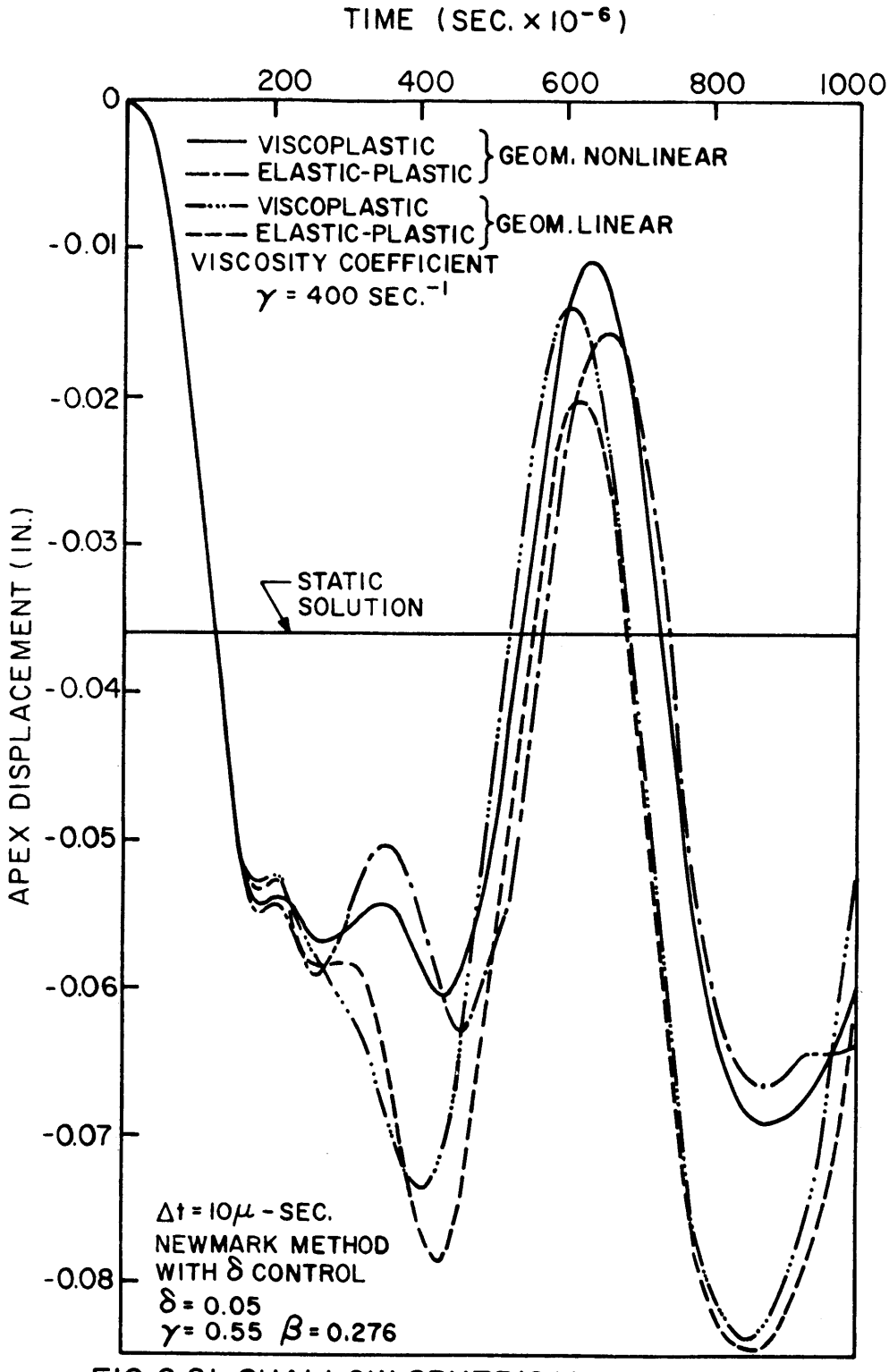

FIG. 6.21 SHALLOW SPHERICAL CAP UNDER UNIFORM EXTERNAL STEP PRESSURE OF 600 PSI — COMPARISON BETWEEN ELASTIC-PLASTIC AND ELASTIC-VISCOPLASTIC RESPONSES

Fig. 6.21 enables direct comparison of these results. Except for the differences in the initial peak values, there is close agreement between the elastic-plastic and viscoplastic responses for both linear and nonlinear theories. This is attributed to the fortuitious choice of the value for γ and indicates that the chosen value of 400 sec.$^{-1}$ is a good estimate of the viscosity coefficient for this material.

7. SUMMARY AND CONCLUSIONS

A numerical method has been presented for nonlinear static and dynamic analysis of shells of revolution under axisymmetric loading. The physical nonlinearities arise from the consideration of elastic-plastic or elastic-viscoplastic material properties, and the geometric nonlinearities are due to large displacements caused by finite rotations. An incremental variational formulation using the Lagrangian mode of description of motion was used to obtain the incremental equations of motion which were subsequently modified to take into account the material constitutive behavior. The displacement increments during each step were assumed to be small which enabled the equations to be considered in their linearized form. The accuracy of the incremental solution procedure was improved by applying an equilibrium correction to each step.

The symmetric Piola-Kirchhoff stress and Lagrangian strain were used in all the constitutive relations. Flow theory of plasticity with von Mises yield criterion and isotropic hardening were employed in the case of elastic-plastic analyses and the tangent stiffness approach was used in the variational formulation. Rate sensitive material behavior, on the other hand, was treated using an initial strain formulation wherein viscoplastic pseudo-loads were obtained as a result of the decomposition of stress increments into "instantaneous elastic" and "delayed viscoplastic" components. The same yield condition and hardening rule were employed as in the case of inviscid plasticity

and the viscoplastic strain rate (lumping together both the plastic and viscous effects) was related to the amount by which the static loading surface was exceeded at any given time.

The modified incremental technique was used for the numerical analysis of nonlinear problems. In the case of dynamic analysis, direct integration of the equations of motion was carried out using step-by-step solution procedures. While the Rayleigh form of viscous damping in the structure may be considered, it is also possible to introduce into the solution any desired amount of artificial viscosity by appropriate choice of parameters in the direct integration algorithms. Finally, the finite element formulation was based on the degenerate isoparametric element with cubic displacement variation. Both thin and moderately thick shells may be considered as a result of the relaxation of Kirchhoff hypothesis.

A number of numerical examples were presented to illustrate the accuracy of the computer programs developed for the analysis of both plane stress and axisymmetric problems. Very good comparisons were obtained with either available exact solutions or existing numerical solutions. The capability of the viscoplasticity formulation, not only to treat rate sensitive materials but also to serve as an artifice for obtaining elastic-plastic solutions, was demonstrated using two different approaches. Several extensions may be made to the computer programs developed during this investigation. A kinematic hardening rule may be introduced into the plasticity relations to enable consideration of both linear and nonlinear hardening of materials. In the case

of viscoplasticity, more experimental studies are needed to guide the choice of viscosity parameters for different materials. Different functional forms may also be established for the scalar function used in viscoplastic constitutive relations, and incorporated very easily in the computer programs. An automated technique for selection of time steps can improve the efficiency in the use of viscoplasticity formulation for arriving at steady state elastic-plastic solutions.

The efficiency of the coding and program organization should be studied carefully, and any possible improvements implemented before these programs are used for the analyses of large systems. Isoparametric quadrilateral elements with additional internal degrees of freedom may be included in order to analyze axisymmetric solids with sharp discontinuities in geometry. The study of dynamic buckling of shells may be developed as a further extension of the present investigation. The modification to extend the analysis capability to general three dimensional problems should be possible without too much difficulty, but the amount of computer time required may become prohibitive for any practical problem.

REFERENCES

1. Timoshenko, S. and Woinowsky-Krieger, S., Theory of Plates and Shells, McGraw-Hill, 1960.

2. Flügge, W., Stresses in Shells, J. Springer, Berlin, 1960.

3. Green, A. E. and Zerna, W., Theoretical Elasticity, Oxford University Press, 1954.

4. Green, A. E. and Adkins, J. E., Large Elastic Deformations and Nonlinear Continuum Mechanics, Oxford University Press, 1960.

5. Truesdell, C. and Toupin, R., Classical Field Theories, Handbuch der Physik, Ed. Flugge, S., Vol. III/1, 1960.

6. Truesdell, C. and Noll, W., The Nonlinear Field Theories of Mechanics, Handuch der Physik, Ed. Flugge, S., Vol. III/3, 1965.

7. Ames, W. F., Nonlinear Partial Differential Equations in Engineering, Academic Press, 1965.

8. Saaty, T. L., and Bram, J., Non-Linear Mathematics, McGraw-Hill, 1964.

9. Mikhlin, S., Approximate Methods for Solution of Differential and Integral Equations, translated from Russian by Scripta Technica, Inc., American Elsevier Publishing Co., Inc., 1967.

10. Forsythe, G. E., and Wasow, W. R., Finite Difference Methods for Partial Differential Equations, John Wiley, 1966.

11. Budiansky, B. and Radkowski, P. P., "Numerical Analysis of Unsymmetrical Bending of Shells of Revolution", AIAA Journal, Vol. 1, No. 8, 1963.

12. Sepetoski, W. K., Pearson, C. E., Drigwell, I. W., and Adkins, A. W., "A Digital Computer Program for the General Axisymmetric Thin Shell Problem", J. of Applied Mechanics, Vol. 29, Dec. 1962.

13. Bushnell, D. and Almroth, B. O., "Finite Difference Energy Method for Nonlinear Shell Analysis," Proc. LMSC/AFFDL Shell Conference, Palo Alto, California, Aug. 1970.

14. Turner, M. J., Clough, R. W., Martin, H. C., and Topp, L. J., "Stiffness and Deflection Analysis of Complex Structures", J. of the Aerospace Sci., Vol. 23, 1956.

15. Argyris, J. H. and Kelsey, S., Energy Theorems and Structural Analysis, Butterworths, London, 1960.

16. Melosh, R. J., "Bases of Derivation of Matrices for the Direct Stiffness Method", AIAA Journal, Vol. 1, No. 7, 1963.

17. Argyris, J. H., Kelsey, S., and Kamel, H., Matrix Methods in Structural Analysis, AGARD - ograph 72, Pergamon Press, 1964.

18. Oden, J. T., Finite Elements of Nonlinear Continua, McGraw-Hill, 1972.

19. Zienkiewicz. O. C., The Finite Element Method in Engineering Science, McGraw-Hill, 1971.

20. Przemieniecki, J. S., Theory of Matrix Structural Analysis, McGraw-Hill, 1968.

21. Felippa, C. A., and Clough, R. W., "The Finite Element Method in Solid Mechanics", Symposium on the Numerical Solution of Field Problems in Continuum Mechanics, Durham, N. Carolina, 1968.

22. Singhall, A. C., "775 Selected References on the Finite Element Method and Matrix Methods of Structural Analysis," Report S-12, Civil Engineering Department, Laval University, Quebec, 1969.

23. Turner, M. J., Dill, E. H., Martin, H. C. and Melosh, R. J., "Large Deflection Analysis of Structures Subjected to Heating and External Loads," Journ. Aerospace Sciences, Vol. 27, No. 2 Feb. 1960.

24. Argyris, J. H., Kelsey, S. and Kamel, H., Matrix Methods in Structural Analysis, AGARD-ograph 72, Pergamon Press, 1964.

25. Argyris, J. H., "Continua and Discontinua," Proc. 1st Conf. on Matrix Method in Structural Mechanics., Wright-Patterson AFB, AFFDL-TR-66-80, 1966.

26. Murray, D. W., and Wilson, E. L., "Finite Element Large Deflection Analysis of Plates", Journal of the Engineering Mechanics Division, ASCE, Vol. 95, EM1, 1969.

27. Gallagher, P. H. and Yang, H. T. Y., "Elastic Instability Predictions for Doubly Curved Shells", Proc. 2nd Conf. on Matrix Method in Structural Mechanics , Wright-Patterson AFB, AFFDL-TR-68-150, 1968.

28. Hsueh, T. M., and Wilson, E. L., "Stability Analysis of Axi-symmetric Shells", Report No. SESM 69-22, University of California, Berkeley, Sept. 1969.

29. Oden, J. T., "Calculation of Geometric Stiffness Matrices for Complex Structures", AIAA Journal, Vol. 4, No. 8, Aug. 1966.

30. Oden, J. T., and Sato, T., "Finite Strains and Displacement of Elastic Membranes by the Finite Element Method", Int. J. Solids Struct., Vol. 3, 1967.

31. Oden, J. T. and Key, J. E., "Numerical Analysis of Finite Axisymmetric Deformations of Incompressible Elastic Solids of Revolution, Int. J. Solids Struct., Vol. 6, No. 5, 1970.

32. Mallet, R. H. and Marcal, P. V., "Finite Element Analysis of Nonlinear Structures", Journal of the Structural Division, ASCE, Vol. 94, No. ST9, Sept., 1968.

33. Marcal, P. V., "Finite Element Analysis of Combined Problems of Nonlinear Material and Geometric Behavior", Technical Report No. N00014-0007/1, Brown University, Providence, R. I., 1969.

34. Oden, J. T., "Finite Element Formulation of Problems of Finite Deformation and Irreversible Thermodynamics of Nonlinear Continua - A Survey and Extension of Recent Developments", Japan-U.S. Seminar on Mathematical Methods of Structural Analysis and Design, Tokyo, Aug. 1969.

35. Felippa, C. A., "Refined Finite Element Analysis of Linear and Nonlinear Two-Dimensional Structures", Ph.D. Dissertation, University of California, Berkeley, Report No. SESM 66-22, 1966.

36. Yaghmai, S., "Incremental Analysis of Large Deformations in Mechanics of Solids with Application to Axisymmetric Shells of Revolution", Ph.D. Dissertation, University of California, Berkeley, 1968, NASA, CR-1350, June 1969.

37. Popov, E. P., Khojasteh-Bakht, M. and Yaghmai, S.,"Analysis of Elastic-Plastic Circular Plates", Journal of the Engineering Mechanics Division, Vol. 93, EM6, ASCE, 1967.

38. Khojasteh-Bakht, M., "Analysis of Elastic-Plastic Shells of Revolution Under Axisymmetric Loading by the Finite Element Method", Ph.D. Dissertation, University of California, Berkeley, Report No. SESM 67-8, 1967.

39. Marcal, P. V. and King, I. P., "Elastic-Plastic Analysis of Two-Dimensional Stress Systems by the Finite Element Method", Int. J. Mech. Sci., Vol. 9, No. 3, 1967.

40. Ziendiewicz, O. C., Valliappan, S. and King, I. P., "Elasto-Plastic Solutions of Engineering Problems "Initial Stress" Finite Element Approach", International Journal for Numerical Methods in Engineering., Vol. 1, Jan. 1969.

41. Armen, H., Pifko, A. and Levine, H. S., "Finite Element Method for the Plastic Bending Analysis of Structures," Proc. 2nd Conference on Matrix Method in Structural Mechanics, Wright-Patterson AFB, AFFDL-TR-68-150, 1968.

42. Hofmeister, L. D., Greenbaum, G. A., and Evensen, D. A., "Large Strain, Elasto-Plastic Finite Element Analysis", AIAA Journal, Vol. 9, No. 7, July 1971.

43. Larsen, P. K., "Large Displacement Analysis of Shells of Revolution Including Creep, Plasticity and Viscoelasticity", Ph.D. Dissertation, University of California, Berkeley, SESM Report No. 71-22, 1971.

44. Klein, S. and Sylvester, R. J., "The Linear Elastic Dynamic Analysis of Shells of Revolution by the Matrix Displacement Method", Proc. of the First AFFDL Conference in Matrix Methods in Structural Mechanics, AFFDL-TR-66-80, Dec. 1968.

45. Wilson, E. L., Farhoomand, I., and Bathe, K. J., "Nonlinear Dynamic Analysis of Complex Structures", International Journal of Earthquake Engineering and Structural Dynamics, Vol. 1, No. 3, 1973.

46. Clough, R. W., "Structural Vibrations and Dynamic Response", Proc. Japan-U.S. Seminar on Matrix Methods of Structural Analysis and Design, Tokyo, Japan, 1969.

47. Clough, R. W., and Wilson, E. L., "Dynamic Finite Element Analysis of Arbitrary Thin Shells", Computers and Structures, Vol. 1, Numbers 1/2, 1971.

48. Stricklin, J. A., Martinez, J. E., Tillerson, J. R., Hong, J. H., and Haisler, W. E., "Nonlinear Dynamic Analysis of Shells of Revolution by the Matrix Displacement Method", AIAA Journal, Vol. 9, No. 4, 1971.

49. Wilson, E. L., "A Computer Program for the Dynamic Stress Analysis of Underground Structures", Report SEL 68-1, University of California, Berkeley, 1968.

50. Perzyna, P., "The Study of the Dynamic Behavior of Rate Sensitive Plastic Materials", Arch. Mech. Stos., Vol. 15, 1963.

51. Lindholm, U. S., "Dynamic Deformation of Metals", Behavior of Materials Under Dynamic Loading, ed. by N. J. Huffington, Jr., ASME, New York, 1965.

52. Cristescu, N., Dynamic Plasticity, North Holland Press, Amsterdam, 1967.

53. Lindholm, U. S., "Some Experiments in Dynamic Plasticity Under Combined Stress", Mechanical Behavior of Materials Under Dynamic Loads, ed. by U. S. Lindholm, Springer-Verlag, New York, 1968.

54. Karnes, C. H., "The Plate Impact Configuration for Determining Mechanical Properties of Materials at High Strain Rates", Mechanical Behavior of Materials Under Dynamic Loads, ed. by U.S. Lindholm, Springer-Verlag, New York, 1968.

55. Hauser, F. E., Simmons, J. A., and Dorn, J. E., "Strain Rate Effects in Plastic Wave Propogation", Response of Metals to High Velocity Deformation, ed. by P. G. Shewmon, and V. F. Zackay, Interscience Publishers, 1960.

56. Hauser, F. E., "Techniques for Measuring Stress-Strain Relations at High Strain Rates", Experimental Mechanics, Vol. 6, No. 8, Aug. 1966.

57. Duffy, J., Hawley, R. H., and Frantz, R. A., Jr., "The Deformation of Lead in Torsion at High Strain Rates", Journal of Applied Mechanics, Vol. 39, No. 3, Sept. 1972.

58. Zienkiewicz, O. C., and Cormeau, I. C., "Visco-Plasticity by Finite Element Process," Arch. Mech. Stos., Vol. 24, Nos. 5-6, 1972.

59. Truesdell, C., The Elements of Continuum Mechanics, Springer-Verlag, New York, 1965.

60. Eringen, A. C., Nonlinear Theory of Continuous Media, McGraw-Hill, New York, 1962.

61. Eringen, A. C., Mechanics of Continua, John Wiley, New York, 1967.

62. Jaunzemis, W., Continuum Mechanics, The Macmillan Co., New York, 1967.

63. Leigh, D. C., Nonlinear Continuum Mechanics, McGraw-Hill, 1968.

64. Malvern, L. E., Introduction to the Mechanics of a Continuous Medium, Prentice Hall, 1969.

65. Larsen, P. K., and Popov, E. P., "Large Displacement Analysis of Viscoelastic Shells of Revolution", to be published in Computer Methods in Applied Mechanics and Engineering (in press).

66. Larsen, P. K., and Popov, E. P., "A Note on Incremental Equilibrium Equations and Approximate Constitutive Relations in Large Inelastic Deformations", to be published in Acta Mechanica (in press).

67. Bridgman, P. W., "The Compressibility of Thirty Metals as a Function of Pressure and Temperature", Proc. American Academy of Science, 58, 1923.

68. Naghdi, P. M., "Stress-Strain Relations in Plasticity and Thermoplasticity", in Plasticity, Proc. 2nd Symposium on Naval Structural Mechanics, Pergamon Press, 1960.

69. Mises, R. V., "Mechanik der Fester Koerper in Plastisch Deformation Zustard", Goettingen Nachr. Math.-Phys., Kh., 1913.

70. Prager, W., "The Theory of Plasticity: A Survey of Recent Achievements", (James Clayton Lecture) Proc. Inst. Mech. Eng., Vol. 169, 1955.

71. Ziegler, H., "A Modification of Prager's Hardening Rule", Quart. Appl. Math., Vol. 17, 1959.

72. Armen, H., Jr., Isakson, G., and Pifko, A., "Discrete Element Methods for the Plastic Analysis of Structures Subjected to Cyclic Loading", AIAA/ASME 8th Structures, Structural Mechanics and Materials Conference, Palm Springs, California, March 1967.

73. Levine, H. S., Armen, H., Jr., Winter, R., and Pifko, A., "Nonlinear Behavior of Shells of Revolution Under Cyclic Loading", Computers and Structures, Vol. 3, No. 3, May 1973.

74. Hill, R., The Mathematical Theory of Plasticity, Clarendon Press, Oxford, 1950.

75. Manjoine, M. J., "Influence of Rate of Strain and Temperature on Yield Stresses of Mild Steel", Trans. ASME, 66, A 211, 1944.

76. Malvern, L. E., "The Propogation of Longitudinal Waves of Plastic Deformation in a Bar of Material Exhibiting a Strain-rate Effect", Journal of Applied Mechanics, Vol. 18, 1951.

77. Lubliner, J., "A Generalized Theory of Strain-Rate-Dependent Plastic Wave Propogation in Bars", Journal of the Mechanics and Physics of Solids, Vol. 12, 1964.

78. Sokolovsky, V. V., "Propogation of Elastic-Visco-plastic Waves in Bars", (in Russian), Prik. Mat. Mekh., Vol. 12, 1948.

79. Von Karman, T., and Duwez, P., "Propogation of Plastic Deformations in Solids", Journal of Applied Physics, Vol. 21, No. 10, Oct. 1950.

80. Rakhmatulin, K. A., "On Propogation of Wave of Unloading", (in Russian), Prik. Mat. Mekh., Vol. 9, No. 1, 1945.

81. Taylor, G. I., "The Plastic Wave in a Wire Extended by an Impact Load", The Scientific Papers of G. I. Taylor, ed. by G. K. Batchelor, Vol. 1, Cambridge University Press, 1958.

82. Perzyna, P., "The Constitutive Equations for Rate Sensitive Plastic Materials", Quart. of Applied Math., Vol. 20, No. 4 1963.

83. Hohenemeser, K., and Prager, W., "Über die Ansätze der Mechanik isotroper Kontinua", ZAAM, Vol. 12, 1932.

84. Perzyna, P., and Wojno, "On the Constitutive Equations of Elastic/Viscoplastic Materials at Finite Strain", Arch. Mech. Stos., Vol. 18, 1966.

85. Wierzbicki, T., "Large Deflections of a Strain Rate Sensitive Plate Loaded Impulsively", Arch. Mech. Stos., Vol. 21, 1969.

86. Calder, C. A., Kelly, J. M., and Goldsmith, W., "Projectile Impact on an Infinite, Viscoplastic Plate", International Journal of Solids and Structures, Vol. 7, Sept. 1971.

87. Perzyna, P., "Fundamental Problems in Visco-plasticity", from Recent Advances in Applied Mechanics, Academic Press, New York, 1966.

88. Martin, H.C., "On the Derivation of Stiffness Matrices for the Analysis of Large Deflection and Stability Problems", Proc. 1st Conference on Matrix Methods in Structural Mechanics, Wright-Patterson AFB, AFFDL-TR-66-80, 1966.

89. Haisler, W. E., Stricklin, J. A. and Stebbins, F. J., "Development and Evaluation of Solution Procedures for Geometrically Nonlinear Structural Analysis by the Direct Stiffness Method", AIAA-ASME 12th Structures, Structural Dynamics, and Materials Conference, Anaheim, California, April 19-21, 1971.

90. Oden, J. T., "Finite Element Applications in Nonlinear Structural Analysis", Proc. of the Conference on Finite Element Methods, Vanderbilt University, Nashville, Tennessee, Nov. 1969.

91. Caughey, T. K., "Classical Normal Modes in Damped Linear Systems", Journal of Applied Mechanics, Paper No. 59-A-62.

92. Newmark, N. M., "A Method of Computation for Structural Dynamics", Proc. ASCE, Vol. 85, No. EM3, 1959.

93. Farhoomand, I., "Nonlinear Dynamic Stress Analysis of Two-Dimensional Solids", Ph.D. Dissertation, University of California, Berkeley, June 1970.

94. Bathe, K. J., and Wilson, E. L., "Stability and Accuracy Analysis of Direct Integration Methods", International Journal of Earthquake Engineering and Structural Dynamics, Vol. 1, No. 3, 1973.

95. Houbolt, J. C., "A Recurrence Matrix Solution for the Dynamic Response of Elastic Aircraft", Journal of the Aerospace Sciences, Vol. 17, 1950.

96. Dunham, R. S., Nickell, R. E., and Stickler, D. C., "Integration Operators for Transient Structural Response", Computers and Structures, Vol. 2, 1972.

97. Nickell, R.E., "A Survey of Direct Integration Methods in Structural Dynamics", Report N00014/0007/9, Division of Engineering, Brown University, Providence, R. I., 1972.

98. Goudreau, G. L., "Evaluation of Discrete Methods for the Linear Dynamic Response of Elastic and Viscoelastic Solids", Ph.D.Dissertation, SESM Report No. 69-15, University of California, Berkeley, 1970.

99. Argyris, J. H., Dunne, P. C., and Angelopoulos, T., "Nonlinear Oscillations Using the Finite Element Technique", Computer Methods in Applied Mechanics and Engineering, Vol. 2, No. 2, May 1973.

100. Kraus, H., Thin Elastic Shells, John Wiley, 1967.

101. De Arantes e Oliviera, E. R., "Mathematical Foundation of the Finite Element Method", Lab. Nacional de Engenharia Civil, Lisbon, 1967.

102. Mikhlin, S. G., Variational Methods in Mathematical Physics, Macmillan Co., 1964.

103. Ergatoudis, J., Irons, B. M., and Zienkiewicz, O. C., "Curved, Isoparametric, 'Quadrilateral' Elements for Finite Element Analysis", International Journal of Solids and Structures, Vol. 4, 1968.

104. Larsen, P. K., and Popov, E. P., "Elastic-Plastic Analysis of Axisymmetric Solids Using Isoparametric Finite Elements", SESM Report 71-2, University of California, Berkeley, 1971.

105. Nagarajan, S., and Popov, E. P., "Elastic-Plastic Dynamic Analysis of Axisymmetric Solids", SESM Report 73-9, University of California, Berkeley, 1973.

106. Wilson, E. L., "SAP, A General Structural Analysis Program", Report No. UCSESM 70-20, University of California, Berkeley, 1970.

107. Ahmad, S., Irons, B. M. and Zienkiewicz, O.C., "Curved Thick Shell and Membrane Elements with Particular Reference to Axisymmetric Problems", Proc. 2nd Conference on Matrix Methods in Structural Mechanics, AFFDL-TR-68-150, 1968.

108. Pawsey, S. F., "The Analysis of Moderately Thick to Thin Shells by the Finite Element Method", Report No. UCSESM 70-12, University of California, Berkeley, 1970.

109. Zienkiewicz, O. C., Taylor, R. L. and Too, J. M., "Reduced Integration Technique in General Analysis of Plates and Shells", International Journal for Numerical Methods in Engineering, Vol. 3, 1971.

110. Abramowitz, M., and Stegun, I. A., Handbook of Mathematical Functions, National Bureau of Standards, 1964.

111. Kornishin, H. S. and Isanbaeva, F. S., Flexible Plates and Panels, Nauka, Moscow, 1968 (in Russian).

112. Weinitschke, H., "On the Nonlinear Theory of Shallow Spherical Shells", SIAM, Vol. 6, No. 3, Sept. 1958.

113. Weinitschke, H., "On Asymmetric Buckling of Shallow Spherical Shells", Journal of Mathematics and Physics, Vol. 44, No. 2, June 1965.

114. Goudreau, G. L. and Taylor, R. L., "Evaluation of Numerical Integration Methods in Elastodynamics", Computer Methods in Applied Mechanics and Engineering, Vol. 2, No. 1, 1972.

115. Baron, M. L., Bleich, H. H. and Weidlinger, P., "Dynamic Elastic-Plastic Analysis of Structures", Journal of the Engineering Mechanics Division, (Proc. ASCE), Vol. 87, No. EM1, 1961.

116. Stricklin, J. A., Martinez, J. E., Tillerson, J. R., Hong, J. H. and Haisler, W. E., "Nonlinear Dynamic Analysis of Shells of Revolution by the Matrix Displacement Method", Department of Aerospace Engineering, Texas A&M University, Report 69-77, Feb. 1970.

117. Prager, W. and Hodge, P. G., Theory of Perfectly Plastic Solids, Dover, 1968.

118. Vallee, J., "Comparison Between the Finite Element Method and the Limit Analysis Method", Graduate Student Report, Department of Civil Engineering, University of California, Berkeley, 1971.

119. Tuholski, N. J., "Elastic-Plastic Analysis of Beams by Plastic Beam and Finite Element Methods", Graduate Student Report, Department of Civil Engineering, University of California, Berkeley, 1972.

APPENDIX A. INTERPOLATION POLYNOMIALS

The following are the interpolation polynomials for linear, quadratic, cubic and quartic elements shown in Fig. 5.1.

Linear element Nodal points (-1, +1)

$$\phi_1(\xi) = \frac{1}{2}(1 - \xi)$$

$$\phi_2(\xi) = \frac{1}{2}(1 + \xi)$$

Quadratic element Nodal points (-1, 0, +1)

$$\phi_1(\xi) = -\frac{1}{2}\xi(1 - \xi)$$

$$\phi_2(\xi) = (1 - \xi^2)$$

$$\phi_3(\xi) = \frac{1}{2}\xi(1 + \xi)$$

Cubic element Nodal points $(-1, -\frac{1}{3}, 0, +\frac{1}{3}, +1)$

$$\phi_1(\xi) = \frac{1}{16}(1 - \xi)(-1 + 9\xi^2)$$

$$\phi_2(\xi) = \frac{9}{16}(1 - 3\xi)(1 - \xi^2)$$

$$\phi_3(\xi) = \frac{9}{16}(1 + 3\xi)(1 - \xi^2)$$

$$\phi_4(\xi) = \frac{1}{16}(1 + \xi)(-1 + 9\xi^2)$$

Quartic element Nodal points $(-1, -\frac{1}{2}, 0, +\frac{1}{2}, +1)$

$$\phi_1(\xi) = \frac{1}{6}\xi(1 - \xi)(1 - 4\xi^2)$$

$$\phi_2(\xi) = -\frac{4}{3}\xi(1 - 2\xi)(1 - \xi^2)$$

$$\phi_3(\xi) = 1 - \xi^2(5 - 4\xi^2)$$

$$\phi_4(\xi) = \frac{4}{3}\xi(1 + 2\xi)(1 - \xi^2)$$

$$\phi_5(\xi) = -\frac{1}{6}\xi(1 + \xi)(1 - 4\xi^2)$$

APPENDIX B. DISPLACEMENT GRADIENT MATRICES

The procedure for evaluation of the displacement gradient matrices $[B_1]$ and $[B_2]$ is outlined in this appendix.

The geometry and displacement field for degenerate isoparametric elements are given by

$$\begin{Bmatrix} r \\ z \end{Bmatrix} = \sum_{i=1}^{N} \phi_i(\xi) \begin{Bmatrix} r_i \\ z_i \end{Bmatrix} + \eta \sum_{i=1}^{N} \frac{1}{2} \phi_i(\xi)\, h_i \begin{Bmatrix} \cos\theta_i \\ \sin\theta_i \end{Bmatrix} \tag{5.2}$$

and

$$\begin{Bmatrix} u \\ w \end{Bmatrix} = \sum_{i=1}^{N} \phi_i(\xi) \begin{Bmatrix} u_i \\ w_i \end{Bmatrix} + \eta \sum_{i=1}^{N} \frac{1}{2} \phi_i(\xi)\, h_i \begin{Bmatrix} -\sin\theta_i \\ \cos\theta_i \end{Bmatrix} \alpha_i \tag{5.3}$$

The chain rule of differentiation gives

$$\begin{Bmatrix} \frac{\partial}{\partial r} \\ \frac{\partial}{\partial z} \end{Bmatrix} = \frac{1}{\det J} [J] \begin{Bmatrix} \frac{\partial}{\partial \xi} \\ \frac{\partial}{\partial \eta} \end{Bmatrix} \tag{B.1}$$

where [J] is the Jacobian matrix given by

$$[J] = \begin{bmatrix} \frac{\partial z}{\partial \eta} & -\frac{\partial z}{\partial \xi} \\ -\frac{\partial r}{\partial \eta} & \frac{\partial r}{\partial \xi} \end{bmatrix} \tag{B.2}$$

and

$$|J| = \det J = \frac{\partial z}{\partial \eta}\frac{\partial r}{\partial \xi} - \frac{\partial z}{\partial \xi}\frac{\partial r}{\partial \eta} \tag{B.3}$$

Combining Eqs. (5.2) and (B.3), one gets

$$|J| = (\phi_{i,\xi}\, r_i + \tfrac{1}{2}\, \eta\, \phi_{i,\xi}\, h_i \cos\theta_i)\, \tfrac{1}{2}\, \phi_j\, h_j \sin\theta_j$$

$$-(\phi_{i,\xi}\, z_i + \tfrac{1}{2}\, \eta\, \phi_{i,\xi}\, h_i \sin\theta_i)\, \tfrac{1}{2}\, \phi_j\, h_j \cos\theta_j$$

Let $P_{ij} = \tfrac{1}{2}\, \phi_{i,\xi}\, \phi_j$ (B.4)

Then $|J| = P_{ij} \Big(h_j\, (r_i \sin\theta_j - z_i \cos\theta_j) + \tfrac{1}{2}\, \eta\, h_i\, h_j$

$$(\sin\theta_j \cos\theta_i - \cos\theta_j \sin\theta_i)\Big)$$

Define:

$$J_1(\xi) = P_{ij}\, h_j\, (r_i \sin\theta_j - z_i \cos\theta_j)$$

$$J_2(\xi) = P_{ij}\, \tfrac{1}{2}\, h_i\, h_j\, (\sin\theta_j \cos\theta_i - \cos\theta_j \sin\theta_i)$$

Then

$$|J| = J_1(\xi) + \eta\, J_2(\xi) \qquad \text{(B.5)}$$

Defining

$$\{PS\} = P_{ij}\, h_j \sin\theta_j$$

$$\{PC\} = P_{ij}\, h_j \cos\theta_j$$

$$\langle SP\rangle = P_{ij}\, h_i \sin\theta_i$$

$$\langle CP\rangle = P_{ij}\, h_i \cos\theta_i \qquad \text{(B.6)}$$

$$\langle RP\rangle = P_{ij}\, r_i$$

$$\langle ZP\rangle = P_{ij}\, z_i$$

one can write $J_1(\xi)$ and $J_2(\xi)$ in the form

$$J_1(\xi) = \langle r\rangle \{PS\} - \langle z\rangle \{PC\}$$

$$J_2(\xi) = \langle h \cos\theta\rangle \{PS\} - \langle h \sin\theta\rangle \{PC\}$$

The global displacement gradients can be derived in a similar manner using Eqs. (5.2, 3) and the chain rule of differentiation, Eqs. (B.1, 2), e.g.

$$\frac{\partial u}{\partial r} = \frac{1}{|J|}\left(\frac{\partial u}{\partial \xi}\frac{\partial z}{\partial \eta} - \frac{\partial u}{\partial \eta}\frac{\partial z}{\partial \xi}\right)$$

$$= \frac{1}{|J|}\left(\frac{1}{2}\phi_j h_j \sin\theta_j \left(\phi_{i,\xi} u_i - \frac{1}{2}\eta\,\phi_{i,\xi} h_i \sin\theta_i \alpha_i\right)\right.$$

$$\left. + \left(\phi_{j,\xi} z_j + \frac{1}{2}\eta\,\phi_{j,\xi} h_j \sin\theta_j\right)\frac{1}{2}\phi_i h_i \sin\theta_i \alpha_i\right)$$

or

$$\frac{\partial u}{\partial r} = \frac{1}{|J|}\left(\langle u\rangle \{PS\} + \langle ZP\rangle \{h \sin\theta\,\alpha\} + \frac{1}{2}\eta\,(\langle SP\rangle \{h \sin\theta\,\alpha\}\right.$$

$$\left. - \langle h \sin\theta\,\alpha\rangle \{PS\})\right) \qquad (B.7)$$

Similarly, expressions can be obtained for $\frac{\partial w}{\partial z}$, $\frac{u}{r}$, $\frac{\partial u}{\partial z}$, and $\frac{\partial w}{\partial r}$.

$$\frac{\partial w}{\partial z} = \frac{1}{|J|}\left(-\langle w\rangle \{PC\} + \langle RP\rangle \{h \cos\theta\,\alpha\} + \frac{1}{2}\eta(\langle CP\rangle\{h \cos\theta\,\alpha\}\right.$$

$$\left. - \langle h \cos\theta\,\alpha\rangle \{PC\})\right) \qquad (B.8)$$

$$\frac{u}{r} = \frac{1}{r}(\phi_i u_i - \frac{1}{2}\eta\,\phi_i h_i \sin\theta_i \alpha_i) \qquad (B.9)$$

$$\frac{\partial u}{\partial z} = \frac{1}{|J|}\left(-\langle u\rangle \{PC\} - \langle RP\rangle \{h \sin\theta\,\alpha\}\right.$$

$$\left. - \frac{1}{2}\eta\,(\langle CP\rangle \{h \sin\theta\,\alpha\} - \{h \sin\theta\,\alpha\}\langle PC\rangle)\right) \qquad (B.10)$$

$$\frac{\partial w}{\partial r} = \frac{1}{|J|}\left(\langle w\rangle \{PS\} - \langle ZP\rangle \{h \cos\theta\,\alpha\}\right.$$

$$\left. + \frac{1}{2}\eta \quad \langle h \cos\theta\,\alpha\rangle \{PS\} - \langle SP\rangle \{h \cos\theta\,\alpha\}\right) \qquad (B.11)$$

In Eqs. (B.7-11), $|J|$ and r are functions of ξ and η. These equations may be written as

$$\frac{\partial u}{\partial r} = \frac{1}{|J|}\left(\langle b_1^* \rangle_1 + \eta \langle b_2^* \rangle_1\right)$$

$$\frac{\partial w}{\partial z} = \frac{1}{|J|}\left(\langle b_1^* \rangle_2 + \eta \langle b_2^* \rangle_2\right)$$

$$\frac{u}{r} = \frac{1}{r}\left(\langle b_1^* \rangle_3 + \eta \langle b_2^* \rangle_3\right)$$

$$\frac{\partial u}{\partial z} = \frac{1}{|J|}\left(\langle b_1^* \rangle_4 + \eta \langle b_2^* \rangle_4\right)$$

$$\frac{\partial w}{\partial r} = \frac{1}{|J|}\left(\langle b_1^* \rangle_5 + \eta \langle b_2^* \rangle_5\right)$$

where the vectors $\langle b_1^* \rangle_i$, $\langle b_2^* \rangle_i$, $i = 1,5$, can be obtained from Eqs. (B.7-11). For example,

$$\underset{(1 \times 3N)}{\langle b_1^* \rangle_1} = \langle \{PS\}_1 \;\; 0 \;\; \langle ZP \rangle_1 h_1 \sin\theta_1 \;\; \{PS\}_2 \;\; 0 \;\; \langle ZP \rangle_2 h_2 \sin\theta_2 \;\; \ldots\ldots \rangle$$

and

$$\underset{(1 \times N)}{\langle b_2^* \rangle_1} = \langle \tfrac{1}{2}\left(\langle SP \rangle_1 - \langle PS \rangle_1\right) h_1 \sin\theta_1 \;\; \tfrac{1}{2}\left(\langle SP \rangle_2 - \langle PS \rangle_2\right) h_2 \sin\theta_2 \;\; \ldots\ldots \rangle$$

For a cubic element, these vectors have the dimensions 1×12 for $\langle b_1^* \rangle_i$ and 1×4 for $\langle b_2^* \rangle_i$

A coordinate transformation from the global (r,z) system to the local (s,t) system yields $\langle b_1 \rangle_i$ and $\langle b_2 \rangle_i$, $i = 1,4$. This can be achieved by a transformation matrix [T], i.e.,

$$\begin{Bmatrix} \frac{\partial u_1}{\partial s} \\ \frac{u}{r} \\ \frac{\partial u_1}{\partial t} \\ \frac{\partial u_2}{\partial s} \end{Bmatrix}_{4 \times 1} = [T]_{4 \times 5} \begin{Bmatrix} \frac{\partial u}{\partial r} \\ \frac{\partial w}{\partial z} \\ \frac{u}{r} \\ \frac{\partial u}{\partial z} \\ \frac{\partial w}{\partial r} \end{Bmatrix}_{5 \times 1} \qquad (B.12)$$

This matrix [T] can be obtained from the relation

$$\begin{Bmatrix} u_1 \\ u_2 \end{Bmatrix} = \begin{bmatrix} \cos\psi & \sin\psi \\ -\sin\psi & \cos\psi \end{bmatrix} \begin{Bmatrix} u \\ w \end{Bmatrix} \qquad (5.5)$$

Calculation of the displacement gradients in the local system in terms of those in the global system, using this equation, leads to

$$[T] = \begin{bmatrix} \cos^2\psi & \sin^2\psi & 0 & \cos\psi \sin\psi & \cos\psi \sin\psi \\ 0 & 0 & 1 & 0 & 0 \\ -\cos\psi \sin\psi & \cos\psi \sin\psi & 0 & \cos^2\psi & -\sin^2\psi \\ -\cos\psi \sin\psi & \cos\psi \sin\psi & 0 & -\sin^2\psi & \cos^2\psi \end{bmatrix} \qquad (B.13)$$

The transformation to the local system can then be made as

$$\begin{bmatrix} \langle b_1 \rangle_1 \\ \langle b_1 \rangle_2 \\ \langle b_1 \rangle_3 \\ \langle b_1 \rangle_4 \end{bmatrix} = [T] \begin{bmatrix} \langle b_1^* \rangle_1 \\ \langle b_1^* \rangle_2 \\ \langle b_1^* \rangle_3 \\ \langle b_1^* \rangle_4 \\ \langle b_1^* \rangle_5 \end{bmatrix} \qquad (B.14)$$

and a similar transformation to obtain $\langle b_2 \rangle_i$, i=1, 4.

The displacement gradient matrices, $[B_1]$ and $[B_2]$ to be used in Eq. (5.19) are then given as

$$[B_1] = \begin{bmatrix} \frac{1}{|J|} & & & \\ & \frac{1}{r} & & \\ & & \frac{1}{|J|} & \\ & & & \frac{1}{|J|} \end{bmatrix} \begin{bmatrix} \langle b_1 \rangle_1 \\ \langle b_1 \rangle_2 \\ \langle b_1 \rangle_3 \\ \langle b_1 \rangle_4 \end{bmatrix} = \begin{bmatrix} \frac{1}{|J|} & \langle b_1 \rangle_1 \\ \frac{1}{r} & \langle b_1 \rangle_2 \\ \frac{1}{|J|} & \langle b_1 \rangle_3 \\ \frac{1}{|J|} & \langle b_1 \rangle_4 \end{bmatrix} \tag{B.15}$$

and

$$[B_2] = \begin{bmatrix} \frac{1}{|J|} & & & \\ & \frac{1}{r} & & \\ & & \frac{1}{|J|} & \\ & & & \frac{1}{|J|} \end{bmatrix} \begin{bmatrix} \langle b_2 \rangle_1 \\ \langle b_2 \rangle_2 \\ \langle b_2 \rangle_3 \\ \langle b_2 \rangle_4 \end{bmatrix} = \begin{bmatrix} \frac{1}{|J|} & \langle b_2 \rangle_1 \\ \frac{1}{r} & \langle b_2 \rangle_2 \\ \frac{1}{|J|} & \langle b_2 \rangle_3 \\ \frac{1}{|J|} & \langle b_2 \rangle_4 \end{bmatrix} \tag{B.16}$$

It may be noted that the computations involved in the integration for incremental stiffness, viscoplastic pseudo-loading and internal resisting forces have been simplified because the dependence on η is expressed merely as a multiplying factor which enables the integrations across the thickness to be carried out separately.

APPENDIX C. DIAGONAL MASS MATRIX

This appendix presents the scheme used to evaluate the lumped masses at the nodal points of cubic degenerate isoparametric elements shown in Fig. 5.2. The total lumped mass or inertia at any node where two elements are interconnected is the sum of the inertia terms assigned to it from each element.

The length and cross-sectional area (i.e. in the r-z plane) of each element are computed using numerical integration at the same time the element stiffness matrices are evaluated. The tributary length and area for each node are approximated by using weight factors obtained from consideration of an element of uniform thickness as shown in Fig. C.1 where the centroids of the tributary lengths and areas are also indicated. The weight factors and centroids for a cubic element are:

Nodal point	Weight factor	Centroid of tributary area	
		ξ	η
1	1/6	-5/6	0
2	1/3	-1/3	0
3	1/3	+1/3	0
4	1/6	+5/6	0

The r-coordinates of the centroids of these areas are obtained

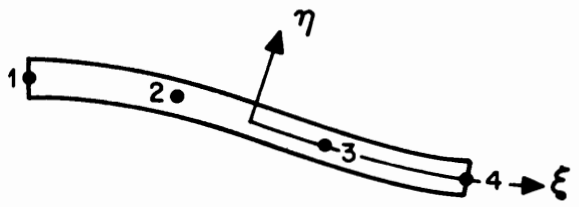

'CUBIC' ELEMENT
UNIFORM THICKNESS h

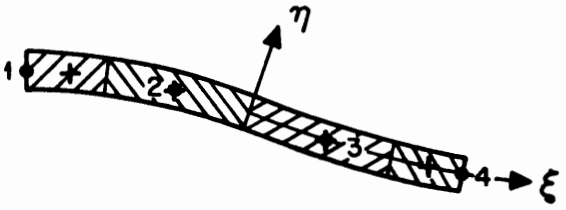

HATCHED ZONES INDICATE TRIBUTARY AREAS
+ INDICATE CENTROIDS OF THE TRIBUTARY AREAS

FIG. C.I 'CUBIC' DEGENERATE ISOPARAMETRIC ELEMENT, WEIGHT FACTORS AND TRIBUTARY AREAS

using nodal point coordinates and interpolation polynomials. For a unit radian in the circumferential direction, the tributary volumes are obtained by multiplying the tributary areas by these radii. Element width is used instead of these radii in the case of plane stress problems. Finally, the lumped mass at each node of the element is the product of the tributary volume and element mass density, and is the inertia term in the element mass matrix corresponding to the two translational degrees of freedom at that node. Rotatory inertia corresponding to the rotational degree of freedom is evaluated as the product of the tributary length and the mass moment of inertia of the circumferential cross section (i.e. in the η-θ plane) at the centroid of the tributary length, i.e. if h_{ic} is the thickness and r_{ic} the radial coordinate at the centroid of the tributary length l_i corresponding to the nodal point i, then the rotatory inertia term is given as (for a unit radian in the circumferential direction)

$$\rho_0 \, r_{ic} \, \frac{h_{ic}^3}{12} \cdot l_i$$

where ρ_0 is the mass density in configuration B_0.